ABSTRACT

Title of Document: A CRASH RISK INDEX FOR FREEWAYS BASED ON CRASH RISK PREDICTION MODELS AND ITS APPLICATIONS

Hyoseuk Chang, Doctor of Philosophy, 2018

Directed by: Professor Ali Haghani

Department of Civil and Environmental Engineering

This research focuses on the development of a crash risk index that quantifies the crash risk coming from impending rear-end or sideswipe crashes. It proposes a generalized framework that can be adopted for traffic safety improvement on freeways to accomplish this. The proposed generalized framework begins with the collection of potential contributing factors that affect crash risk. It involves traffic parameters, such as basic traffic parameter that can be obtained from detectors, lane-based traffic parameters, number of trucks, ramp flow, and surrogate measures of lane-changing, and environmental characteristics, such as rainfall, snow, visibility, pavement, and

lighting condition. The most significant contributing factors are identified by random forest method and three statistical tests for five different segment types. Based on the identified factors Bayesian random intercept logistic regression is used to build crash risk prediction models for five segment types. The outcome of them is used to develop a crash risk index that quantifies crash risk for the segment. The developed crash risk index is applied to a 13.14-mile stretch of I-110 northbound in California to monitor the change in crash risk in real time. The results of monitoring demonstrate that the crash risk indices result in high crash risk before the crash occurs. Lastly, new variable speed limits (VSL), which is a proactive intervention, aiming to reduce the high crash risk indicated by the crash risk indices are proposed. The results indicate that the proposed VSL control reduces the high crash risk below thresholds and achieves a reduction in travel time as well. It is expected that if this whole framework would be utilized on a freeway, it will help traffic operators to identify hazardous traffic conditions better and to implement proactive interventions to alleviate crash risk in the right location at the right time.

A CRASH RISK INDEX FOR FREEWAYS BASED ON CRASH RISK PREDICTION MODELS AND ITS APPLICATIONS

By

Hyoseuk Chang

Dissertation submitted to the Faculty of the Graduate School of the
University of Maryland, College Park, in partial fulfillment
of the requirements for the degree of

Doctor of Philosophy

2018

Advisory Committee:

Professor Ali Haghani, Chair

Professor Paul Schonfeld

Professor Martin Dresner

Professor Cinzia Cirillo

Doctor Kaveh Farokhi Sadabadi

Dedication

To my grandmother who has been praying for me until now.

Acknowledgements

It is my honor to have my advisor, Professor. Ali Haghani, for his enlightening and persistent encouragement. I would never have been able to finish my dissertation without the guidance of my advisor. I am deeply indebted to him for training me to think in a more creative way during my Ph.D. degree and for supporting me to live in a good environment. From the bottom of my heart, I would like to express my appreciation for his help on my research career.

I would also like to express my gratitude to the members of my doctoral examination committee – Dr. Paul Schonfeld, Dr. Martin Dresner, Dr. Cinzia Cirillo, and Dr. Kaveh Farokhi Sadabadi for giving me suggestions on this dissertation and for serving on the committee. Their comments were very helpful in the successful completion of this dissertation.

I am very thankful to my supervisor at the federal highway research center, Anushapatel Nujjetty and TJ. They always showed support and encouragement. It has been a pleasure to work with them and working there was a huge opportunity for me to see how people approach traffic safety issues.

I would like to express my deepest appreciation to my family for their infinite love and support and to my grandmother for always praying for me. Without their love, I would not have been able to make it through these hard times.

Table of Contents

List of Tables

List of Figures

Chapter 1 Introduction

1.1 Background

Freeway traffic safety management has gained much attention since crashes not only take lives but also result in serious congestion costs. In recent years, particular attention has been given towards the development of real-time crash prediction models which predict the likelihood of crash occurrences using traffic parameters. The most important step in predicting crash occurrences is the identification of hazardous traffic conditions that possibly lead to raising crash risk. The longer hazardous traffic conditions last, the greater the crash risk. Traffic safety can be enhanced when such hazardous traffic conditions are identified and avoided.

Numerous studies have been conducted to identify significant contributing factors which affect hazardous traffic conditions and raise crash risk. The findings of these studies have established statistical links between crash risk and traffic parameters. Recent studies have also sought to improve understanding of the relationship between crash risk and geometric characteristics, between crash risk and environmental characteristics. However, a solid understanding of the relationship between crash risk and combined other factors, such as traffic parameters, geometric characteristics, and environmental characteristics is still lacking. Many studies have concluded that contributing factors affecting crash risk not only depend on geometric and environmental characteristics but also the intensity of the contributing factors vary with respect to different geometric characteristics. Despite these findings, not all potential contributing factors have been examined synthetically. Moreover, several traffic parameters which have been found to affect crash risk significantly (e.g., lane-based traffic parameters, number of trucks, ramp flow, and surrogate measures of lane-change maneuvers) have not been properly considered in the existing models.

In brief, improving understanding of these complex and interconnected relationships will help transportation professionals to better identify hazardous traffic conditions with high crash risk before crashes occur. Furthermore, the establishment of a concrete framework involving the identification of significant contributing factors and estimating crash risk in real time ultimately will help to develop proactive traffic safety management strategies.

1.2 Research Objectives

This study intends to pursue the following principal objectives:

- Examine all effective traffic parameters, geometric characteristics, and environmental characteristics and consider them in a comprehensive way;
- Establish a generalized framework that involves examining all potential contributing factors, developing a crash risk index and monitoring crash risk in real time;
- Develop proactive traffic safety management strategies aiming at reducing the observed high crash risk.

1.3 Dissertation Organization

Figure 1.1 illustrates the principal tasks and organization of this study. A brief description of each chapter is presented next.

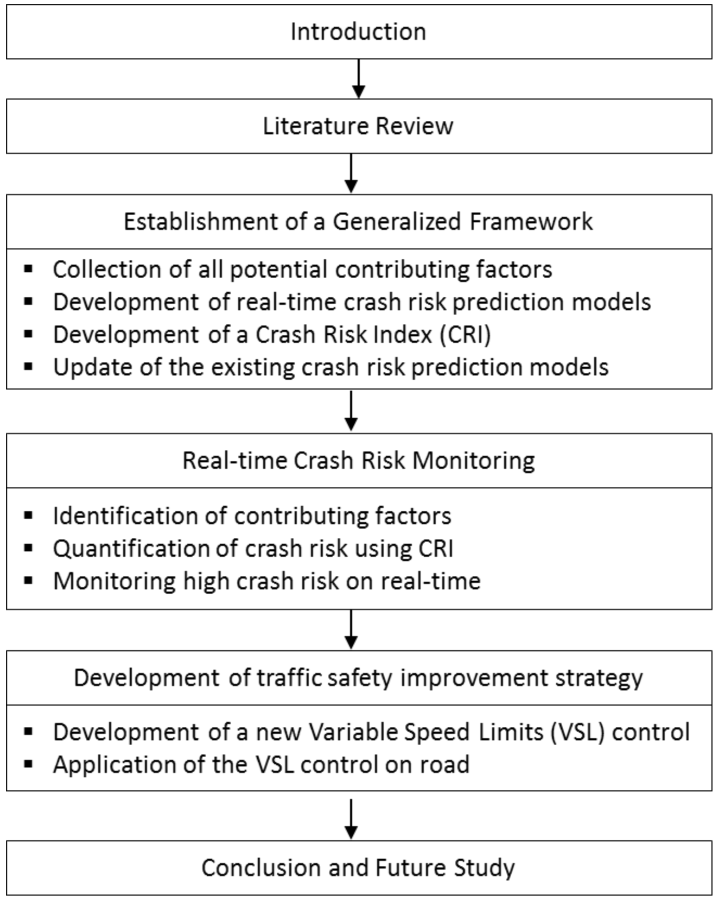

Figure 1.1 Organization of This Dissertation

- Literature Review – Chapter 2 presents a comprehensive literature review of existing studies which focused on identifying contributing factors affecting crash risk on freeways according to crash types, crash severity, geometric characteristics, and environmental characteristics. Also, the transferability of existing crash risk prediction models is reviewed. Advantages and limitations of developed crash risk indices are also addressed along with their potential enhancements in this chapter.

- Establishment of a Generalized Framework – Chapter 3 illustrates the framework of the proposed generalized procedure based on critical issues that need to be taken into account.

It first specifies the required input and then presents a Bayesian random intercept logistic regression model, aiming to obtain the constant effect of each selected contributing factor on the change in crash risk. Based on the constant effects, crash risk index, which aims to monitor crash risk in real time on freeways is presented. Lastly, this section introduces a Bayesian updating approach that improves temporal transferability of the real-time crash risk prediction models developed in this study.

- Real-Time Crash Risk Monitoring – Chapter 4 presents the application of the generalized framework. It first presents the identified actual contributing factors for five segment types on I-110 northbound in California and then builds five Bayesian random intercept logistic regression models with the contributing factors identified. Odds ratios that are one of the outcomes of the models are utilized to develop crash risk indices for each segment type. Then the crash risk indices are applied towards monitoring changes in crash risk on a 13.14-mile segment of I-110N in California. High crash risk is presented before crash occurrences, and high crash risk even remains after the first crash occurred.

- Development of Traffic Safety Improvement Strategy – Chapter 5 presents Variable Speed Limits (VSL) as a proactive countermeasure for traffic safety improvement. To do that, a methodology of a VSL control is proposed and is applied to a 2.6-mile stretch of a sample segment in I-110N freeway in California. This chapter presents the change in high crash risk and travel time with the VSL and with no VSL.

- Conclusion and Future Studies – Chapter 6 summarizes the findings of these completed tasks, the contributions of this research, and future studies.

Chapter 2 Literature Review

2.1 Introduction

Given the large body of literature on various aspects of predicting crash risk, this chapter presents a comprehensive review of discovering contributing factors, updating crash risk prediction models, and existing crash risk indices. The purposes of this chapter are to reveal lacks of existing studies on identifying contributing factors and to enhance the existing crash risk prediction models for more accurate crash risk prediction in real time along with the development of a crash risk index. A summary of review results associated with each of the purposes is presented in the remaining sections.

2.2 Contributing Factors

A crash is a complicated event that can be influenced by a multitude of factors such as geometric characteristics, environmental characteristics, and current traffic conditions. A crash occurs as a result of hazardous traffic conditions combined with other external factors. Hazardous traffic conditions typically manifest themselves differently each time. Thus, it is important to examine all potential factors together so that hazardous traffic conditions can be explicitly and accurately identified before the crash occurrence and an appropriate traffic safety management can be implemented to mitigate these conditions. Hence, numerous studies have put much effort into identifying contributing factors capable of estimating crash risk ahead of crash occurrence.

Early studies conducted mainly using traffic parameters such as flow, speed, and occupancy obtained from detectors. The most utilized traffic parameters were average flow, average speed, and average occupancy as well as the standard deviation of flow, the standard deviation of speed, and the standard deviation of occupancy while the coefficient of variation of traffic parameters was also occasionally used. Abdel-Aty et al. (2004) used traffic data obtained from detectors upstream and downstream from a crash location to identify contributing factors. They found that a 5-min average occupancy at an upstream detector station 5 to 10 minutes ahead of the crash occurrence along with a 5-min coefficient of variation in the speed at a downstream detector station were significant factors in estimating crash risk. Oh et al. (2001) applied a nonparametric Bayesian method to determine whether speed variation in 5-min intervals was a good indicator of crash occurrence. They compared disruptive conditions to normal conditions and found that the standard deviation of speed was the most significant factor. However, many studies realized that crash mechanism is not generic throughout the gamut of freeways and that hazardous traffic conditions are often contingent on situational variables which vary on a case by case basis. For instance, Lee et al. (2006) found that the percentage of crashes on curved and straight road sections are different for both sideswipe and rear-end crashes. Hossain et al. (2011) showed that crash mechanisms might differ substantially between basic freeway segments (BFS) and ramp vicinities. Xu et al. (2013) showed that traffic parameters contributing to raising crash risk were different across different weather conditions. Hassain et al. (2015) found that the traffic parameters leading to increased crash risk are different under clear visibility and reduced visibility. From the previous studies, it can be concluded that the contributing factors are different with respect to crash types, crash severity, and different segment types and that environmental characteristic is also important factor raising crash risk as well as traffic parameters. Hence, recent studies have focused on unveiling relationships between crash risk and traffic parameters combined with geometric characteristics and environmental characteristics. Thus, next sections show the contributing factors found to affect crash types and crash severity.

2.2.1 Crash Type

A majority of crashes on freeways are rear-end and sideswipe crashes. Rear-end crashes are more likely to occur in lanes where vehicle interactions between leading and following vehicles are more intensive. Rear-end crashes are more affected by a driver's car following behavior which can be measured by speed and headway of the vehicles in the same lane. Kim et al. (2007) found that higher volume and lower truck percentage in a given segment of a freeway increased the probability of rear-end crashes. Lee et al. (2011) found that as the difference in speed across lanes increases, rear-end crashes are more likely to occur in the left lane. On the other hand, sideswipe crashes are associated with lane-change behavior. Sideswipe crashes mostly occur at the moment when a vehicle squeezes into a target lane with improper lane change maneuvers from a current lane. Unlike rear-end crashes, differences in traffic parameters between adjacent lanes are associated with sideswipe crashes. Chovan et al. (1994) found that lane change crashes commonly occurred when a subject vehicle changed lanes and hit a vehicle in the adjacent lane traveling at similar speed. Unfortunately, it is relatively difficult to observe lane change behaviors from traffic data. Accordingly, some surrogate measurements of lane change have been developed. Lee et al. (2006) suggested a geometric mean of ratios of flows between adjacent lanes referred to as the overall average flow ratio (OAFR) to indicate the likelihood of sideswipe crashes. In other words, OAFR indicates the total number of lane changes in all lanes. This is a variable which accounts for the variation in traffic conditions across lanes. They observed that as OAFR increased, lane change frequency also increased. They emphasized that the variation in traffic flow across lanes would be more important in estimating lane change. Khattak et al. (1998) found that trucks are more involved in sideswipe crashes than rear-end crashes due to the trucks' length and truck drivers' difficulty with seeing drivers in an adjacent lane. There are some other observations: Brackstone et al. (1998) concluded that lane change rate increases with flow under uncongested conditions and decreases with flow under congested conditions. This is because as flow increases under uncongested conditions, more drivers take advantage of higher speeds by changing lanes. However, as flow reaches capacity, acceptable gaps between vehicles for lane changes consequently decrease and the lane change rate decreases. After congestion occurs, it becomes even harder for drivers to find acceptable gaps; therefore, the lane change rate continues to decrease. This suggests that the level of congestion is closely related to lane change. Park and Ritchie (2004) observed that lane change tends to increase the variation in speed and subsequent high variation in speed may also increase the likelihood of crash occurrence. Golob et al. (2004) found that lane change crashes tend to occur when variation in flow is low, and variation in speed is high. Pande and Aty (2007) explored differences in traffic parameters between lanes at the upstream detector station of a crash location because the interaction between traffic flows in individual lanes might affect the lane changing behavior of drivers as well as the risk involved in lane changing maneuvers. The average differences in occupancies between adjacent lanes upstream of the crash location involved more crash risk. Lee et al. (2011) investigated the effects of the traffic parameters related to individual drivers' lane-changing and car-following behaviors on the occurrence of sideswipe and rear-end crashes on freeways. The analysis demonstrated that the significant traffic parameters affecting crash occurrence are distinctly different between sideswipe crashes and rear-end crashes. The flow-related variables were significant in the sideswipe crash models whereas the speed-related variables were significant in the rear-end crash models. These results suggested that the lane-by-lane traffic parameters are considered to be surrogate measures of lane-changing that are associated with the occurrence of sideswipe crashes. Ahn and Cassidy (2008) investigated effects of merging and diverging on freeway traffic oscillations near ramps. The finding showed that freeway traffic oscillations were shown to form and grow due to vehicle lane-change maneuvers. The lane-change maneuvers were made due to ramp flow. They concluded that traffic oscillations formed by lane-change maneuvers propagated upstream through the queue so that a state of greater crash risk existed at the end of the queue. In addition to this, Brackstone, McDonald, and Wu (1998) found that the lane change to the right-side target lane is mainly affected by the gap availability in the target lane. Also, the lane change to the left-side target lane is mainly affected by the speed difference between the current lane and the target lane. Previous studies have confirmed that traffic parameters that increase crash risk not only differ with respect to each crash type but also differ in the intensity of the traffic parameters that affect both rear-end and sideswipe crashes. Table 2.1 presents a summary of these previous studies.

Table 2.1 Contributing Factors according to Crash Type

Author	Crash Type	Contributing Factor
Kim et al. (2007)	Rear-end	Higher flow and lower truck percentage
Lee et al. (2011)	Rear-end	The difference in speed across lanes
Chovan et al. (1994)	Sideswipe	Lane changes
Lee et al. (2006)	Sideswipe	Overall average flow ratio (OAFR), variation in flow
Khattak et al. (1998)	Sideswipe	Number of trucks
Brackstone et al. (1998)	Sideswipe	Level of congestion
Park and Ritchie (2004)	Sideswipe	High variation in speed
Golob et al. (2004)	Sideswipe	Low variation in flow and high variation in speed
Pande and Aty (2007)	Sideswipe	The average difference between adjacent lane occupancies
Lee et al. (2011)	Rear-end	Speed-related variables
	Sideswipe	Flow-related variables (lane-by-lane traffic flow parameters)
Ahn and Cassidy (2008)	Sideswipe	Ramp flow

2.2.2 Crash Severity

Previous studies found that the identified contributing factors and the effect on crash risk would be different with respect to crash severity. Li and Bai (2006) modeled the relationships between fatal crashes and wide ranges of crash variables. Of the predictors they identified, environmental factors, such as darkness, dusk, were found to increase the chances of having a fatality. Li and Bai (2009) investigated significant crash risk factors that contribute to high-severity crashes in highway work zones. They showed that poor light conditions contributed to a much larger percent of fatal crashes, which indicates that poor light conditions could increase the probability of causing fatalities when a severe crash occurred. In this analysis, good light condition refers to the daylight condition, fair condition refers to the dawn, dusk, or dark-with-streetlights condition, and poor condition refers to the dark-without-streetlights condition. Li and Bai (2008) also found that the light condition affects the crash severity that poor light condition increases the chance of a fatal crash. Xu et al. (2013) developed a model that predicts the crash likelihood at different levels of severity with a particular focus on severe crashes. The results showed that the traffic flow characteristics contributing to crash likelihood were quite different at different levels of severity. The PDO (property-damage-only) crashes were more likely to occur under congested traffic flow conditions with highly variable speed and frequent lane changes, while the KA (fatal/incapacitating injury crashes) and BC (non-incapacitating/possible injury crashes) crashes were more likely to occur under less congested traffic flow conditions. High speed, coupled with a large speed difference between adjacent lanes under uncongested traffic conditions, was found to increase the likelihood of severe crashes (KA). For example, the upstream traffic density, the downstream traffic volume, the weather conditions, the peak period, and road surface width were found to be significantly correlated with the risk of injury and fatality once a crash happens. Also, the average speed measured at the upstream detector station, the difference in speeds between adjacent lanes at the upstream station and the downstream traffic flow were significantly correlated with the risk of fatal or incapacitating injury upon crash occurrence. Golob and Recker (2003) revealed the relationships among urban freeway accidents, traffic flow, weather, and lighting conditions. The results indicated that hit-objected collisions and collision involving multiple vehicles that are associated with lane-change maneuvers are more likely to occur on wet roads, while rear-end collisions are more likely to occur on dry roads during daylight. Controlling for weather and lighting conditions, there is evidence that accident severity is influenced more by volume than by speed.

2.2.3 Geometric Characteristic

According to HCM (2010), a freeway is a continuous facility that consists of a basic segment, a weaving segment, and a merge and diverge segment. Merge and diverge segments are defined as segments in which two or more traffic streams combine to form a single traffic stream (merge), or single traffic stream divides to form two or more separate traffic streams (diverge). The merge influence area is defined as from the point where edges of travel lanes of merging roadways meet to 1500 feet downstream of that point. The diverge influence area is defined as from the point where edges of travel lanes of diverging roadways meet to 1500 feet upstream of that point. These definitions are illustrated in Figure 2.1.

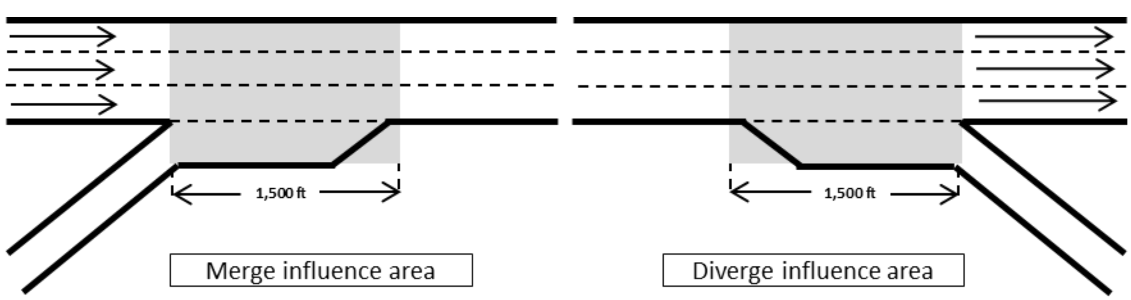

Figure 2.1 Merge Influence Area and Diverge Influence Area

A weaving segment is defined as a segment in which two or more traffic streams traveling in the same general direction cross paths along a significant length of the freeway without the aid of traffic control devices (except for guide signs). A weaving segment is formed when a diverge segment closely follows a merge segment or a one-lane off-ramp closely follows a one-lane on-ramp and the two are connected by a continuous auxiliary lane. Thus, weaving influence is the base length of a weaving segment plus 500 feet upstream of the entry plus 500 feet downstream of the exit point of a weaving segment. This is shown in Figure 2.2.

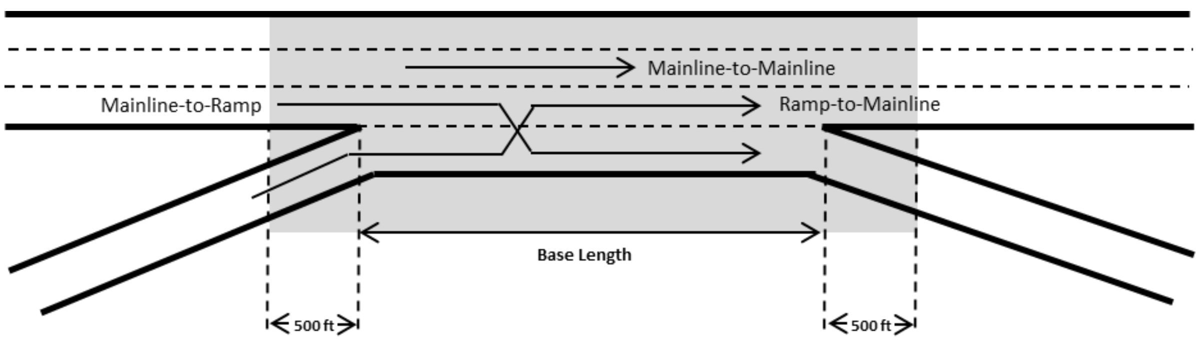

Figure 2.2 Weaving Segment Influence Area

Basic freeway segments are all segments that are not merge, diverge, or weaving segments. Driving behaviors and traffic conditions may differ with respect to each segment type. For example, weaving segments are one of the most complicated segments for drivers to navigate since on- and off-ramp traffic merges and diverges, and weaves may occur in a limited space. Thus, weaving segments may easily become recurrent bottlenecks during peak hours because the capacity of weaving segments is much lower than that of basic segments when controlling for free-flow speed, truck percentage, etc. (HCM, 2000). This may more easily lead to crashes since three different streams of traffic are forced to compete with one another in the limited space and time. Ramp segments are the second most complicated segments that require a great degree of lane-change maneuvers between on- or off- ramps and basic segments. Traffic conflicts are made upstream of off-ramps and downstream of on-ramps in such a way that variation in traffic parameters tends to be high.

The majority of previous studies have been limited in that they sought mainly to identify significant factors leading to crashes in basic segments. Hossain and Muromachi (2012, 2013a, 2013b) studied basic segments and ramp vicinities. They found that the congestion index and the speed difference between upstream and downstream detectors had the biggest impact on the crash frequency on basic segments, while ramp flow had the highest influence in determining crash types within ramp vicinities. Yu and Aty (2013) developed support vector machine models to estimate crash occurrence for basic segments. They found the average speed at downstream detectors, the average speed at crash location, the crash location standard deviation of occupancy, and the crash location standard deviation of flow to be significant factors.

Several studies discovered that the crash mechanisms on various segment types were not the same. Khattak et al. (1998) found that sideswipe crashes were more likely to occur on curved roads with greater numbers of lanes. Lee et al. (2006) showed that the percentage of crashes on curved and straight road sections are different for both sideswipe and rear-end crashes. Since the publication of the first Highway Capacity Manual in 1950, weaving segments have gained much attention for their capacity reduction. However, regarding predicting crash risk, there has only been a meager number of studies conducted. Qi et al. (2014) explored the relationship between geometric design and crashes on weaving segments. Their results showed that shorter segment length, greater required number of lane changes for diverging vehicles, higher diverging traffic flow, and lower merging traffic flow might result in higher crash rates. Wang et al., (2015) predicted crash risk within weaving segments taking into account geometric, traffic, and weather data. They showed that the flow and the speed difference between the beginning and the end of a weaving segment have a significant positive impact on crash risk and the average speed at the beginning of a weaving segment is found to be negatively related to crash risk.

In addition to weaving segments, there have also been several studies on crash risk for ramp segments. Lee and Aty (2006) estimated crash risk on ramp segments and at ramp intersections by using log-linear models. They found that the higher flow and the lower speed would result in higher crash risk. They also found that crash rates on loop and outer connection ramps were higher than on diamond ramps. Hossain and Muromachi (2011) attempted to understand crash mechanisms for five different segments: basic freeway segments, upstream and downstream of off-ramps, and upstream and downstream of on-ramps. While the average and standard deviation of the difference in traffic parameters between adjacent lanes contributed more to crashes for the basic freeway segments, the ramp flow and the variation in speed between upstream and downstream of off-ramps contributed more to crashes. Hossain and Muromachi (2013) employed random multinomial logit models to identify crash prone traffic patterns. The level of congestion and the average speed difference between upstream and downstream traffic best-explained crashes for the basic mainline segments whereas, the ramp flow and the average difference in occupancy between upstream and downstream traffic have the highest influence in crashes within the ramp vicinities. Wang et al., (2015) conducted a real-time crash risk analysis for freeway ramp segments. The results found the logarithm of traffic flow, the average speed, visibility, and the standard deviation of speed to be significant factors for multiple-vehicle (MV) crashes on ramp segments. All studies are summarized in Table 2.2.

Table 2.2 Contributing Factor According to Geometric Characteristics

Author	Geometry	Contributing Factor
Oh et al. (2001)	Basic segments	The standard deviation of speed
Aty et al. (2004)	Basic segments	Upstream average lane occupancy Downstream variation of speed
Pande et al. (2006b) Lee et al. (2006)	Basic segments	Upstream average speed Downstream average speed The downstream difference in occupancy on adjacent lanes Downstream standard deviation of flow and speed
Hossain and Muromachi (2012, 2013a, 2013b)	Basic segments	Congestion index The speed difference between upstream and downstream
	Ramp segments	Ramp flow
Yu and Aty (2013)	Basic segments	Downstream average speed Crash location average speed Crash location standard deviation of occupancy Crash location standard deviation of flow
Qi et al. (2014)	Weaving segments	Shorter segment length More lane changes Higher diverging flow Lower merging flow
Wang et al. (2015)	Weaving segments	Flow and speed difference between beginning and end of weaving segments Average speed at the beginning of weaving segments
Lee and Aty (2006)	Ramp segments	Higher flow Lower speed
Hossain and Muromachi (2011)	Basic segments	Average difference in flow parameters between adjacent lanes The standard deviation of the difference in flow parameters between adjacent lanes
	Ramp segments	Ramp flow

		Variation in speed between upstream and downstream
Hossain and Muromachi (2013)	Basic segments	Level of congestion The average speed difference between upstream and downstream
	Ramp segments	Ramp flow Average difference in occupancy between upstream and downstream
Wang et al. (2015)	Ramp segments	Logarithm of flow Average speed The standard deviation of speed Visibility

The studies above have confirmed that the significant contributing factors to crash risk are distinct depending on segment types and furthermore, that the factors found within each of the types said lacked overall consistency across various studies. Hossain and Muromachi (2013) accentuated that crash mechanism is not generic throughout freeways and that they vary from basic mainline segments to ramp vicinities. Accordingly, crash-prone traffic conditions may change across space on freeways, and crash risk fluctuates along with geometric variation. Therefore, geometric heterogeneity should be taken into account if accurate crash risk predictions are to be made.

2.2.4 Environmental Characteristics

2.2.4.1 Weather Condition

Adverse weather conditions are known to increase crash risk. The crash severity on wet pavement due to rain and on reduced visibility are more likely to end in fatality. Bertness (1980) compared crash frequency and severity under rainy and clear weather conditions using a matched-pair approach. The results showed that crash frequency increased by 100% and the average number of injured persons involved in crashes increased by 70% under rainy weather conditions. Fridstrom et al. (1995) showed that rainy weather increased the monthly injury crash frequency. Keay and Simmonds (2005) also found that the crash risk under rainy weather conditions was 0.7 times larger than that under clear weather condition. Several studies also evaluated the impact of snowy weather on crash frequency. Eisenberg and Warner (2005) investigated the impact of snowfall on crash rate. The results showed that snowfall increased the crash frequency but decreased the risk of fatal and serious injury crashes. Qiu and Nixon (2008) conducted a meta-analysis, which is the statistical procedure for combining data from multiple studies, to evaluate the impact of weather on crashes by generalizing the research findings from previous studies between 1967 and 2005. The research results demonstrated that snowy weather could increase the crash rate by 84% and the injury rate by 75%. Existing studies have proven that adverse weather conditions significantly increased crash rates and injury rates and wet pavement and reduced visibility due to rain or snow marginally increased the crash likelihood. On average, from 2002 to 2012 in the United States, 23% of crashes were weather-related, and 74% of weather-related crashes happened on wet pavement. Meanwhile, weather-related crashes have caused from 94 million to 272 million hours of delay each year.

However, weather conditions have not been universally studied in crash risk prediction. A few studies have considered weather conditions to predict crash risk. Madanat and Liu (1995) first used traffic and weather data together to develop a binary logit prediction model to predict crashes in real-time. They found that visibility and rainfall would affect crash occurrence. Lee et al. (2002) showed that the significant factors affecting the likelihood of crashes were weather conditions, the speed variation along the section, the speed difference across lanes, and the occupancy. Hourdos et al. (2006) built a logistic regression model based on a unique detection and surveillance infrastructure system deployed on a freeway section that has the highest crash rate in Minnesota. The modeling results suggested that certain traffic patterns and weather conditions were good indicators of crash-prone conditions for high crash freeway sections. Ahmed et al. (2013) first used airport weather data in real-time crash risk assessment based on Bayesian logistic regression. The results indicated that the use of airport weather information was a valid method to assess real-time crash risk. Hassan et al. (2013) built a matched case-control logistic regression model to compare traffic parameters on visibility conditions. The results showed that the traffic parameters leading to crash risk are different under clear visibility and reduced visibility. Xu et al. (2013) considered weather conditions as one of the main contributing factors to crash risk and attempted to understand the relationships between traffic parameters and crash risk under the following adverse weather conditions: clear weather, rainy weather, and reduced visibility weather. The analysis showed that traffic parameters contributing to crash risk were different across different weather conditions. The average speed difference between upstream and downstream detector stations had the largest impact on crash risk in reduced visibility weather, followed by that in rainy weather. Therefore, weather conditions should also be included in models seeking to improve crash risk prediction. Of weather conditions, rainfall, snow, and visibility are the most significant factors to be taken into consideration.

2.2.4.2 Pavement and lighting condition

In addition to weather condition, pavement and lighting condition were also found an impact factor on crash risk. Wang et al. (2015) showed that in addition to traffic and geometric factors, wet pavement surface significantly increases the crash ratio by 77% on weaving segments. In another study, they found that wet road surfaces would increase the possibility of an SV (single-vehicle) crash on ramps. The results also found that visibility is a significant factor for the occurrence of SV and MV (multivehicle) crashes on ramps. Kim et al. (2007) found that bad weather increases the probability of fatality by 128%, and darkness with no street lights increases the probability of fatality by 110%. Pai (2011) found that adverse weather, wet roads, and no light streets were most common in rear-end crashes. Mountain and Jarrett (1996) stated that weather, quality of street lighting, and condition of the road surface used in a regression model would have different underlying mean accident frequencies. Stone and Broughton (2003) found that darkness increased the accident incidence rates and fatality rates. Golob (2003) stated that Hit-object collisions and collisions involving multiple vehicles that are precipitated by weaving maneuvers are more likely to occur on wet roads. This finding is consistent with the degradation of vehicle performance characteristics associated with wet road conditions (e.g., braking distance and skidding resistance). Particularly, multiple vehicle collisions caused by weaving maneuvers are more likely to occur on wet roads during daylight than on either dry or wet roads during darkness may be indicative of drivers' overconfidence in both their own and their vehicles' performance capabilities—a confidence that is superseded by the visual limitations imposed by darkness. Conversely, rear-end collisions are more likely to occur on dry roads during daylight, again perhaps reflecting the notion of general driver overconfidence that succumbs to cautions dictated by the adverse weather. Hourdos et al. (2006) used a video capturing technology for detecting and developing an online model of crash-prone conditions. For environmental factors, they examined pavement conditions (e.g., wet or dry), visibility condition (e.g., clear or reduced) and sun position (e.g., night, cloudy, sun in back or side, and sun in front). The outcome showed that wet pavement and reduced visibility due to rain or snow marginally increase the crash likelihood and sun facing the driver strongly increases the crash likelihood. Therefore, in addition to rainfall, snow, and visibility, pavement and lighting conditions should also be taken into consideration on crash risk prediction.

2.2.5 Lack of previous studies

Many studies have put much effort into finding contributing factors depending on crash types, crash severity, and segment types. Various traffic parameters and environmental characteristics were collected and examined to accomplish this. Although each study has made some contributions towards identifying contributing factors with respect to each category, there still exist some deficiencies that remain to be addressed:

- The existing studies have not examined all potential factors synthetically. A crash is an event which occurs as a result of a combination of geometric characteristics and environmental characteristics. The examination of all potential traffic parameters should be conducted based on different segment types and all environmental factors that were studied previously should also be properly integrated so that the most significant contributing factors affecting crash risk can be identified.
- Not all traffic parameters have been employed in the literature. For example, lane-by-lane traffic parameters are considered as a surrogate measure of lane-changing that are associated with sideswipe crashes. The number of trucks is a significant factor that is associated with both sideswipe and rear-end crashes. Ramp flow is a significant factor that has the most impact on crash risk for ramp segments. If possible, all traffic parameters that have been proven to be significant factors in the previous literature should be employed in crash risk prediction. Table 2.3 summarizes the traffic parameters have been considered in previous studies.

Table 2.3 Considered Traffic Parameters

Author	Geometry	Environ mental Cha.	Lane-based traffic parameters	Number of truck	Ramp flow	Surrogate measure of lane-changing
Oh et al. (2001)	Basic segment	X	X	X	X	X
Aty et al. (2004)	Basic segment	X	X	X	X	X
Lee et al. (2006)	Basic segment	X	O	X	X	X
Hossain et al. (2011)	Basic segment	X	X	X	X	O
Yu et al. (2013)	Basic segment	O	X	X	X	O
Hossain et al. (2012)	Basic segment	X	O	X	X	O
Wang et al. (2015)	Weaving segment	X	O	X	X	O
Wang et al. (2015)	Ramp segment	O	X	X	O	X
Lee and Aty (2006)	Ramp segment	X	X	X	O	X
Hassain et al. (2011)	Ramp segment	X	X	X	O	O
Hassain et al. (2012)	Ramp segment	O	X	X	O	X

2.3 *Transferability*

Many studies have developed real-time crash risk prediction models that reveal the relationship between crash risk and the contributing factors. They can help to identify hazardous traffic conditions with high crash risk, and consequently, proactive traffic safety management strategies can be developed to reduce the crash risk evaluated by the crash risk prediction models. Thus, it is needed to build an accurate and reliable real-time crash risk prediction model so that any traffic safety management strategies aiming to reduce the crash risk can be effective.

Many studies have made much effort on building crash risk prediction models and have proved that the models are effective in identifying hazardous traffic conditions. However, one of the key matters is transferability that a developed model needs to be utilized across time and space. Pande et al. (2011) examined the spatial transferability of the crash risk prediction model, which was developed based on data taken from a freeway corridor, and then applied to other freeway corridors. The results showed that the developed model produced a very poor predictive performance for other freeway corridors with different traffic patterns. Shew et al. (2013) developed a crash risk prediction model based on the data collected from the US-101 freeway in California. The predictive performance of the model was tested with the data collected from the nearby I-880 freeway. The results showed that the difference in crash prediction accuracy between the US-101 dataset and the I-880 dataset was as large as 15% for the given false alarm rate. When it comes to contributing factors, Aty et al. (2008) identified different contributing factors for different years at the same location. Table 2.4 summarizes the identified contributing factors at the same location over the years as well as the identified contributing factors at different places along the same segment type.

Table 2.4 Identified Contributing Factors in Different Years and Places

Author	Year	Contributing Factor
Aty et al.	2004	Average occupancy The coefficient of the variance of speed at downstream detectors
Aty et al.	2005	The coefficient of the variance of speed
Aty et al.	2006	The average speed at upstream and downstream detectors The average difference in occupancy between adjacent lanes The standard deviation of flow at downstream detectors The standard deviation of speed at downstream detectors
Aty et al.	2008	The average speed The standard deviation of speed The average flow The standard deviation of flow
Author	**Place**	**Contributing Factor**
Hossain and Muromachi	Japan	The average difference in speed between upstream and downstream detectors
Oh et al	Korea	The standard deviation of speed
Aty et al	FL, USA	The average occupancy The coefficient of the variance of speed at downstream detectors
Chengcheng	CA, USA	The average difference in speed between upstream and downstream detectors The standard deviation of speed at downstream detectors

These results suggest that real-time crash risk prediction models cannot be directly transferred from one freeway to another due to the variability in traffic conditions, driver populations, and geometric characteristics. However, once a model is well-specified to capture the relationship between crash risk and traffic conditions for a freeway, it would be cost-effective to transfer such a model across time and space. The transferability of a crash risk prediction model includes two aspects: spatial transferability and temporal transferability. Spatial transferability involves an application of a crash risk prediction model developed for a freeway to other freeways. Temporal transferability involves an application of a crash risk prediction model developed in the year to the next year at the same freeway.

Several studies have been conducted to improve the transferability of crash frequency prediction models. For example, Hadayeghi et al. (2006) examined the temporal transferability of zonal-level crash frequency prediction models. It is found that the model developed using 1996 data could not be used for predicting crash frequency in 2001. Then, the Bayesian updating approach and calibration factors were used to update the 1996 models. The updated models could produce reasonably good predictive performances on the 2001 samples. Sawalha and Sayed (2006) compared three different methods for improving the transferability of the negative binomial models. A maximum likelihood method was proposed for recalibrating the transferred model. The results showed that the maximum likelihood method was better than the method proposed by the Interactive Highway Safety Design Model (IHSDM). Chen et al. (2011) applied the Bayesian model averaging (BMA) approach to improve the transferability of crash frequency prediction models. The results showed that the BMA approach was superior to conventional model calibration methods. These studies focused on the transferability of aggregate crash frequency prediction models. The studies are limited to predict crash frequency in the next year or at other locations. There are few studies on the feasibility of the transferability on predicting crash risk in real time. Thus, the transferability of real-time crash risk prediction models across time and space is needed to be addressed.

2.4 Crash Risk Index (CRI)

Some quantitative indicators referred to as a crash risk index, which can be used to identify hazardous traffic conditions on freeways directly, have been developed to provide operators and drivers with crash risk information in real time.

Several rear-end crash risk indices have been developed including time-to-collision (Saccomanno et al. (2008); Oh and Kim (2010)), stopping distance index (Oh et al. (2006), (2009)), modified time to collision (Ozbay et al. (2008)), and individual vehicle speeds and headways (Hourdos et al. (2006)). For example, Oh et al. (2006) derived the rear-end crash risk index to quantify the potential for rear-end crashes based on safe stopping distances in situations with a following car, generally associated with rear-end crash scenarios, and further employed it for developing criteria to evaluate levels of rear-end crash risk. The rear-end crash risk index is calculated as the ratio of the number of unsafe car-following events to the maximum possible number of car-following events at freeway detector stations as illustrated in Equation 2.1.

$$RCRI = \frac{number\ of\ rear-end\ conflicts}{exposure} = \frac{\sum_i SDI_i}{N_{car}^{max}(\frac{T}{3600})N_l} \qquad (2.1)$$

Where RCRI is the rear-end collision index, SDI_i is the stopping distance index (0: safe, 1: unsafe), N_{car}^{max} is the maximum number of car-following events per hour (derived from freeway capacity), N_l is the number of freeways lanes, and T is the analysis period(s).

However, this only enables the prediction of rear-end crash risk and is not employable for sideswipe crash prediction. Furthermore, existing detector stations are not capable of extracting individual vehicle's information, so it is difficult to apply such methodology to places where inductive loop detectors are not installed. Li et al. (2014) quantified rear-end crash risk during propagation of kinematic waves in real-time based on the theory that the likelihood of a rear-end crash increases as both spatial and temporal proximities to the tail of an expanding or receding queue become smaller. This can only work to quantify the degree of rear-end crash risk at the end of backward-moving waves, and it is hard to monitor middle of traffic flow that may be affected by external factors, such as lane changes and geometric heterogeneity. Xu et al. (2013) conducted a Fisher discriminant analysis to develop a crash risk index as a method to derive a linear combination of traffic parameters. The discriminant function that transforms a set of traffic parameters into a single discriminant score used to identify hazardous traffic conditions that may lead to a crash occurrence. The crash risk index is expressed by:

$$CRI = d_0 + d_1X_1 + d_2X_2 + \cdots + d_nX_n \tag{2.2}$$

Where CRI denotes the crash risk index, $X_1, X_2, \ldots, X_n$ are traffic parameters existing as independent variables, and $d_0, d_1, d_2, \ldots, d_n$ are discriminant coefficients for the independent variables.

Leur and Sayed (2000) developed a crash risk index that does not rely on crash data. The crash risk index was developed as a driver-based, subjective assessment of the potential road safety risks for in-service roadways. The crash risk index is expressed by:

$$Risk = function\ of\ (exposure, probability, and\ consequence) \tag{2.3}$$

Where exposure is a measure to quantify the "exposure" of road users to potential roadway hazards, the probability is a measure to quantify the chance of a vehicle being involved in a collision, and the consequence is a measure to quantify the severity level resulting from a potential collision.

Exposure is evaluated by the traffic flow that encounters a hazardous road feature and consequence is evaluated as a result of vehicle speed. Each component is collected and calculated depending on participants' subjective responses to a drive-through safety review. Each participant is asked to give a rating of the road safety risk at 45 locations along the route. Oh, et al. (2009) developed a real-time safety index based on the concept of safe stopping distance and time collision. They captured unsafe traffic situations of car-following and lane-changing events based on individual vehicle trajectory data. The safe stopping distance and time to collision (TTC) between leading and following vehicles were used to derive a rear-end collision risk index. Although they were applied to lane-changing events, it is not enough to capture lane-changing associated crash risk. Aty et al. (2007) used a matched case-control logistic regression model to assess crash risk in two separate models using the log odds of significant traffic parameters. One was to determine crash risk during the low-speed flow regime (speed < 37.5mph) and another was to determine crash risk during the high-speed flow regime (speed >= 37.5mph). For example, below is the model for the low-speed flow regime:

$$Crash_{Risk} = 2.64827LogCVSF2 + 0.88842LogCVSF3 + 1.33966LogAOE2 + 0.97766LogAOH3 - 0.43603SVF2 \tag{2.4}$$

Where LogCVSF2 = Log of the standard deviation of the speed divided by the average speed five to ten minutes before the time of interest at the location of interest; LogCVSF3 = Log of the standard deviation of the speed divided by the average speed 10 to 15 minutes before the time of interest at the location of interest; LogAOE2 = Log of the average occupancy 5 to 10 minutes before the time of interest and 0.5 mi upstream of the detector of interest; LogAOH3 = Log of the average occupancy 10 to 15 minutes before the time of interest and one mi downstream of the detector of interest; and, SVF2 = Standard deviation of volume 5 to 10 minutes before the time of interest at the station of interest.

Crash risk cannot be only restricted by speed since a crash is a complicated event affected by multitude factors and the log odds cannot show the constant effect of each parameter on crash risk since the coefficient of parameters could be altered by changes in other parameters. Thus, it is not sufficient to reveal the constant impact of each parameter on the change in crash risk.

2.5 Closure

In summary, this chapter has provided a comprehensive review of existing research efforts that have sought to find significant contributing factors among traffic parameters and environmental characteristics with respect to crash types, crash severity, and segment types. Also, we presented the transferability of developed crash frequency prediction models and suggested the feasibility of the transferability on predicting crash risk in real time. Several crash risk indices have also been introduced in the literature to help operators and drivers receive updated crash risk information as they travel on freeways in real time. Those findings, if properly utilized, could potentially proactively improve traffic safety on freeways.

Although a comprehensive review of identification of contributing factors and crash risk indices that can predict crash risk before crash occurrences have been reported in this chapter, some deficiencies still exist that remain to be overcome.

- All traffic parameters and environmental characteristics that have been proven to affect crash risk before crash occurrence should be collected and employed together in an ideal crash risk prediction model. Traffic parameters include lane-by-lane parameters, number of trucks, ramp flow, and fundamental traffic data that come from detectors and environmental characteristics include rainfall, snow, visibility, pavement, and lighting conditions.
- It is required that the identification of contributing factors should be analyzed separately under different segment types.
- Previous studies showed that a crash prediction model developed is hard to be transferred to other places and time periods due to distinct contributing factors depending on places and time periods. Therefore, it is desirable to establish a generalized procedure as a tool

for identifying contributing factors and developing a crash risk index so that appropriate proactive traffic safety strategies could be implemented aiming at reducing the crash risk.

- The crash risk indices developed and reported in the literature were only capable of predicting rear-end crashes and were made using the trajectory of individual vehicles which cannot be extracted from ordinary detectors. If a crash risk index that could predict the risk of any crash type in real time could be developed, it would be more helpful to operators and drivers.

Chapter 3 Establishment of a Generalized Framework

3.1 Introduction

This chapter proposes a generalized framework that is a procedure to identify contributing factors and to develop a crash risk index. In response to the deficiencies identified in the literature review, the proposed generalized framework intends to incorporate geometric characteristics, traffic parameters, and environmental characteristics together; and to develop a crash risk index that quantifies crash risk for the impending crash occurrence. The details of each component in the generalized framework are presented in the remaining sections.

3.2 Major Research Features

This study aims to develop a generalized framework that can be applied to any freeways to identify significant contributing factors affecting crash risk under different segment types. It also aims to develop a crash risk index that estimates the degree of crash risk on a target segment, so that appropriate proactive traffic safety management strategies are implemented to reduce the high crash risk on the segment. Some major features that will be included in this study are listed below:

- Identification of significant factors according to each segment type.
- Taking into account all potential traffic parameters which have been proven to be significant factors in the previous studies.
- Developing a crash risk prediction model.
- Developing a crash risk index based on the crash risk prediction model above, and applying it to monitor crash risk on segment-based freeways.
- Updating the crash risk prediction models

3.3 Generalized Framework

Figure 3.1 depicts a comprehensive framework for the generalized procedure including data collection, identifying contributing factors, building a Bayesian random intercept logistic regression model, developing a crash risk index, monitoring crash risk, and updating the model.

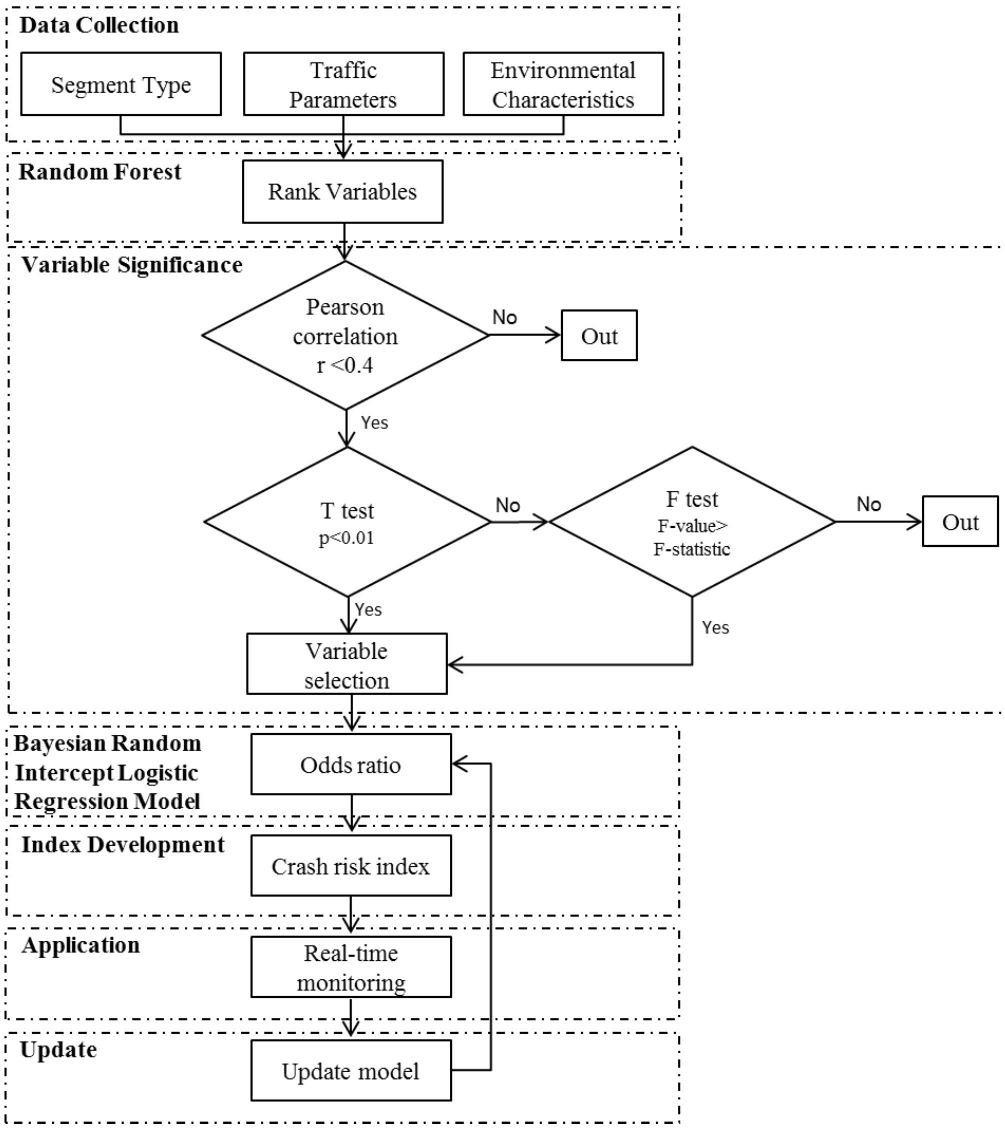

Figure 3.1 A Framework of the Generalized Procedure

3.3.1 Data Collection

3.3.1.1 Geometric Characteristics

As mentioned in Chapter 2, according to HCM (2010) a freeway is classified into basic segments, weaving segments, and merge and diverge segments. The merge and diverge segment can be combined into ramp segments. HCM presents a different methodology for the level of service and capacity with respect to each segment type because the patterns of several moving traffic streams are different in each segment. Accordingly, the hazardous traffic conditions can also be expected to differ depending on geometric type such that ramp segments can be affected by ramp flow and weaving segments can be affected by outgoing traffic streams and incoming traffic streams. Thus, it is desirable that each type should be studied separately. Particularly, basic segments can be classified into a curved segment (0 < radius of curvature <= 3000 ft), a straight segment, and a rolling segment. The curvature of road segments reflects the level of difficulty in lane changing maneuvers and rolling segments reflect different acceleration capabilities of different vehicle types influencing car-following and lane changing maneuvers as well. Thus, due to the different traffic patterns and driving behaviors on each segment type, the traffic conditions affecting crash risk are expected to be different.

Therefore, this study classifies freeway segments into five segment types: basic straight segments, basic curved segments, basic rolling segments, weaving segments, and ramp segments. Essentially, a segment is defined from one upstream detector station to one downstream detector station since previous studies have shown that changes in traffic parameters between an upstream and a downstream detector station contribute significantly towards generating hazardous traffic conditions. Thus, the traffic data extracted from the two detector stations are utilized for analysis. Fig 3.2 illustrates the split of a certain length of a freeway into one of five segment types, and each type constitutes one upstream detector station and one downstream detector station.

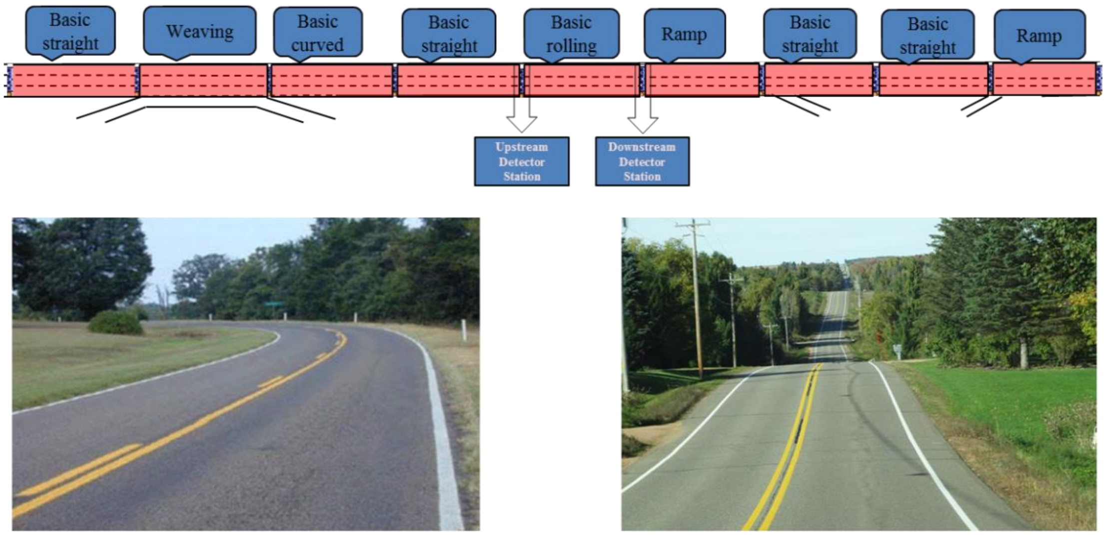

Basic curved segment

Basic rolling segment

Figure 3.2 Five Segment Types

3.3.1.2 Traffic Parameters

According to the collection of effective traffic parameters affecting crash risk from previous studies, 34 traffic parameters have been proven to be significant in predicting crash risk. Hence, all these 34 traffic parameters should be collected as candidate variables for selecting contributing factors as shown in Table 3.1. To collect the traffic data at crash times, traffic data were extracted in the time interval between 5 and 10 min before the crash occurrence times. For example, if a crash occurred at 8:15 PM, the considered traffic data is from 8:05 to 8:10 PM. The purpose of this is to compensate for any inaccuracies in the reported crash occurrence time (Christoforou et al. (2010); Golob and Recker, (2004)). It also helps to identify hazardous traffic conditions ahead of crash occurrence time to make preemptive countermeasures possible (Pande et al., 2011; Xu et al., 2013c). Wang et al. (2015) compared traffic data extracted 5-10 min and 0-5 min before the crash occurrence time. The traffic data extracted 0–5 min before crash occurrences could more accurately describe crash-prone conditions. While, the traffic data extracted 5–10 min before crash occurrence could provide sufficient time for the traffic management center to analyze, react, and provide warnings to drivers. The crash times were typically recorded as the time when drivers called the police or emergency services. Hence, the recorded crash times were actually the times after crash occurrences. If the 0–5 min traffic data are used, some traffic conditions would already have been impacted by the crashes and would no longer be crash-prone conditions. Therefore, the traffic data extracted 5–10 min before the recorded crash times are not yet influenced by the crashes.

In a matched case-controlled dataset, the traffic data before the crashes are taken as cases while non-crash traffic data are taken as controls. In this study, the factors used to match cases and controls are location, direction, the day of the week, and data collection time. Using these matching factors, five non-crash traffic data for a given crash traffic data are randomly collected. In the matched case-controlled study design, a typical case-to-control ratio of 1:5 has been widely accepted. There were some trials where the ratio of case to control was 1:3, 1:4, or 1:5. In these instances, statistical power generally increased as the ratio changed from 1:3 to 1:5, but it was found that the statistical power did not increase significantly beyond a case-to-control ratio of 1:4. Hence, this study uses a case-to-control ratio of 1:5. Five non-crash traffic data that are taken at the same time period and same day of the week of each crash event are collected for comparison with crash-prone traffic conditions.

This study focuses only on the crashes that occurred during peak periods, 06:00 AM – 09:00 AM and 04:00 PM – 07:00 PM, to minimize the confounding effects of external factors other than hazardous traffic conditions. Previous studies suggested that crashes which occurred during the evening and early morning when traffic volume is quite low were more closely related to some other factors such as human errors rather than traffic conditions (Aty and Pande, 2005). This study also focuses on the crashes during weekdays (Monday to Thursday) and crashes on holidays are excluded from further analysis because those traffic patterns are often irregular in comparison to normal weekdays, making it difficult to observe regular non-crash traffic conditions.

Table 3.1 Collected Traffic Parameters

Basic traffic parameter		Lane-based traffic parameter	
Upstream	Downstream	Upstream	Downstream
The average speed	The average speed	The average difference in speed between lanes	The average difference in speed between lanes
The average flow	The average flow	The average difference in flow between lanes	The average difference in flow between lanes
The average occupancy	The average occupancy	The average difference in occupancy between lanes	The average difference in occupancy between lanes
The standard deviation of speed	The standard deviation of speed		
The standard deviation of flow	The standard deviation of flow		
The standard deviation of occupancy	The standard deviation of occupancy		
The average difference in speed between upstream and downstream detector stations			

The average difference of flow between upstream and downstream detector stations			
The average difference of occupancy between upstream and downstream detector stations			
Surrogate measures of lane-changing maneuver		**Others**	
Upstream	Downstream	Upstream	Downstream
OAFR	OAFR	The average ramp flow	The average ramp flow
The coefficient of variation in speed	The coefficient of variation in speed	Congestion index	Congestion index
The coefficient of variation in flow	The coefficient of variation in flow	The average number of truck	The average number of truck
The difference of CVS between upstream and downstream			

A total of 34 traffic parameters are collected, including the averages and the standard deviations of basic traffic parameters (e.g., flow, speed, and occupancy), the difference in basic traffic parameters between adjacent lanes, as well as the difference in basic traffic parameters between upstream and downstream stations. In addition to basic traffic parameters, several indices are also calculated to represent certain traffic flow characteristics. Overall average flow ratio (OAFR) represents the total number of lane changes in all lanes. OAFR is computed by:

$$AFR_i(t) = \frac{\frac{v_i(t)}{v_{i-1}(t)} \times NL_{i,i-1}(t) \times \frac{v_i(t)}{v_{i+1}(t)} \times NL_{i,i+1}(t)}{NL_{i,i-1}(t) + NL_{i,i+1}(t)} \tag{3.1}$$

where

$AFR_i(t)$ = the average flow ratio in subject lane i during time interval t (representing lane change from lane i to adjacent lanes i-1 and i+1);

$v_i(t)$ = the average flow in subject lane i during time interval t (vehicles/unit time);

$v_{i-1}(t)$ = the average flow in inner lane (i-1) adjacent to lane i, if lane i-1 exists, during time interval t (vehicles/unit time);

$NL_{i,i-1}(t)$ = the number of lane changes form lane i to i-1, if lane i-1 exists, during time interval t;

$v_{i+1}(t)$ = the average flow in outer lane (i+1) adjacent to lane i, if lane i+1 exists, during time interval t (vehicles/ unit time); and

$NL_{i,i+1}(t)$ = the number of lane changes form lane i to i+1, if lane i +1 exists, during time interval t.

$$\begin{aligned} \text{OAFR(t)} &= \sqrt[n]{AFR_1(t) \times AFR_2(t) \times \cdots \times AFR_n(t)} \\ &= [\textstyle\prod_{i=1}^{n} AFR_i(t)]^{1/n} \end{aligned} \tag{3.2}$$

Where OAFR(t) is the overall AFR in all lanes during time interval t and n is the number of lanes. The coefficient of variation in speed (CVS) represents the standard deviation of speed divided by the average speed. This measure is designed to account for the tendency for increased variation in speed with increased average value. The coefficient of variation in flow (CVF) represents the tendency for increased variation in flow with increased average value. The congestion index represents the congestion conditions on a roadway and is computed by:

$$Congestion\ Index\ (CI) = \frac{FF - Actual_{sp}}{FF}, FF = 85^{th}\ percentile\ speed \qquad (3.3)$$

Furthermore, the average ramp flow which represents traffic conditions on ramp segments and the average number of trucks that is associated with sideswipe crashes are collected.

3.3.1.3 Environmental Characteristic

3.3.1.3.1 Weather condition

Weather data are collected to capture the impact of weather conditions on the change in crash risk. The weather data are obtained from the www.wunderground.com website, which provides hourly weather information from weather stations across the United States. Weather data for each crash case are extracted from the closest weather station. The weather data collected are rainfall, snow, and visibility.

3.3.1.3.2 Pavement and lighting condition

Pavement condition is categorized as dry and wet. Wet pavement is considered if at least light rain is continued for 30 minutes before a crash occurred. Note that light rain is less 0.1 inch. Also, lighting condition is categorized as daylight, dark with streetlights and dark with no streetlights. As the previous studies revealed, pavement and lighting condition influence the crash severity.

3.3.2 Random Forest

Random Forest (RF) is one of the most recent and promising machine learning techniques. Random Forest is a refinement of bagged trees. The term came from random decision forests that was first proposed by Ho (1998). It combines Breiman's "bagging" idea and Ho's "random subspace method" to establish a collection of decision trees with controlled variations (Breiman, 2001). A single decision tree suffers from high variance or bias. In contrast, Random Forest offers unbiased estimates of classification error as trees are added to the forest. Also, the Law of Large Numbers guarantees that Random Forest is robust against over-fitting. The main idea of Random Forest is that every tree is built using a deterministic algorithm based on two factors. First, at each node, the best split is chosen from a random subset of the predictors rather than all of them to determine the splitting decision. Second, every tree is built using a bootstrap sample of the observations.

The Random Forest procedure eliminates the need for dividing the data into training and validation sub-datasets because when a particular tree is grown from a bootstrap aggregate sample, one-third of the cases are left out and not used in the development of the tree. These cases are called out-of-bag (OOB) data. This OOB data becomes the validation dataset which is used to obtain an unbiased error estimate as well as estimates of variable importance. To test whether the attempted number of trees is sufficient to reach relatively stable results, a plot of OOB error rate against various tree numbers is developed. The best number of trees is that which has the minimum error rate along with a similar constant error rate (Breiman (2001); Pang et al. (2006); Grimm et al. (2008); Kuhn et al. (2008)). Proposed by Breiman (2001), it is well known for ranking variables based on importance from a given set of variables.

The Random Forest algorithm estimates the importance of a variable by the total decrease in node impurities denoted by the Gini coefficient from splitting on the variable, averaged over all trees. Note that the Gini coefficient is a measure of how each variable contributes to the homogeneity, from 0 (homogeneous) to 1 (heterogeneous), of the nodes and leaves in the resulting random forest. In this study, the Random Forest technique is employed using the R program. The R program provides a mean decrease Gini “IncNodePurity” diagram for selecting the important variables affecting the binary target variable. Using the Gini coefficient, the quality (Node Purity) of a split for every variable (node) of a tree is measured. Every time a split of a node is made on a variable m, the Gini impurity criterion for the two descendant nodes is less than the parent node. Thus, adding up the Gini decreases for each variable over all trees in the forest provides a quantitative value of variable importance. More important variables result in nodes with higher purity and have a higher decrease in Gini. A higher IncNodePurity implies a higher variable importance (Kuhn et al., 2008). The major steps of the Random Forest algorithm are as follows:

1. Let L be the complete dataset with M variables and N records, and let B be the total number of Classification and Regression Trees (CART) trees in the RF. Let L_b be the b^{th} bootstrap sample created by randomly selecting n samples with replacement from L. The rest of the data, that is, L$-L_b$, are called the out-of-bag data (OOB) of the b^{th} bootstrap sample.
2. Next, for the b^{th} tree T_b, instead of growing a CART tree with M variables, m variables are randomly selected from M variable space at every node, and the best splitter among m capable of producing two maximum pure nodes is used to split the node at each level.
3. For estimating OOB error rate, at every bootstrap iteration the L $- L_b$ datasets are used to calculate the misclassification rate r_b of tree T_b. This is achieved by running down the L–L_b dataset into T_b grown in Step 2. The class of each of the data points is decided according to majority voting (which can be weighted). Last, the r_b of all the B trees are aggregated to calculate the OOB error rate.
4. Variable importance in RF differs from conventional statistical approaches. Here, it is measured by permuting the values of each variable (one variable at a time) and then calculating the new error rate. The permuted variable with the highest error rate is considered the most important variable, as any error in measuring its value has the highest impact on the classification performance of RF.

One of the practices of Random Forest in real-time traffic safety evaluation is to estimate variable importance. In this study, a cut-off purity value is used to choose the most important covariates affecting the binary target variable (crash versus non-crash). Initially, the cut-off purity value is used to remove less important variables. However, this study only uses the cut-off purity value as a tool for ranking all variables, and all the ranked variables are used for analysis. The reason is that less important variables will also impact the generation of hazardous traffic conditions and any variables affecting crash risk thus cannot be ignored. The resulting ranked variables are used as inputs in the next step.

3.3.3 Variable Significance

3.3.3.1 Pearson Correlation Test

Correlations between two variables are a measure of how much they are related. As a known problem, the accuracy of a result can be reduced if some or all of the independent variables are correlated. The most common measure of correlation in statistics is the Pearson Correlation Coefficient. It shows the linear relationship between two sets of data. It has a value between +1 and −1, where 1 is a total positive linear correlation, 0 is no linear correlation, and −1 is a total negative linear correlation. For two independent variables, x and y, the coefficient of r is computed by

$$r = \frac{n\sum x_i y_i - \sum x_i \sum y_i}{\sqrt{n\sum x_i^2 - (\sum x_i)^2}\sqrt{n\sum y_i^2 - (\sum y_i)^2}} \tag{3.4}$$

This study uses the Pearson Correlation Coefficient. If two variables are found to be highly correlated, (coefficient >0.4 or coefficient <-0.4) the variable with the higher rank is chosen for further analysis and the variable with the lower rank is removed.

3.3.3.2 T-test

For each chosen variable from Pearson Correlation test, T-test assesses whether the averages of it at crash-occurred traffic conditions and non-crash traffic conditions are statistically different from each other at the significance level of 0.01. The formula for the t-test is in Equation 3.5.

$$t = \frac{\bar{X}_{crash} - \bar{X}_{noncrash}}{\sqrt{\frac{\sigma_{crash}}{n_{crash}} + \frac{\sigma_{noncrash}}{n_{noncrash}}}} \tag{3.5}$$

The numerator of the ratio is the difference between the averages of the two groups. The denominator is a measure of the variability or dispersion of the values. The denominator of this ratio is known as the standard error of the difference. The T-test is used to determine statistical significance between two sets of data, or in this case, indicating whether the chosen explanatory variables are significantly different in crash and non-crash traffic situations. Therefore, the variables in cases where the T-test yields a p-value of less than 0.01 are chosen as final contributing factors and the variables where the p-value is greater than 0.01 are further examined in the next step.

3.3.3.3 F-test

The t-value measures the size of the difference between averages relative to the variation of two groups. In other words, larger variation can make t-values lower so that the t-test can turn out to be insignificant. Crashes are events resulting from variation in traffic parameters. Thus, the variables that turned out to be insignificant from the T-test are examined with F-test again to see whether the variances of the two groups are different. An F-test compares the ratio of two variances. If the variances are equal, the ratio of the variances will be equal to 1. Therefore, if the calculated F-value of the variable is greater than the F critical value from an F table, it is chosen as a final contributing factor, and if not, the variable is removed.

3.3.4 Bayesian Random Intercept Logistic Regression Model

This study utilizes Bayesian random intercept logistic regression to develop the real-time crash risk prediction models according to five segment types on freeways. The purpose of using this statistical approach is to explore the effects of traffic parameters and environmental factors selected on five freeway segment types while controlling for the effects of other factors such as crash time (i.e., peak hours) and geometric characteristics (i.e., basic straight, basic curved, basic rolling, weaving, and ramp segments).

The Bayesian logistic regression model extends conventional logistic regression model to a Bayesian framework by adding a prior distribution of each parameter to the model. Coefficients of each parameter in a Bayesian logistic regression model are estimated based on prior information available and observed data. In contrast to the fixed parameters estimated by the maximum likelihood estimation (MLE), the Bayesian logistic regression model regards parameters as random variables. It provides full uncertainty of the parameters via posterior distribution. Also, Bayesian regression modeling has an advantage of avoiding an over-fitting problem caused by a limited number of training data with large feature size (Helai, Chor, & Haquea, 2008; Lee et al. 2011; Mitra & Washington, 2007). Logistic models and their extensions have been widely used in real-time safety studies with data from different sources, such as loop detectors (Abdel-Aty et al. 2004), microwave radar sensors (Yu et al. 2013), Automatic Vehicle Detection (AVI) data (Abdel-Aty et al. 2012; Ahmed and Abdel-Aty, 2012), and vehicle trajectory data (Oh and Kim, 2010).

Since crashes are naturally random events and are affected by numerous factors, in addition to traffic parameters and environmental characteristics, other factors might also have significant impacts on crash risk, such as driving behaviors, vehicle types, and drivers’ mistakes. To account for the heterogeneity in the dataset, the Bayesian random intercept logistic regression is adopted for predicting real-time crash risk under five segment types. In the Bayesian random intercept logistic model, the constant can be written as:

$$\beta_{0i} = \beta_0 + u_{0i},\ i = 1,2, \dots , n \tag{3.6}$$

where u_0 is a randomly distributed term. In this study, the random coefficient u_0 is specified to be normally distributed with mean zero and variance $\sigma^2, e.g. u_0 \sim N\ (0, \sigma^2)$. Hence, Bayesian random intercept logistic regression can be written as:

$$y_i \sim Bernoulli(p_i)$$

$$\text{logit}(p_i) = \beta_{0i} + \beta_1 x_{1i} + \beta_2 x_{2i} + \beta_3 x_{3i} + \dots + \beta_k x_{ki} \tag{3.7}$$

where y_i represents the crash indicator (= 1 if a crash occurred, and 0 otherwise) for the ith observation in the sample, p_i denotes the crash probability for the ith observation, x_{ki} denotes the value of variable k for the sample i, β_{0i} is the random intercept and β_k is the coefficient of variable k. The likelihood function can be written as:

$$\text{f}(Y|\beta) = \prod_{i=1}^{n} P_i$$

$$= \prod_{i=1}^{n}\left[\left(\frac{e^{\beta_{0i}+\beta_1 x_{1i}+\beta_2 x_{2i}+\dots+\beta_k x_{ki}}}{1+e^{\beta_{0i}+\beta_1 x_{1i}+\beta_2 x_{2i}+\dots+\beta_k x_{ki}}}\right)^{y_i}\left(1-\frac{e^{\beta_{0i}+\beta_1 x_{1i}+\beta_2 x_{2i}+\dots+\beta_k x_{ki}}}{1+e^{\beta_{0i}+\beta_1 x_{1i}+\beta_2 x_{2i}+\dots+\beta_k x_{ki}}}\right)^{(1-y_{i})}\right] \tag{3.8}$$

A Bayesian inference approach based on the Markov Chain Monte Carlo (MCMC) method is adopted to simulate the posterior distribution of β. The estimates of the mean, standard deviation, and quartiles of the parameter of each explanatory variable can be determined by the posterior distribution provided by the Bayesian approach. Based on the specification of Bayes' theorem, the posterior distribution of parameters can be estimated using the following function:

$$\text{f}(\beta|Y) = \frac{f(Y,\beta)}{f(Y)} = \frac{f(Y|\beta)\pi(\beta)}{\int f(Y,\beta)\mathrm{d}\beta} \propto f(Y,\beta)\pi(\beta) \tag{3.9}$$

where $f(Y|\beta)$ denotes the posterior joint distribution of parameters β conditional on dataset Y. $f(Y,\beta)$ represents the joint probability distribution of dataset Y and model parameters β. $f(Y|\beta)$ is the likelihood conditional on parameters β, specified by Equation 3.8. Function π(β) is the prior distribution of parameter β. The selection of the prior distribution can include: (a) informative prior distributions if something is known about the unknown parameters based on experts' knowledge or existing research; or (b) non-informative prior distributions if little is known about the unknown parameters. This study uses the non-informative prior distributions for each parameter. The usual prior distributions with large variances can be used for the non-informative prior distributions, hence adopting an expression of prior ignorance for each parameter. The following non-informative prior distributions are used:

$$\beta \sim \mathrm{N}(0_k, 10^6 I_k) \tag{3.10}$$

where 0_k is a k x 1 vector of zeros; I_k is a k x k identity matrix. β follows a normal distribution. Based on the specification of the prior distributions for parameter β, the posterior distribution $\mathrm{f}(\beta|Y)$ can be derived as:

$$\mathrm{f}(\beta|Y) \propto f(Y, \beta)\pi(\beta)$$

$$\propto \exp\left\{\sum_{i=1}^{N}(\beta_0 + \beta_1 x_{1i} + \beta_2 x_{2i} + \cdots + \beta_k x_{ki})y_i - \sum_{i=1}^{N} log\left[1 + e^{\beta_0+\beta_1 x_{1i}+\beta_2 x_{2i}+\cdots+\beta_k x_{ki}}\right] - \frac{1}{2}\frac{(\beta_0)^2+(\beta_1)^2+\cdots+(\beta_k)^2}{10^6}\right\} \tag{3.11}$$

To generate realizations from the posterior joint distribution $\mathrm{f}(\beta|Y)$, the Metropolis-Hasting sampling approach sequentially draws parameters from Equation 3.11. The inference can then be made on the basis of the remaining draws after discarding the draws during the burn-in period.

3.3.4.1 Predictive Performance

In this study, a model with a binary outcome (crash = 1 and non-crash = 0) classifies an observation as a crash if the predicted crash risk of the observation exceeds a pre-specified threshold. Otherwise, it will be classified as a non-crash. The predictive performance of a model with a binary outcome can be measured with two complementary indicators: the true positive rate (sensitivity) that is the proportion of events correctly predicted as a crash, and the true negative rate (specificity) that is the proportion of non-events correctly predicted as a non-crash. Both sensitivity and specificity depend on the threshold value. The Receiver Operating Characteristic (ROC) curve is frequently used to evaluate the predictive performance of models with binary outcomes (Ahmed et al. 2012; Xu et al. 2013a, c). The ROC curves illustrate the relationship between the sensitivity and the false alarm rate (1-specificity) for various thresholds. To develop a ROC curve, one needs to calculate the sensitivity and the false alarm rate for multiple thresholds. The area under the ROC curve (AUC) can be used as an evaluative measure of the predictive performance. The AUC falls between 0 and 1. A larger AUC indicates a better predictive performance.

3.3.4.2 Odds Ratio

Odds are defined as the probability of an outcome occurring divided by the probability of an outcome not occurring, i.e., $P(Y = 1)/(1-P(Y = 1))$. Odds ratio represents the odds that an outcome will occur given a particular predictor, compared to the odds of the outcome occurring in the absence of that predictor. Odds ratios are most commonly used in case-control studies. When a logistic regression is calculated, regression coefficient (b1) represents the estimated increase in the log odds of the outcome per unit increase in the value of the predictor. In other words, the exponential function of the regression coefficient (e^{b1}) is the odds ratio associated with a one-unit increase in the predictor. Odds ratios are used to compare the relative odds of the occurrence of the outcome of interest (i.e., crash occurrence), given predictors (e.g., traffic parameters, environmental characteristics). The odds ratio can also be used to determine whether a particular predictor is a risk factor for a particular outcome, and to compare the magnitude of various risk factors for that outcome;

OR = 1: Predictor does not affect odds of the outcome

OR>1: Predictor associated with higher odds of the outcome

OR<1: Predictor associated with lower odds of the outcome

In this study, the odds ratio for each contributing factor is defined as the relative amount by which the odds of the outcome (crash occurrence) increase or decrease when the value of the contributing factor is increased by 1 unit while the other factors are kept fixed. In other words, the odds ratio represents the constant effect of a contributing factor X on the likelihood that one outcome will occur.

In general, change in outcome occurrence is described with probability or odds ratio. However, Probability and odds have different properties that give odds some advantages in statistics. For example, in logistic regression, the odds ratio represents the constant effect of a predictor X on the likelihood that one outcome will occur and the logistic regression model often wants a measure of the unique effect of each predictor X on the outcome. If we try to express the effect of X on the likelihood of a categorical outcome having a specific value through probability, the effect is not constant. What that means is there is no way to express in one number how the predictor X affects the categorical outcome in terms of probability. The effect of the predictor X on the probability of the outcome has different values depending on the value of the predictor X. While it is generally preferable to use probabilities because they're intuitive, they are just not going to be able to describe that effect in a single number. The odds ratio is a single summary score of the effect, and the probabilities are more intuitive. When the predictor X is continuous, the odds ratio is constant across values of X, but probabilities aren't. This logic works exactly the same way as interest rates. Assume that an annual interest rate is 8%. An investor would earn $8 if he or she invested $100, or $40 if he or she invested $500 at the end of the year. The rate stays constant, but the actual amount earned differs based on the amount invested. Odds ratios work the same. An odds ratio of 1.08 will give an 8% increase in the odds at any value of predictor X. Likewise, the difference in the probability depends on the value of predictor X. So if we decide to report the increase in probability at different values of predictor X, we will have to do it at low, medium, and high values of predictor X. We can't use a single number on the probability scale to convey the relationship between the predictor and an outcome. This study uses odds ratios to evaluate the impacts of each contributing variable on crash risk.

3.3.4.3 WinBUGS

The WinBUGS software package is used to specify the Bayesian random intercept logistic regression models. WinBUGS software is developed by the Bayesian inference Using Gibbs Sampling (BUGS) project (BUGS 1996-2008). This group was concerned with flexible software for Bayesian analysis of complex statistical models using Markov Chain Monte Carlo (MCMC) methods. Bayes' key contribution is to use a probability distribution to represent all the uncertainty involved in the event space. Three parallel MCMC chains are constructed in WinBUGS for each Bayesian random intercept logistic regression model. Each MCMC chain consists of 10,000 iterations, including an initial "burn-in" of 2,000 iterations. The estimations of each parameter's non-informative prior distributions are used as the initial values. The convergence of the posterior distribution samples is checked by the visual inspection of the trace plots, posterior density plots, and autocorrelation function plots.

3.3.4.4 Model Validation

The whole dataset is split into training and scoring datasets. For the training dataset, 70% of the original dataset is used for model development, and 30% of it is used to evaluate crash risk.

3.3.5 Crash Risk Index Development

A quantitative indicator that can directly show the degree of crash risk on a segment in real time is developed. Crash risk index (CRI) is formulated by three components including odds ratios of contributing factors obtained from the Bayesian random intercept logistic regression models, 5-

min interval historical non-crash traffic data, and 5-min based current traffic data. The CRI is written as:

$$CRI_i^k = \sum Odds\ ratio_N^k \cdot (N_{current\ 5min}^k - N_{non-crash\ 5min}^k) \qquad (3.12)$$

where CRI is crash risk index, k is the segment types (1 = basic straight segments, 2 = basic curved segments, 3 = basic rolling segments, 4 = weaving segments, and 5 = ramp segments), i is the 5-min time period, and N is the contributing factor.

It should be noted that the components of crash risk index are different for different freeways and therefore, for each freeway, a crash risk index must be developed that is suitable for that freeway based on its characteristics.

3.3.6 Update

The Bayesian updating approach is used to improve the temporal transferability of the crash risk prediction models built in this study. This approach can update an old model as new data become available. Assuming that a real-time crash risk prediction model has been developed based on the historical sample Y1 and that a new sample Y2 is then obtained, the posterior distribution can be updated using Bayes' theorem as follows:

$$\pi(\beta|Y_1, Y_2) \propto f(Y_1, Y_2|\beta)\pi(\beta) = f(Y_2|Y_1, \beta)\, f(Y_1|\beta)\pi(\beta) \propto f(Y_2|\beta)\pi(\beta|Y_1) \qquad (3.13)$$

Thus, when updating a crash risk prediction model, the estimation results of the old model developed by the sample Y1 can be used as the informative prior distribution $\pi(\beta|Y_1)$ and can be incorporated into new sample Y2 in a new updated posterior distribution. The main difference between updating an existing model and developing a new Bayesian random intercept logistic regression model lies in the specification of the prior distributions shown in Eq. 3.10. When updating an existing model, the prior distributions shown in Eq. 3.10 are replaced with the informative prior distribution $\pi(\beta|Y_1)$ that are obtained from the existing model developed by data Y1. Based on the new data Y2, the same Metropolis–Hasting sampling approach can be used to estimate the parameters for the updated model. It is obvious that the Bayesian updating approach provides an easy-to-use mechanism to update an existing crash risk prediction model.

3.4 Closure

This chapter proposed a generalized framework to define and analyze these complex and interconnected relationships that can help transportation professionals to better identify hazardous traffic conditions with high crash risk before crashes occur. The generalized framework is globally applicable for the identification of significant contributing factors affecting crash risk and for the evaluation of the distinct impact each factor has on the change in crash risk. It has described each part of the generalized framework from data collection to updating a Bayesian random intercept logistic regression model. 34 traffic parameters are examined combined with five environmental data according to five segment types so that each segment type has its own particular contributing factors. Random Forest and the three statistical analysis tests can be used to select the most appropriate contributing factors. The resulting odds ratios from Bayesian random intercept logistic regression models can be utilized to develop a crash risk index. The crash risk index is expected to monitor traffic conditions for predicting high crash risk per a unit of the segment in real time.

Chapter 4 Development of A Crash Risk Index and Real-Time Crash Risk Monitoring

4.1 Introduction

This chapter presents an actual application of the proposed generalized framework to a 13.14-mile segment on the northbound direction of the I-110 freeway in California. Each section describes how each component of the generalized framework has been applied in practice. This Chapter aims to develop a crash risk index as an indication of high crash risk for impending crash occurrence and to show the application of it in the real world. Lastly, section 4.7 shows how the crash risk pattern appears before the crash occurs. The details of the results are presented in the remaining sections.

4.2 Data Collection

For a given crash event, the paired traffic, geometric, weather, pavement, and lighting condition data were collected from a 13.14-mile segment in the northbound direction of the I-110 freeway in California. There are 28 loop detector stations with an average spacing of 0.4 miles and two weather stations within the selected segments. The collected data covers the entire 2015 period. A total of 342 crashes were identified and used in this study.

The aggregated 5-min average speed, flow, and occupancy data for each lane were collected from the Highway Performance Measurement System (PeMS) maintained by the California Department of Transportation (Caltrans). The traffic data were extracted from the two nearest detector stations of the crash locations: one upstream station and one downstream station. For each crash in the dataset, the traffic data for a 5-min period ending 5 min to 10 min before the crash time was collected. The non-crash traffic data during a 5-min period sharing the same time and day of the week were also collected. These were extracted from other weeks during the study period when crashes did not occur within one hour before and after that given crash time. It is expected that the 5-min gap from the crash time will compensate for any delay in reporting the exact crash time. For example, if a crash occurred at 8:15 PM, the considered traffic data were collected from 8:05 to 8:10 PM. The purpose of doing so is to detect high crash risk ahead of the crash time. It should be noted that the reported crash times were adjusted according to abrupt changes in traffic parameters such that a sudden decrease in speed and sudden increase in occupancy at the upstream station of the crash location happen together.

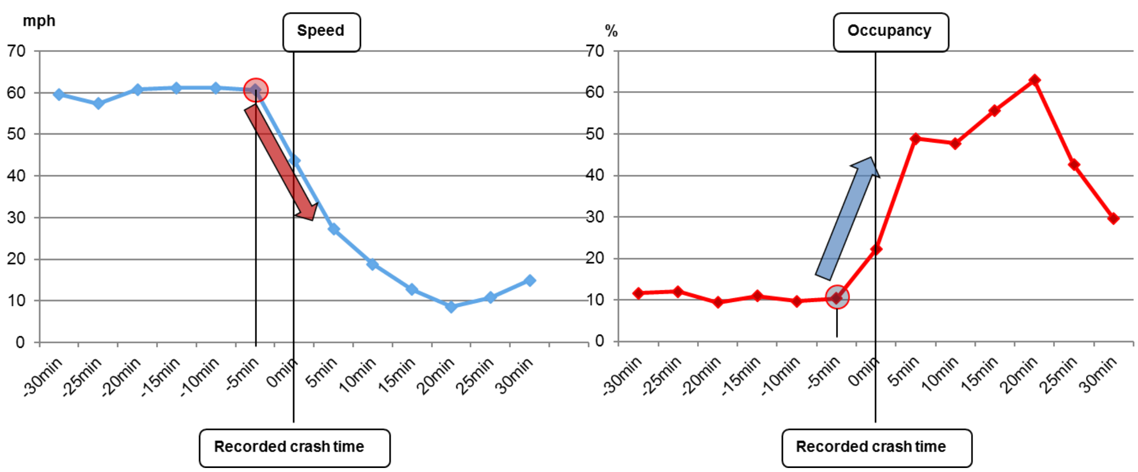

Figure 4.1 Adjustment of the Reported Crash Time

As shown in Figure 4.1, the speed started to drop 5 minutes before the reported crash time, and the occupancy started to increase 5 minutes before the reported crash time. Thus, the actual crash time was adjusted from 3/18/2015, 17:26 to 3/18/2015, 17:21. In this way, the actual crash times for all crash events were adjusted by combining the reported crash times and traffic data collected from upstream stations. If there was no significant abrupt change in speed and occupancy together, the reported crash time was used for further analysis. As a result, there was on average a 5.1 min difference between the reported and the adjusted crash times.

The weather data was collected from www.wundergound.com website, which provides hourly weather information from weather stations across the United States. Three weather-related data were collected from the closest weather stations, including rainfall, snow, and visibility.

Crash data were obtained from the Statewide Integrated Traffic Records System (SWITRS) maintained by Caltrans. It provides information for all reported crashes (e.g., crash time, location, duration, and description).

The geometric data were obtained from the PeMS database. 25 segments were analyzed in this study, and each segment was so classified into one of five segment types by which the crash events were split where the crash occurred. Among the 342 crashes, 72 crashes which occurred on basic straight segments, 29 crashes which occurred on basic rolling segments, 18 crashes which occurred on basic curved segments, 53 crashes which occurred on weaving segments, and 177 crashes which occurred on ramp segments were identified. It should be noted that seven crashes occurred on straight-rolling segments and curve-rolling segments which have two geometric characteristics. Hence, these seven crashes were duplicated to the corresponding segment type in both segment types. As a result, a total of 349 crash traffic data and 1,745 non-crash traffic data were collected and used for the analysis.

To compare what contributing factors are identified at different locations, crash events, traffic data, geometric data, weather data and pavement and lighting condition data were collected from a 32.30-mile segment in the northbound direction of the I-95 freeway in Florida. The I-95 has been known to have the highest crash-related fatality rate in the US. There are 72 loop detector stations with an average spacing of 0.4 miles and two weather stations within the selected segments. The collected data covers the entire 2015 period as well. A total of 78 crashes were identified and used in this study. It should be mentioned that there were many detectors with empty traffic data and many crashes occurred on an on-ramp or off-ramp locations. Therefore, those crashes were excluded. Traffic data and crash data were collected from Florida Department of Transportation, and geometric data were collected manually using Google Earth. The weather data on rainfall, snow, and visibility were collected from the nearest weather stations via the www.wundergound.com website.

The whole dataset was split into training and validation datasets. For the training dataset, 70% of the whole dataset had a total of 244 crashes including 50 basic straight segment crashes, 13 basic curved segment crashes, 20 basic curved segment crashes, 37 weaving segment crashes and 124 ramp segment crashes. The training dataset was used to develop Bayesian random intercept logistic regression models and 30% of the whole dataset which is validation dataset including 22 basic straight segment crashes, 5 basic curved segment crashes, 16 basic rolling segment crashes, 16 weaving segment crashes, and 53 ramp segment crashes was used to compute crash risk and to validate the performance of the Bayesian random intercept logistic regression models.

4.3 Contributing Factor

34 traffic parameters, along with three weather variables and pavement and lighting condition variables (a total of 39 variables) were ranked according to five segment types by Random Forest. The ranked variables are presented in Figure 4.2. Note that all candidate variables use abbreviation as shown in Table 4.1.

Table 4.1 Variable Description

Symbol	Description
ASU/ASD	The average speed at upstream detector / average speed at downstream detectors
AOU/AOD	The average occupancy at upstream detector / average occupancy at downstream detectors
AFU/AFD	The average flow at upstream detector / average flow at downstream detectors
SSU/SSD	The standard deviation of speed at upstream detector / standard deviation of speed at downstream detectors
SOU/SOD	The standard deviation of occupancy at upstream detector / standard deviation of occupancy at downstream detectors
SFU/SFD	The standard deviation of flow at upstream detector / standard deviation of flow at downstream detectors
ADSUD	The average difference in speed between upstream and downstream detectors
ADOUD	The average difference in occupancy between upstream and downstream detectors
ADFUD	The average difference in flow between upstream and downstream detectors
ADSLU	The average difference in speed between lanes at upstream detectors
ADSLD	The average difference in speed between lanes at downstream detectors
ADOLU	The average difference of occupancy between lanes at upstream detectors
ADOLD	The average difference of occupancy between lanes at downstream detectors
ADFLU	The average difference of flow between lanes at upstream detectors
ADFLD	The average difference of flow between lanes at downstream detectors
ATU	The average number of trucks at upstream detectors
ATD	Th average number of trucks at downstream detectors
CVSU	The coefficient of variation in the speed at upstream detectors
CVSD	The coefficient of variation in the speed at downstream detectors
CVFU	The coefficient of variation in flow at upstream detectors
CVFD	The coefficient of variation in flow at downstream detectors
DCVSUD	The difference of CVS between upstream and downstream detectors
CIU	The congestion index at upstream detectors

CID	He congestion index at downstream detectors
OAFRU	The overall average flow ratio at upstream detectors
OAFRD	The overall average flow ratio at downstream detectors
ARU	The average ramp flow at upstream detectors
ARD	The average ramp flow at downstream detectors
Rain	Rainfall
Snow	Snow
VISIBILITY	Visibility
Light condition	Daylight, Dark with street lights, and Dark with no street lights
Pavement	Dry and wet

RF- CA, rank

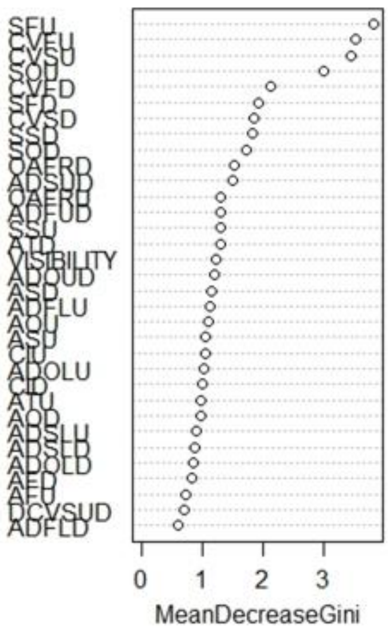

Basic straight segment

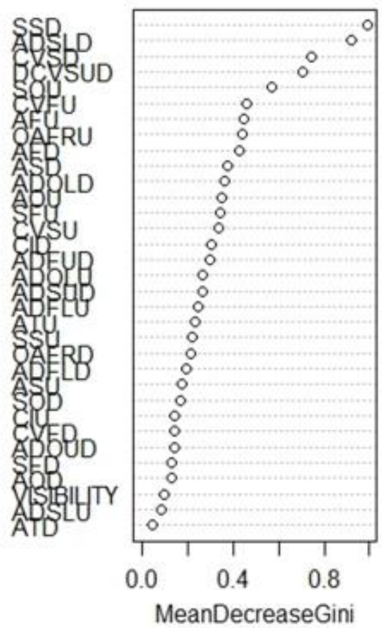

Basic curved segment

RF- CA, rank

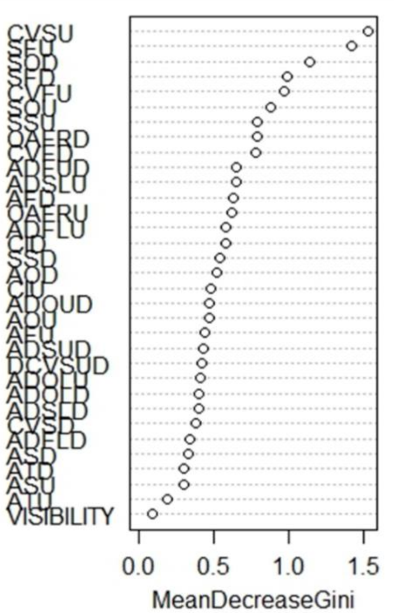

Basic rolling segment

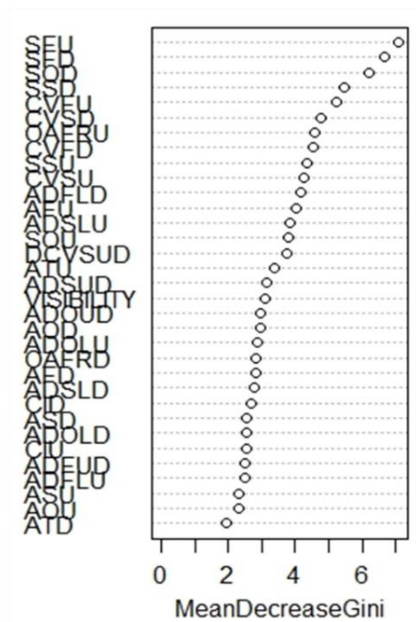

Ramp segment

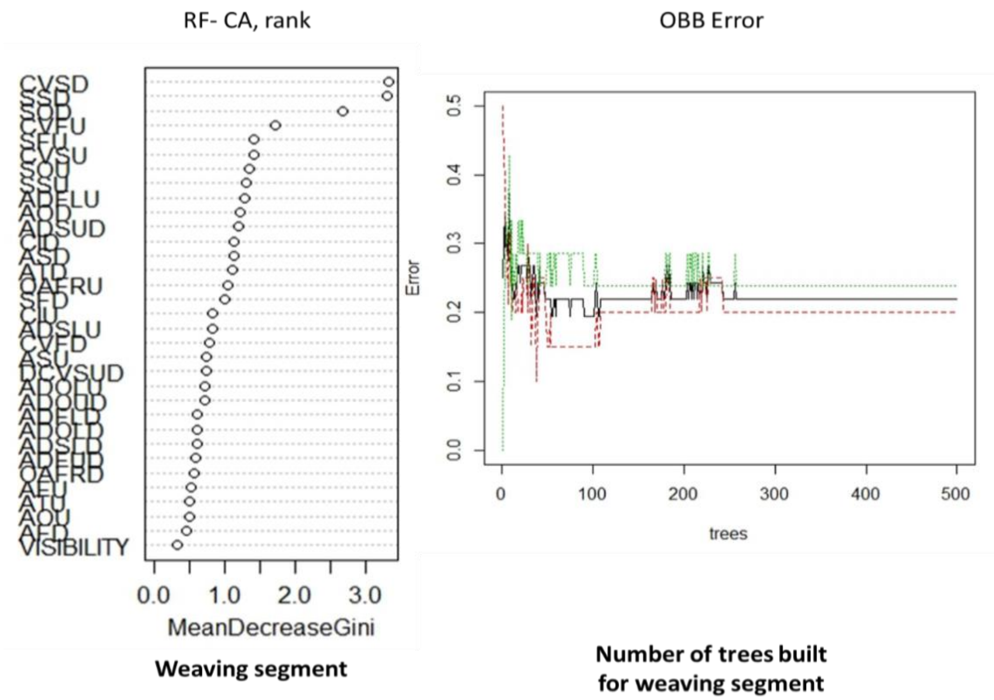

Figure 4.2 Ranked Variables

RF resulted in the lowest OOB error when it built around 250 trees for weaving segments, for example. As shown in Figure 4.2, the importance of variables ranked differently for each segment. Basic straight segments had flow related variables as the most important variable, whereas basic curved segments had speed related variables as the most important variable. The results indicated that difference in traffic parameters between upstream and downstream detector stations and change in traffic parameters at one point is most likely to affect crash risk. The variable OAFRU was highly ranked for basic curved segments and ramp segments. This indicates that lane change maneuvers are more likely to affect crash risk relative to other segments. The variables ATU and ATD were highly ranked for ramp segments and weaving segments. As the number of trucks increases on weaving or ramp segments, the crash risk is more likely to increase.

With the ranked variables, a Pearson Correlation Coefficient was computed for each pair of variables. If the two variables were found to be highly correlated, the variable with higher rank was chosen for further analysis and the lower ranked variable was removed. For example, the Pearson correlation coefficient of first ranked variable SFU with all variables is shown in Table 4.2. Table 4.2 shows that SFU is correlated with CVFU, CVSU, SOU, CVFD, SFD, and SSU. Thus, these five variables are removed and the correlation of next highest ranked variable which is CVSD with all lower ranked variables is checked. During this process, the correlation of all variables are checked with each other and the variables that have little or no correlation with higher ranked variable are selected in this step. Then, for each chosen variable, T-test assessed whether its averages of it in the traffic conditions in which crash occurred and non-crash traffic conditions were statistically different from each other at 0.01 significance level. The variables that were found to be statistically significant were chosen as a contributing factor, and the insignificant variables were again examined with F-test.

If the calculated F-value of the variable is greater than the critical F critical, it was chosen as a contributing factor. Otherwise, the variable was removed.

Table 4.3 shows the contributing factors that significantly affected crash risk on the I-110 northbound for the five segment types in 2015.

Table 4.2 The Result of Pearson Correlation Test

1^{ST} Variable	The next ranked variable	Pearson correlation coefficient
SFU	CVFU	0.922
SFU	CVSU	0.512
SFU	SOU	0.495
SFU	CVFD	0.526
SFU	SFD	0.519
SFU	CVSD	0.244
SFU	SSD	0.315
SFU	SOD	0.383
SFU	OAFRD	0.056
SFU	ADSUD	0.010
SFU	OAFRU	0.062
SFU	ADFUD	-0.230
SFU	SSU	0.421
SFU	ARD	-0.211
SFU	VISIBILITY	0.017
SFU	ADOUD	-0.006
SFU	ASD	0.084
SFU	ADFLU	-0.024
SFU	AOU	0.021
SFU	ASU	-0.034
SFU	CIU	0.034
SFU	ADOLU	0.025
SFU	CID	-0.084

Table 4.3 Contributing Factors on I-110 Northbound in CA in 2015

Segment type	Contributing factor
Basic straight segment	• The average difference in flow between upstream and downstream detectors • The average difference in speed between upstream and downstream detectors • The coefficient of variation in the speed at downstream detector • OAFR at upstream detectors • OAFR at downstream detectors • The standard deviation of flow at upstream detectors • Visibility • Light condition
Basic curved segment	• The coefficient of variation in flow at the upstream detector • The average difference of coefficient in variation of speed between upstream and downstream detectors • OAFR at upstream detectors • The standard deviation of speed at downstream detectors • Pavement • Light condition
Basic rolling segment	• The coefficient of variation in flow at downstream detectors • OAFR at upstream detectors
Weaving segment	• The average difference in speed between upstream and downstream detectors • The average number of trucks at downstream detectors • The coefficient of variation in flow at upstream detectors • The coefficient of variation in the speed at downstream detectors • Pavement
Ramp segment	• The average difference of flow between lanes at downstream detectors • The average difference in speed between lanes at upstream detectors • OAFR at upstream detectors • The standard deviation of flow at downstream detectors • The standard deviation of flow at upstream detectors • The standard deviation of speed at downstream detectors • Pavement

Variation in traffic parameters and OAFR turned out to affect crash risk for basic segments, indicating that crashes on basic segments are susceptible to both rear-end crashes and sideswipe crashes. Regarding weather variables, visibility was found to be a significant factor for basic straight segments. The average number of trucks turned out to be significant for weaving segments. Variation in traffic parameters between lanes and OAFR were significant factors for ramp segments. The crash risk could be affected when it gets dark on basic straight segments and basic curved segments. Wet pavement affects crash risk on basic curved segments, weaving and ramp segments. Basic curved segments are the place where it is affected by both pavement and lighting conditions.

When it comes to the I-95 in Florida, the same procedure was conducted to identify contributing factors, and the results are shown in Table 4.4.

Table 4.4 Contributing Factors on I-95 northbound in FL in 2015

Geometric type	Contributing factors
Basic straight segment	• The average difference in flow between lanes at the upstream detector • The average difference in flow between upstream and downstream detectors • The average difference in occupancy between lanes at downstream detector • The average difference in speed between lanes at the upstream detector • The average difference in speed between upstream and downstream detectors • The coefficient of variation in flow at downstream detector • The standard deviation of speed at the upstream detector • Visibility
Basic curved segment	• The average difference in flow between upstream and downstream detectors • The average difference in speed between lanes at downstream detector • The difference in Coefficient of variation in speed between upstream and downstream detectors • Pavement
Weaving segment	• The average difference in occupancy between lanes at downstream detector • The difference in coefficient of variation in speed between upstream and downstream detectors • Visibility • Pavement
Ramp segment	• The average difference in speed between upstream and downstream detectors • The difference in the coefficient of variation in speed between upstream and downstream detectors • The standard deviation of flow at downstream detector • The standard deviation of occupancy at downstream detector

The I-95 in Florida consists of four segment types. Compared with the contributing factors in California, variation in traffic parameters between lanes had a greater impact on crash risk for basic segments. The analysis further showed that the average number of trucks does not have an impact for weaving segments and lane change maneuvers do not have as much of an impact as they do on the I-110 northbound in California for weaving segments and ramp segments.

4.4 Bayesian Random Intercept Logistic Regression Model

With the contributing factors on I-110N in California in Table 4.2, Bayesian random intercept logistic regression was used to develop crash risk prediction models for the five segment types. This aimed to explore distinct effects of each contributing factor of each segment type on crash risk. The estimation results of the crash risk prediction models for the five segment types are given in Tables 4.5 to 4.9.

Table 4.5 Crash Risk Prediction Model for Basic Straight Segments on I-110 in CA in 2015

Variables	**Parameters estimates (beta coefficient)**				**Odds ratios**
	Mean	Std.dev.	2.5%	97.5%	
Intercept	-4.037	0.478	-5.129	-3.824	-
ADFUD	-0.014	0.004	-0.022	-0.007	0.986
ADSUD	0.003	0.021	-0.038	0.044	1.003
CVSD	0.003	0.031	-0.059	0.065	1.003
OAFRU	-0.003	0.032	-0.064	0.061	0.998
OAFRD	-0.003	0.031	-0.064	0.059	0.998
SFU	0.035	0.008	0.021	0.051	1.036
VISIBILITY	-0.026	0.029	-0.081	0.030	0.975
LIGHT CONDITION	0.038	0.010	0.019	0.053	1.039

Table 4.6 Crash Risk Prediction Model for Basic Curved Segments on I-110 in CA in 2015

Variables	**Parameters estimates (beta coefficient)**				**Odds ratios**
	Mean	Std.dev.	2.5%	97.5%	
Intercept	-4.794	0.292	-5.102	-4.414	-
CVFU	-0.027	0.314	-0.638	0.594	1.023
DCVSUD	0.027	0.313	-0.592	0.647	1.079
OAFRU	-0.234	0.294	-0.802	0.345	0.826
SSD	0.129	0.066	0.006	0.267	1.140
LIGHT CONDITION	0.052	0.056	0.034	0.079	1.053
PAVEMENT	0.014	0.012	0.008	0.025	1.014

Table 4.7 Crash Risk Prediction Model for Basic Rolling Segments on I-110 in CA in 2015

Variables	**Parameters estimates (beta coefficient)**				**Odds ratios**
	Mean	Std.dev.	2.5%	97.5%	
Intercept	-3.852	0.263	-4.287	-3.529	-
CVFD	0.107	0.316	-0.506	0.732	1.170
OAFRU	0.007	0.249	-0.479	0.492	1.039

Table 4.8 Crash Risk Prediction Model for Weaving Segments on I-110 in CA in 2015

Variables	Parameters estimates (beta coefficient)				Odds ratios
	Mean	Std.dev.	2.5%	97.5%	
Intercept	-4.012	0.332	-4.499	-3.825	-
ADSUD	0.064	0.026	0.014	0.115	1.066
ATD	0.080	0.020	0.044	0.122	1.083
CVFU	0.001	0.032	-0.060	0.064	1.002
CVSD	0.004	0.031	-0.057	0.065	1.004
PAVEMENT	0.033	0.024	0.019	0.059	1.034

Table 4.9 Crash Risk Prediction Model for Ramp Segments on I-110 in CA in 2015

Variables	Parameters estimates (beta coefficient)				Odds ratios
	Mean	Std.dev.	2.5%	97.5%	
Intercept	-5.111	0.262	-5.728	-4.842	-
ADFLD	-0.070	0.016	-0.102	-0.040	0.932
ADSLU	-0.010	0.034	-0.079	0.056	0.991
OAFRU	0.033	0.038	-0.034	0.117	1.035
SFD	0.005	0.004	-0.003	0.013	1.005
SFU	0.008	0.003	0.003	0.013	1.008
SSD	0.046	0.017	0.014	0.079	1.047
PAVEMENT	0.065	0.038	0.038	0.089	1.067

In most cases, the variation in traffic parameters has positive coefficients, indicating that as the variation in traffic parameters increases, crash risk also increases. For example, if the standard deviation of flow at upstream detectors is positive, then greater standard deviation of flow at upstream detectors increases crash risk.

However, the flow-related variables were found to be negatively related to crash risk for basic straight segments and basic curved segments, indicating that greater average difference in flow between upstream and downstream detectors (ADFUD) decreases crash risk. Furthermore, as overall average flow ratio (OAFR) increases, the crash risk decreases. Additionally, the average difference in flow between lanes at downstream detectors (ADFLD) and the average difference in speed between lanes at upstream detectors (ADSLU) were also found to be negatively related to crash risk for ramp segments. Under congested traffic conditions, a greater difference in flow between lanes indicates fewer gaps between vehicles resulting in fewer gaps for a lane change. Thus, the crash risk is decreased as the average difference in flow between lanes become greater. Visibility was also found to play a significant role in crash risk. Under poor visibility, car following and lane changing become much more difficult for drivers, so vehicles become very cautious when following leading vehicles or when trying to change a lane.

The standard deviation of speed was a good indicator of traffic turbulence. When there is a significant speed difference, deceleration or acceleration would need to be used to guarantee a safe following distance. Under these circumstances, rear-end crashes are likely to occur for basic curved segments and ramp segments because the standard deviation of speed at downstream detectors has a positive impact on crash risk for both basic curved segments and ramp segments. Ramp segments and weaving segments are more likely to be affected by sideswipe crash risks because the overall average flow ratio at upstream detectors (OAFRU), the coefficient of variation in flow at upstream detectors (CVFU), and the coefficient of variation in speed at downstream detectors (CVSD) were found to affect crash risk positively.

OAFR and flow variation related variable are measures of lane-change maneuvers that are associated with sideswipe crashes. The average number of trucks was found to affect crash risk for weaving segments positively. Trucks interrupt mandatory lane changes, so the number of trucks can be an obstacle for merging and diverging vehicles.

Pavement and lighting condition variables are categorical variables. For pavement condition, 0 is set as dry, and 1 is set as wet condition. For lighting condition, 0 is set as daylight, 1 is set as dark with street light, and 2 is set as dark with no streetlight. All segment types are likely to be affected by environmental characteristics, except basic rolling segments. Crash risk gets increased at night and on wet pavement condition. Especially, crash risk tends to be higher at dark with no streetlight.

Odds ratios were used to evaluate the impacts of each variable on crash risk for five segment types. As mentioned, odds ratios indicate the constant effect of each variable on the odds of the outcome. That is, it is an estimate of the expected change in the crash risk of having a crash versus a non-crash per unit increase in the corresponding variable. Note that the odds ratio is equal to the exponential of a beta coefficient. A positive beta coefficient for a variable means that the odds of a crash occurrence increase with a unit increase in the value of that variable. An odds ratio value of 1 indicates no significant relationship with crash risk, but a value of less than 1 indicates a negative relationship with crash risk, and a value greater than 1 indicates a positive relationship with crash risk.

The odds ratio of standard deviation of flow at downstream detectors (SFD) for basic straight segments was 1.036, indicating that the crash risk increases by 3.6% as SFD increases by 1 unit. On the other hand, the odds ratio of the overall flow ratio at upstream detectors (OAFRU) for basic curved segments was 0.826, indicating that the crash risk decreases by 17.4% as OAFRU increases by 1 unit. Furthermore, the odds ratio associated with a unit increase in the OAFRU for basic curved segments and basic rolling segments was 0.826 and 1.039 respectively, which means that a unit increase in the OAFRU was associated with -17.4% and 3.9% change, respectively. The results showed that the intensity and direction of a variable are distinct across segment types.

4.5 *Crash Risk Index Development*

A crash risk index (CRI) capable of quantifying crash risk is derived. This index is an invaluable tool for traffic operators in evaluating crash risk on roads. Furthermore, it enables the developmental support of effective countermeasures to prevent crash occurrences on freeways. It should be noted that this section focuses on developing a crash risk index to quantify hazardous traffic conditions. The crash risk index (CRI) is formulated by three components including odds ratios of contributing factors obtained from the Bayesian random intercept logistic regression models, 5-min interval based historical non-crash traffic data, and 5-min interval based current traffic data. With those components, five crash risk indices are developed as follows:

- For basic straight segments,

$$CRI_i^1 = 3.6 * (SFU_{cu5} - SFU_{no5}) + 0.3 * (ADSUD_{cu5} - ADSUD_{no5}) - 1.4 * (ADFUD_{cu5} - ADFUD_{no5}) + 0.3 * (CVSD_{cu5} - CVSD_{no5}) - 0.2 * (OAFRU_{cu5} - OAFRU_{no5}) - 0.3 * (OAFRD_{cu5} - OAFRD_{no5}) - 2.6 * (VISIBILITY_{cu5} - VISIBILITY_{no5}) + 3.9 * (Light_{cu5}) \quad (4.1)$$

- For basic curved segments,

$$CRI_i^2 = 14 * (SSD_{cu5} - SSD_{no5}) + 2.3 * (CVFU_{cu5} - CVFU_{no5}) + 7.9 * (DCVSUD_{cu5} - DCVSUD_{no5}) - 17.4 * (OAFRU_{cu5} - OAFRU_{no5}) + 1.4 * (PAVEMENT_{cu5}) + 5.3 * (Light_{cu5}) \quad (4.2)$$

- For basic rolling segments,

$$CRI_i^3 = 17 * (CVFU_{cu5} - CVFU_{no5}) + 3.9 * (OAFRU_{cu5} - OAFRU_{no5}) \quad (4.3)$$

- For weaving segments,

$$CRI_i^4 = 6.6 * (ADSUD_{cu5} - ADSUD_{no5}) + 8.3 * (ATD_{cu5} - ATD_{no5}) + 0.2 * (CVSD_{cu5} - CVSD_{no5}) + 0.4 * (CVFU_{cu5} - CVFU_{no5}) + 3.4 * (PAVEMENT_{cu5}) \quad (4.4)$$

- For ramp segments,

$$CRI_i^5 = 4.7 * (SSD_{cu5} - SSD_{no5}) + 0.8 * (SFU_{cu5} - SFU_{no5}) + 0.5 * (SFD_{cu5} - SFD_{no5}) - 0.9 * (ADSLU_{cu5} - ADSLU_{no5}) - 6.8 * (ADFLD_{cu5} - ADFLD_{no5}) + 3.5 * (OAFRU_{cu5} - OAFRU_{no5}) + 6.7 * (PAVEMENT_{cu5}) \quad (4.5)$$

Where CRI_i^{k} is the crash risk index on segment type k at 5-min time period i.

The scoring dataset which is 30% of the whole dataset was used to score the crash risk on five segment types. Table 4.10 presents CRI scores for all the 5 min to 10 min traffic situations before crash occurrences and non-crash traffic situations at the crash locations and at the crash time on other days when there is no crash.

Table 4.10 CRI Scores for Five Segment Types

Type	Condition	Minimum	Maximum	Mean	SD
1	Crash	-368.545	949.970	201.625	237.935
	Non-crash	-258.342	196.281	-17.172	89.794
2	Crash	-82.086	222.187	88.246	74.521
	Non-crash	-91.209	56.353	-7.400	42.930
3	Crash	-13.750	8.000	0.879	4.716
	Non-crash	-14.045	4.722	-2.519	4.686
4	Crash	-157.872	617.823	107.626	193.266
	Non-crash	-142.469	131.973	-2.812	53.184
5	Crash	-137.759	377.191	65.316	107.688
	Non-crash	-246.664	241.316	-25.632	62.480

The result shows that CRI of crash traffic conditions appears to be relatively higher than those of non-crash traffic situations, implying that traffic conditions of impending crashes have a high possibility of crash occurrences. Interestingly, the standard deviation of CRI in crash traffic conditions is higher on all segment types which means that the traffic situations become unstable before the crash occurs.

The CRI computed for each segment type are not comparable because each segment type shows different minimum and maximum due to five separate CRI compositions. To be comparable to each other, we standardized the scores by rescaling them to 0 to 100 range values, and the rescaled CRI scores are presented in Table 4.11. As expected, all segment types had maximum CRI in crash traffic conditions. The mean CRI score for both crash traffic conditions and non-crash traffic conditions for basic rolling segments were relatively higher than those of other types. This means that basic rolling segments are more likely to have high crash risk than other types.

Table 4-11 Rescaled CRI Scores

Type	Condition	Minimum	Maximum	Mean	SD
1	Crash	0	100	43	18
	Non-crash	8	43	27	7
2	Crash	3	100	52	27
	Non-crash	0	47	25	14
3	Crash	1	100	67	21
	Non-crash	0	85	52	20
4	Crash	0	100	34	24
	Non-crash	2	37	20	7
5	Crash	17	100	50	17
	Non-crash	0	78	36	10

4.6 *Predictive Performance*

The predictive power of the crash risk prediction models is tested. The models classified an observation as a crash if the predicted CRI score of the observation exceeded a predetermined threshold. Otherwise, it was classified as a non-crash case. The prediction accuracy of the crash and non-crash cases depended on the predetermined threshold. This study developed receiver operating characteristic (ROC) curves to estimate the predictive performance of the five crash risk prediction models with different CRI score thresholds. A ROC curve is a graphical plot of the sensitivity (y-axis) vs. 1 – specificity (x-axis). The ROC curves illustrate the relationship between the true positive rate (sensitivity) and the false positive rate (1-specificity) for thresholds from 0 to 100. Sensitivity and specificity calculated with different thresholds were used to develop ROC curve for each crash risk prediction model. Figure 4.3 illustrates the ROC curves for the Bayesian random intercept logistic regression models.

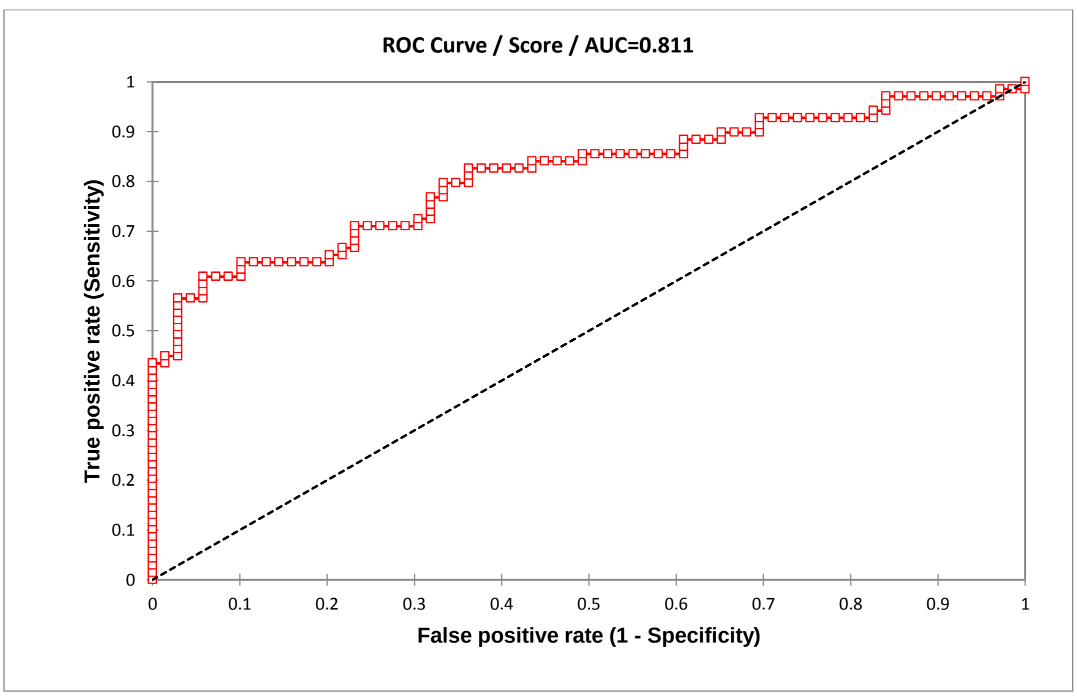

ROC curve for basic straight segments

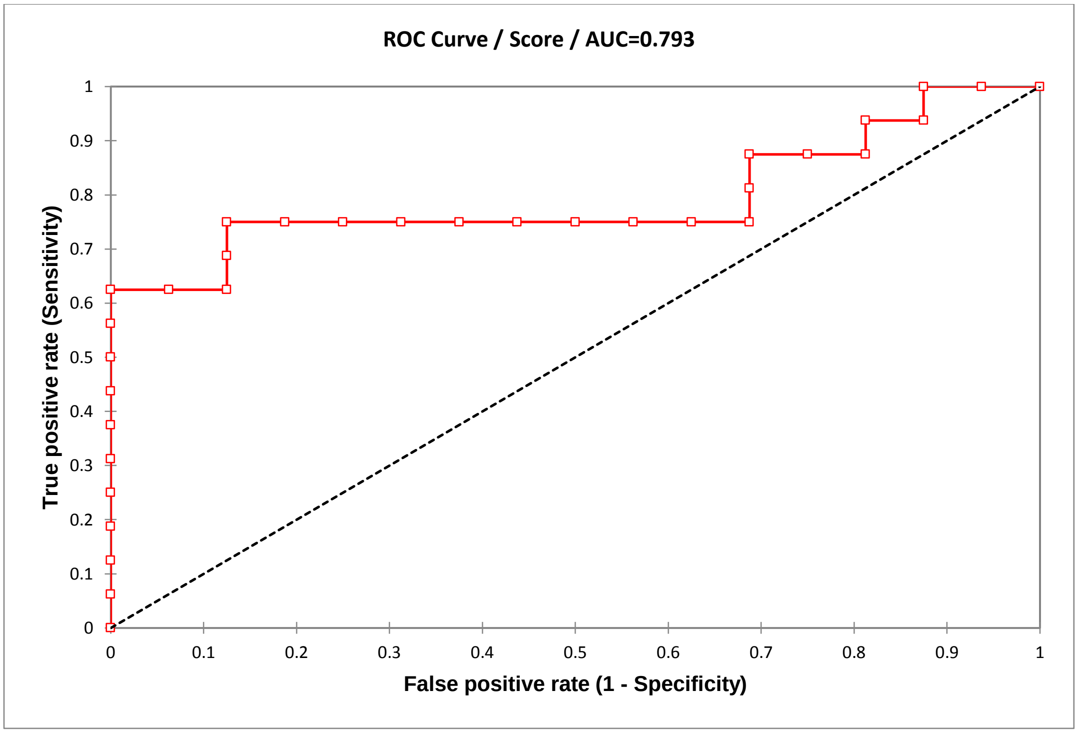

ROC curve for basic curve segments

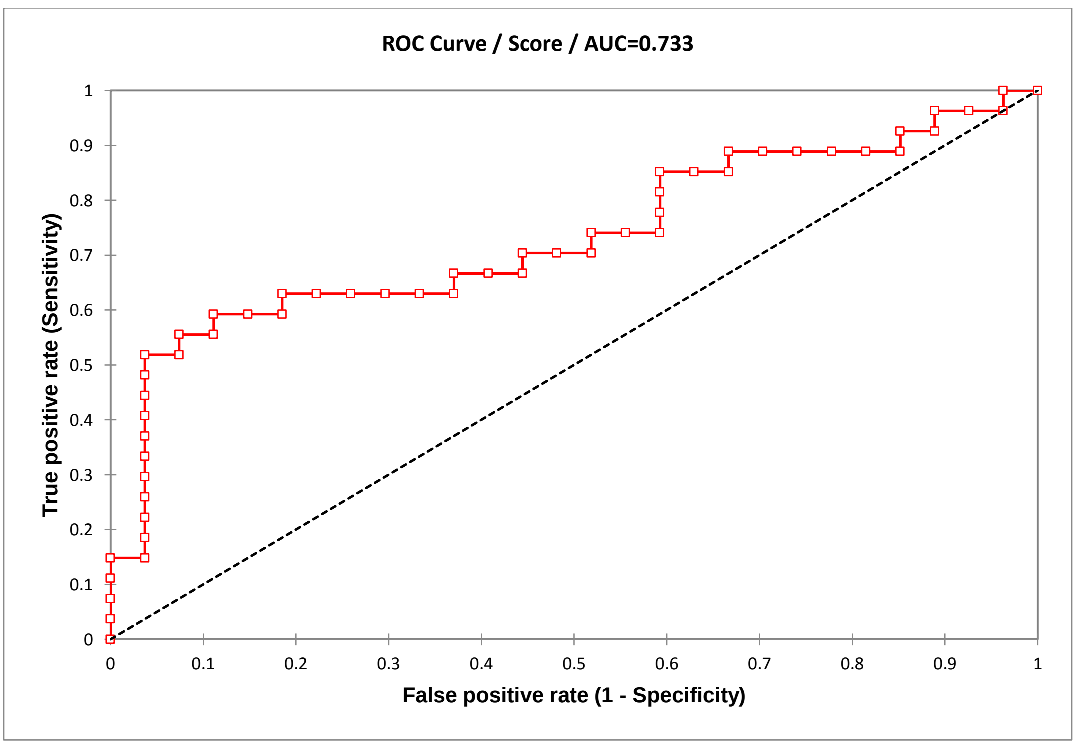

ROC curve for basic rolling segments

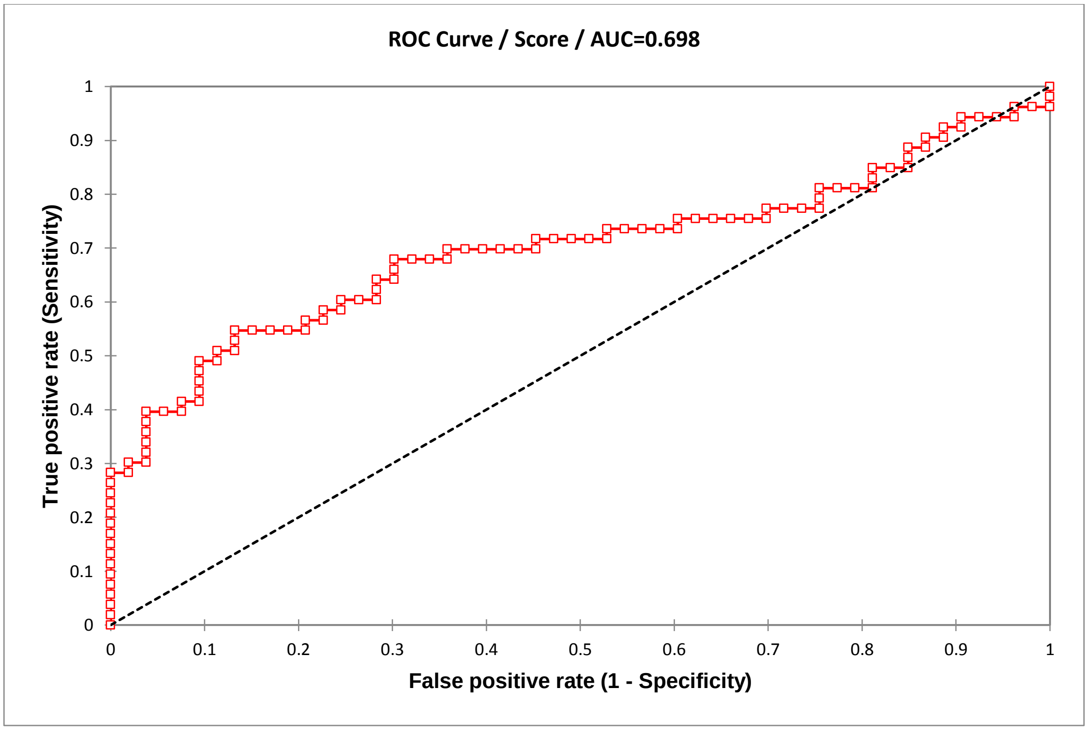

ROC curve for weaving segments

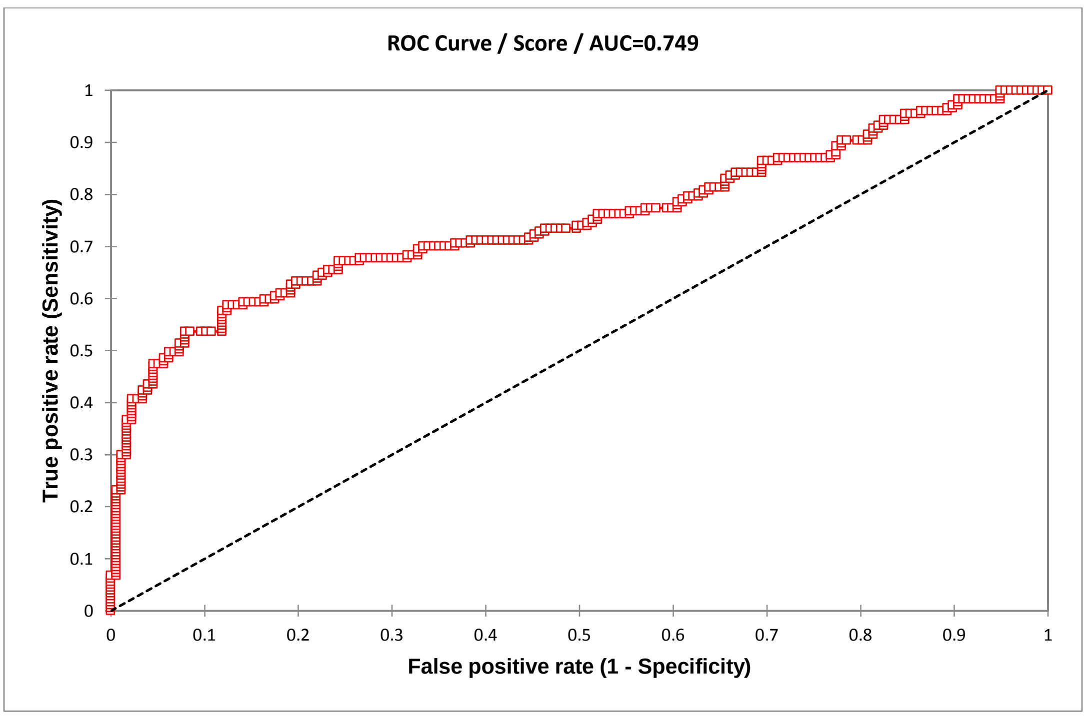

ROC curve for ramp segments

Figure 4.3 ROC Curves of Crash Risk Prediction Models for the Five Segment Types

The areas under the ROC curves (AUC) for the models were found to be 0.811, 0.793, 0.733, 0.698, and 0.749, respectively, indicating that the crash risk prediction models have prediction performances of 81.1%, 79.3%, 73.3%, 69.8%, and 74.9%, respectively.

Table 4.12 presents the sensitivity measured by the percent of predicted crashes at each segment type depending on several false positive (false alarm) rates.

Table 4.12 True Positive Rate under Different False Positive Rates

False positive rate	True Positive Rate (Sensitivity)				
	1	2	3	4	5
0.05	56.5%	62.5%	51.9%	39.6%	47.5%
0.1	60.9%	62.6%	55.6%	49.1%	53.7%
0.2	63.8%	75.0%	63.0%	54.7%	63.3%
0.3	71.0%	75.2%	63.1%	64.2%	67.8%
0.4	82.6%	75.2%	66.7%	69.8%	71.2%
0.5	85.5%	75.2%	70.4%	71.7%	74.0%

As shown in Figure 4.3, the sensitivity increased as the false positive rate increased. This trade-off between the true positive rate and the false positive rate must be considered when setting a threshold value and needs to be determined carefully to meet a particular requirement for practical implementation.

In this study, a threshold that can maximize Youden index (= sensitivity + specificity -1), which is a summary measure of a ROC curve, has been selected to evaluate predictive performance. Youden index measures the effectiveness of CRI and enables the selection of an optimal threshold value among CRI scores as an indication of high crash risk. It is utilized when selecting an optimal threshold value in many scientific areas such as radiology, psychiatry, epidemiology, and manufacturing inspection systems.

$$\begin{aligned}\text{Youden index} &= \text{sensitivity} + \text{specificity} - 1 \\ &= \text{sensitivity} - \text{false positive rate}\end{aligned}$$

Youden index can be maximized at high sensitivity and low false positive rates. Table 4.13 shows threshold values made by Youden index and follows prediction accuracy of crashes and non-crashes.

Table 4.13 Prediction Performance of Five Crash Risk Prediction Models

Type	Threshold (CRI score)	Sensitivity	Specificity	False positive rate	Overall accuracy
1	40	60.9%	94.2%	5.8%	77.5%
2	31	75.0%	87.5%	12.5%	81.3%
3	68	55.6%	92.6%	7.4%	74.1%
4	27	54.7%	86.8%	13.2%	70.8%
5	45	58.8%	87.6%	12.4%	73.2%

The results indicate that each type has maximized the Youden index at the threshold values which means that each type has achieved the greatest overall accuracy at the threshold values.
For comparison purposes, Table 4.14 summarizes previous studies' prediction accuracy of crashes and non-crashes.

Table 4.14 Predictive Performance of Crash Risk Prediction Models in Previous Studies

Authors	Sensitivity	Specificity	False positive rate
Oh et al. (2001)	55.8%	72.1%	27.9%
Oh et al. (2005)	35.2%	73.5%	26.5%
Abdel-Aty et al. (2004)	69.4%	52.8%	47.2%
Abdel-Aty et al. (2005)	56.0%	80.0%	20.0%
Hossain and Muromachi (2010)	63.3%	80.0%	20.0%
Hassan and Abdel-Aty (2011)	67.2%	64.7%	35.3%
Ahmed et al. (2012)	72.9%	57.9%	42.0%

Compared to the predictive performance of the crash risk prediction models in previous studies as shown in Table 4.14, this study has a better predictive performance. Figures 4.4 to 4.6 show comparisons of the prediction accuracy of crashes and non-crashes and false positive rates with previous studies. The prediction accuracy of non-crashes for these developed models was much better than those of previous studies, and the false positive rate was much lower than those of previous studies. These results demonstrate that the developed models' predictive performance for discriminating between crashes and non-crashes is much stronger than what had been previously accomplished in the literature.

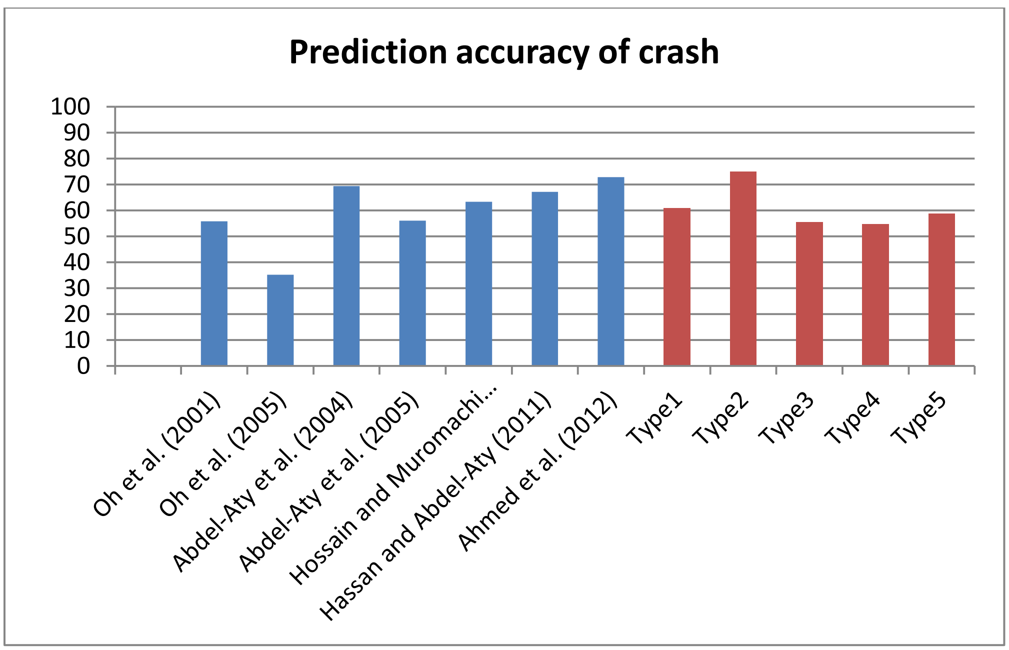

Figure 4.4 Comparison of prediction accuracy of crashes

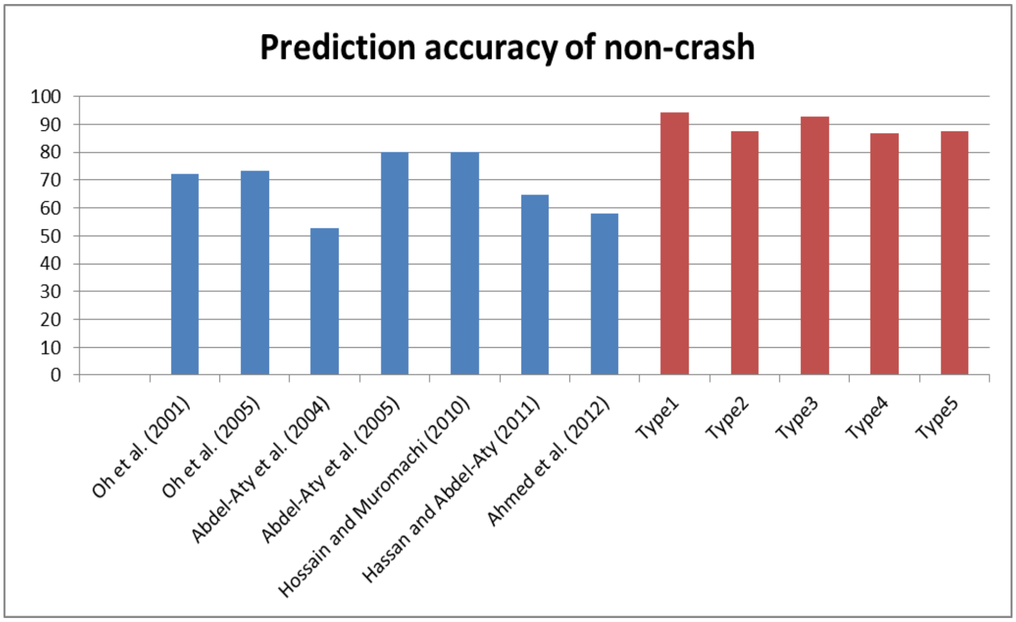

Figure 4.5 Comparison of prediction accuracy of non-crashes

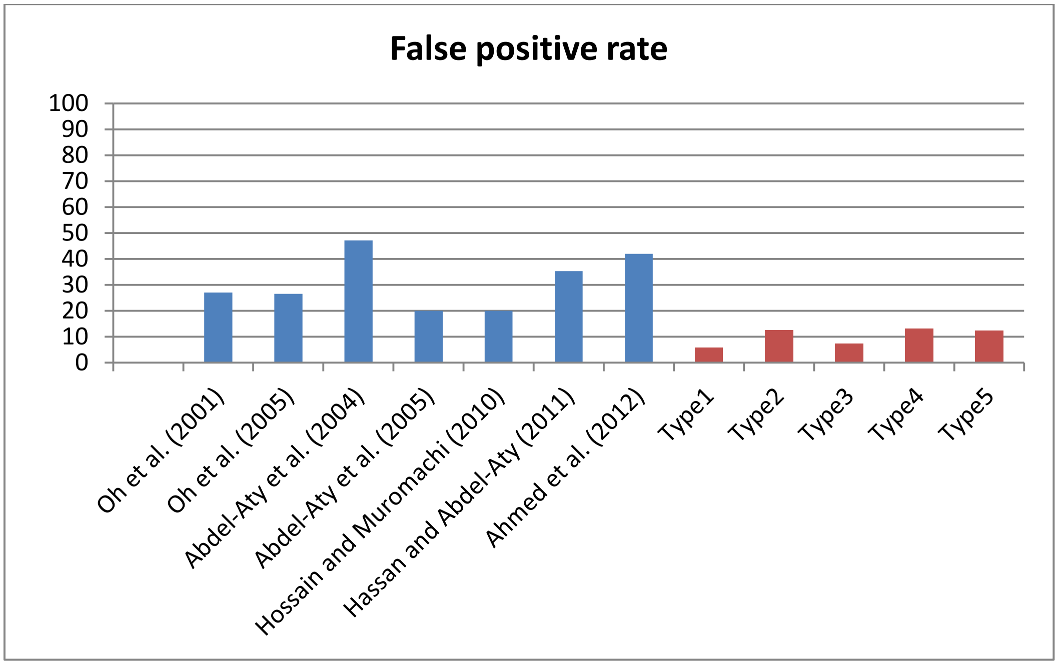

Figure 4.6 Comparison of False Positive Rates

4.7 *Sensitivity Analysis of Thresholds*

The predictive performance of the CRIs are evaluated based on thresholds. In fact, the predictive performance depends on the choice of thresholds. Thus, crash risk scores exceeding the thresholds have been only considered as high crash risk and some scores that are very close to the thresholds, but below the thresholds are not categorized as high crash risk. Consequently, this can make some real crashes identified incorrectly as non-crash cases. For example, assume that CRI for a traffic condition is 39 and CRI for another traffic condition is 41 at the threshold of 40. The former is categorized as non-high crash risk, but the latter is categorized as high crash risk. Therefore, this section conducts sensitivity analysis of thresholds to see how the predictive performance varies with different thresholds for five segment types. The receiver operating characteristic (ROC) curves that this study developed are used to estimate the predictive performance of the five CRIs with different thresholds. As mentioned above, a threshold has a value between 0 and 100 and sensitivity analysis is conducted in 10-point increments. The results of sensitivity analysis for five CRIs are presented in Table 4.15 to 4.19.

Table 4.15 Sensitivity Analysis of Thresholds for Basic Straight Segment Type

Threshold (CRI score)	Sensitivity	Specificity	False positive rate	Overall accuracy
10	98.6%	0.00%	100.0%	49.3%
20	98.6%	1.4%	98.6%	50.0%
30	89.9%	34.8%	65.2%	62.4%
40	60.9%	94.2%	5.8%	77.6%
50	36.2%	96.5%	3.5%	66.4%
60	18.8%	96.9%	3.1%	57.9%
70	8.7%	97.2%	2.8%	53.%
80	2.9%	98.4%	1.6%	50.7%
90	1.8%	99.1%	0.9%	50.5%

Table 4.16 Sensitivity of Analysis of Thresholds for Basic Rolling Segment Type

Threshold (CRI score)	Sensitivity	Specificity	False positive rate	Overall accuracy
10	94.3%	11.1%	88.9%	52.7%
20	93.1%	13.5%	86.5%	53.3%
30	92.6%	14.8%	85.2%	53.7%
40	88.9%	18.5%	81.5%	53.7%
50	88.9%	25.9%	74.1%	57.4%
60	70.4%	55.6%	44.4%	63.0%
70	50.5%	94.3%	5.7%	72.4%
80	25.9%	96.3%	3.7%	61.1%
90	7.4%	98.1%	1.9%	52.8%

Table 4.17 Sensitivity of Analysis of Thresholds for Basic Curved Segment Type

Threshold (CRI score)	Sensitivity	Specificity	False positive rate	Overall accuracy
10	97.4%	6.3%	93.7%	51.9%
20	77.0%	42.0%	58.0%	59.5%
30	75.0%	87.5%	12.5%	81.3%
40	62.5%	89.1%	10.9%	75.8%
50	59.2%	90.1%	9.9%	74.7%
60	56.3%	92.2%	7.8%	74.3%
70	43.8%	93.8%	6.2%	68.8%
80	25.1%	94.2%	5.8%	59.7%
90	12.5%	96.8%	3.2%	54.7%

Table 4.18 Sensitivity of Analysis of Thresholds for Weaving Segment Type

Threshold (CRI score)	Sensitivity	Specificity	False positive rate	Overall accuracy
10	92.5%	11.3%	88.7%	51.9%
20	73.6%	45.3%	54.7%	59.5%
30	39.6%	96.2%	3.8%	67.9%
40	24.5%	96.8%	3.2%	60.7%
50	22.6%	97.8%	2.2%	60.2%
60	15.1%	98.2%	1.8%	56.7%
70	9.4%	98.5%	1.5%	54.0%
80	7.5%	99.2%	0.8%	53.4%
90	5.7%	99.2%	0.8%	52.5%

Table 4.19 Sensitivity of Analysis of Thresholds for Ramp Segment Type

Threshold (CRI score)	Sensitivity	Specificity	False positive rate	Overall accuracy
10	98.8%	2.8%	97.2%	50.8%
20	98.3%	5.1%	94.9%	51.7%
30	90.4%	22.0%	78.0%	56.2%
40	67.8%	71.8%	28.2%	69.8%
50	44.6%	95.5%	4.5%	70.1%
60	27.1%	98.9%	1.1%	63.0%
70	15.3%	99.4%	0.6%	57.4%
80	6.2%	99.5%	0.5%	52.9%
90	2.8%	99.5%	0.5%	51.2%

The tables show that sensitivity and false positive rate increase as the threshold is set at lower values and that the threshold that makes the greatest overall accuracy is different according to segment type. These results indicate that the threshold point for each segment type that achieved the greatest overall accuracy is very close to the one that is made by the Youden index. This proves that the Youden index can be utilized as a basis for choosing a threshold that maximizes the overall accuracy.

4.8 *Crash Risk Monitoring*

This section presents a practical application of the CRIs to predict high crash risk by monitoring change in crash risk scores. A time period when the CRI score is above the threshold is referred to as high crash risk. Hence, time periods having high crash risk were found by the threshold values determined in Table 4.13.

Crash risk monitoring was conducted for the I-110N in California. Figure 4.7 illustrates the entire 13.14-mile segment, including seven basic straight segments, one basic curved segment, two basic rolling segments, three weaving segments, and twelve ramp segments. Crash data provides segment locations, crash time, and duration.

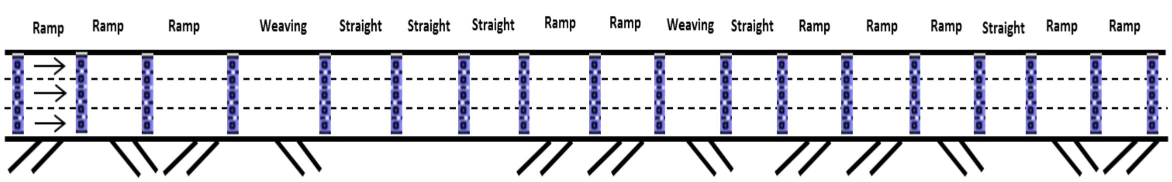

Figure 4.7 The Entire 13.14-mile Stretch on the I-110N in CA Divided into Segments

4.8.1 Basic Straight Segment

Seven basic straight segments exist in the 13.14-mile stretch, and each of these segments has crash cases. For example, the greatest number of crashes, 34, occurred on a segment between upstream detector station 774658 and downstream detector station 772501. Table 4.20 presents three examples of these crash cases where the crash risk was monitored during 5-min intervals, 30 minutes before a crash occurred. Figure 4.8 presents the data composition of crash and non-crash traffic conditions for crash number 63. The computed values of contributing factors for each 5-minute period are used to come up with the CRI score.

Table 4.20 CRI Scores for the Basic Straight Segments

Crash num:19	CRI score	Crash num:63	CRI score	Crash num:103	CRI score
1/20/2015 8:45	34	2/18/2015 19:40	59	4/13/2015 16:55	34
1/20/2015 8:50	34	2/18/2015 19:45	48	4/13/2015 17:05	26
1/20/2015 8:55	38	2/18/2015 19:50	50	4/13/2015 17:10	27
1/20/2015 9:00	26	2/18/2015 19:55	48	4/13/2015 17:15	22
1/20/2015 9:05	32	2/18/2015 20:00	47	4/13/2015 17:20	19
1/20/2015 9:10	37	2/18/2015 20:05	45	4/13/2015 17:25	19
1/20/2015 9:15	44	2/18/2015 20:10	64	4/13/2015 17:30	30
1/20/2015 9:20	46	2/18/2015 20:15	63	4/13/2015 17:35	21

TIME	crash(current traffic condition)							historical non-crash traffic condtion							CRI
	ADFUD	ADSUD	CVSD	OAFRU	OAFRD	SFU	VISIBILITY	ADFUD	ADSUD	CVSD	OAFRU	OAFRD	SFU	VISIBILITY	
2/18/2015 19:40	115.245	11.500	0.003	1.021	1.028	38.184	10	113.667	9.767	0.010	1.040	1.045	9.899	10	59
2/18/2015 19:45	114.298	11.500	0.009	1.014	1.026	9.192	8	128.333	9.800	0.006	0.973	1.045	21.685	10	48
2/18/2015 19:50	119.487	11.400	0.020	1.009	1.028	12.021	9	135.333	9.600	0.022	1.021	1.040	19.092	10	50
2/18/2015 19:55	116.278	11.500	0.000	1.014	1.024	12.021	10	147.333	14.667	0.032	1.128	1.039	26.634	10	48
2/18/2015 20:00	133.267	9.100	0.086	1.092	1.017	21.213	10	109.333	19.067	0.011	1.116	1.041	15.792	9	47
2/18/2015 20:05	134.388	8.100	0.000	1.115	1.019	7.071	10	143.000	20.800	0.009	1.075	1.033	20.978	10	45
2/18/2015 20:10	185.187	8.400	0.042	1.026	1.027	33.234	9	161.333	23.267	0.041	1.068	1.034	7.307	9	64
2/18/2015 20:15	204.234	9.000	0.029	1.060	1.022	35.355	9	144.667	26.667	0.077	1.109	1.032	9.192	10	63

Figure 4.8 Data Composition of Crash and Non-Crash Traffic Condition for Crash Number 63

For instance, crash number 19 occurred on January 20th, 9:20. The CRI scores of crash number 19 showed that the crash risk gradually increased and reached a high crash risk level after 9:10 where the CRI score was 44, above the threshold of 40 for basic straight segments. A crash eventually occurred 10 minutes later at 9:20. Crash number 63 showed high crash risk for the whole 30 minutes before the crash occurring at 20:15. However, crash number 103 indicated below threshold crash risk for the entire 30 minutes before the crash. A total of 69 crashes were monitored for basic straight segments, and high crash risk appeared for on average of 18 minutes before crash occurrences. Figure 4.9 illustrates the change in CRI scores before crashes occurred.

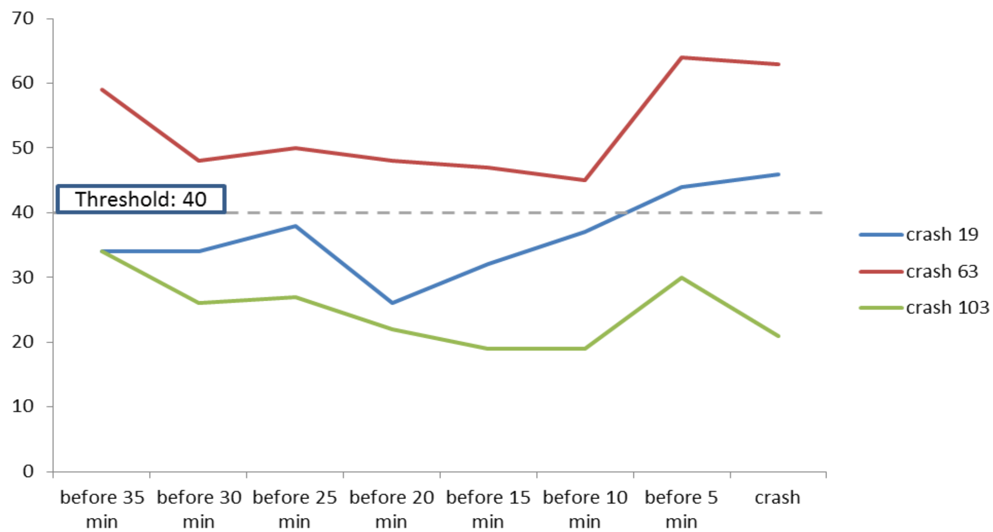

Figure 4.9 Change in CRI Score for the Basic Straight Segments

4.8.2 Basic Curved Segment

One basic curved segment exists in the 13.14-mile stretch in California, and the segment had 16 crash cases. Table 4.21 presents three crash cases where the crash risk was monitored during 5-min intervals, 30 minutes before a crash occurred.

Table 4.21 CRI Scores for the Basic Curved Segments

Crash num:71	CRI score	Crash num:153	CRI score	Crash num:108	CRI score
2/25/2015 16:35	27	6/1/2015 18:10	19	10/28/2015 15:25	24
2/25/2015 16:40	45	6/1/2015 18:15	37	10/28/2015 15:30	53
2/25/2015 16:45	52	6/1/2015 18:20	22	10/28/2015 15:35	29
2/25/2015 16:50	32	6/1/2015 18:25	26	10/28/2015 15:40	49
2/25/2015 16:55	39	6/1/2015 18:30	36	10/28/2015 15:45	41
2/25/2015 17:00	25	6/1/2015 18:35	41	10/28/2015 15:50	44
2/25/2015 17:10	21	6/1/2015 18:40	54	10/28/2015 15:55	30
2/25/2015 17:15	26	6/1/2015 18:45	39	10/28/2015 16:00	31

For instance, crash number 71 occurred on February 25th, 17:10. The CRI scores of case number 71 showed high crash risk for 10 minutes from 16:35 -16:45. However, the crash risk dropped below the threshold of 31 before the crash occurred at 17:15. Crash number 153 showed high crash risk from 18:25 until the crash occurrence. The high crash risk remained 20 minutes before the crash. Crash number 108 presented high crash risk from 15:25 to right before the crash. The high crash risk lasted for 35 minutes. A total of 16 crashes were monitored, and high crash risk appeared for on average of 29 minutes before the crash occurred. Figure 4.10 illustrates the change in CRI scores before crashes occurred.

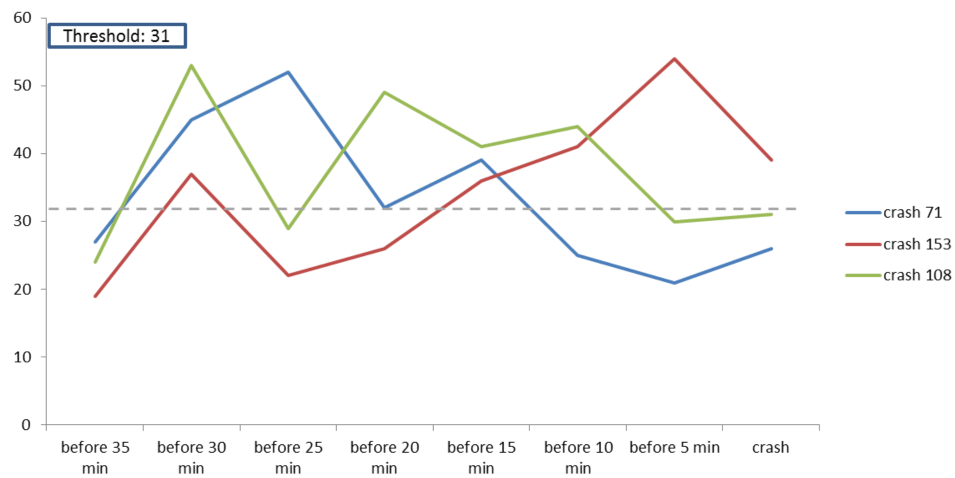

Figure 4.10 Change in CRI Score for the Basic Curved Segments

4.8.3 Basic Rolling Segment

Three basic rolling segments exist in the 13.14-mile stretch, and they had 27 crash cases. For example, the greatest number of crashes, 13, was observed to occur on a segment where is between upstream detector station 772501 and downstream detector station 718046. Table 4.22 presents three crash cases monitored crash risk during 5-min intervals, 30 minutes before a crash occurred.

Table 4.22 CRI Scores for the Basic Rolling Segments

Crash num:118	CRI score	Crash num:67	CRI score	Crash num:127	CRI score
11/12/2015 16:45	74	9/17/2015 16:30	69	5/6/2015 6:15	71
11/12/2015 16:50	66	9/17/2015 16:35	73	5/6/2015 6:20	66
11/12/2015 16:55	66	9/17/2015 16:40	77	5/6/2015 6:25	69
11/12/2015 17:00	72	9/17/2015 16:45	72	5/6/2015 6:30	65
11/12/2015 17:05	69	9/17/2015 16:50	70	5/6/2015 6:35	72
11/12/2015 17:10	71	9/17/2015 16:55	70	5/6/2015 6:40	67
11/12/2015 17:15	69	9/17/2015 17:00	65	5/6/2015 6:45	71
11/12/2015 17:20	71	9/17/2015 17:05	65	5/6/2015 6:50	71

For instance, crash number 118 occurred on November 12th, 17:20. The CRI scores for crash number 118 showed that the crash risk gradually increased surpassing the threshold for basic rolling segments until 16:55 with a CRI score of 72. A crash eventually occurred 25 minutes later at 17:20. The other two crash cases also showed high crash risk before the crashes occurred. Although they appeared not to be a high crash risk, their scores were very close to high crash risk regime. A total of 27 crashes were monitored for this segment, and high crash risk appeared for on average of about 35 minutes before crash occurrences. Figure 4.11 illustrates the change in CRI scores before crashes occurred.

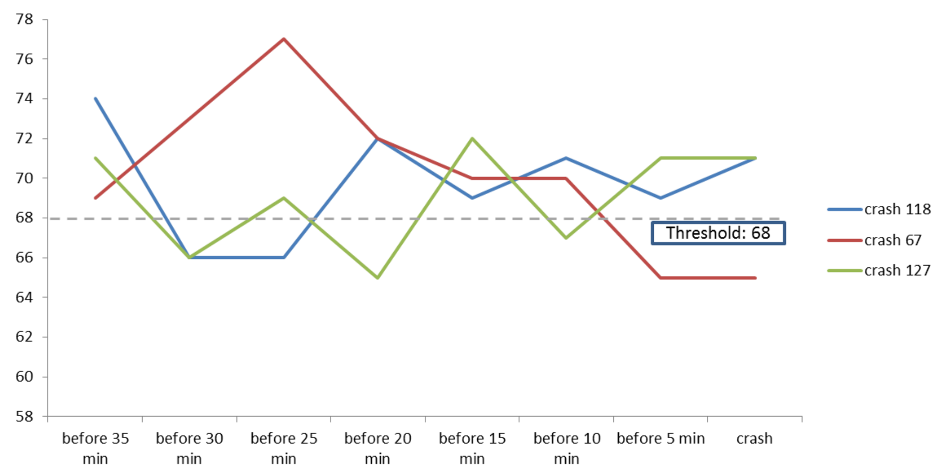

Figure 4.11 Change in CRI Score for the Basic Rolling Segments

Interestingly, four crashes occurred in the same segment at similar time periods. The first crash occurred at 17:35, the second at 17:50, the third at 18:15, and the fourth at 18:30. Table 4.23 shows the change in CRI scores between crashes. High crash risk was detected for nearly 25 minutes before the first crash at 17:00 and remained until the last crash occurred. Figure 4.12 illustrates the change in CRI scores before crashes occurred. As it is shown, high crash risk remained during the four crash occurrences.

Table 4.23 Change in CRI Score for Crash numbers 55,56,57,58

Crash number: 55,56,57,58	CRI score
2/11/2015 17:00	75
2/11/2015 17:05	67
2/11/2015 17:10	64
2/11/2015 17:15	73
2/11/2015 17:20	70
2/11/2015 17:25	69
2/11/2015 17:30	67
2/11/2015 17:35	70
2/11/2015 17:40	71
2/11/2015 17:45	73
2/11/2015 17:50	71
2/11/2015 17:55	72
2/11/2015 18:00	72
2/11/2015 18:05	69
2/11/2015 18:10	70
2/11/2015 18:15	71
2/11/2015 18:20	68
2/11/2015 18:25	68
2/11/2015 18:30	71

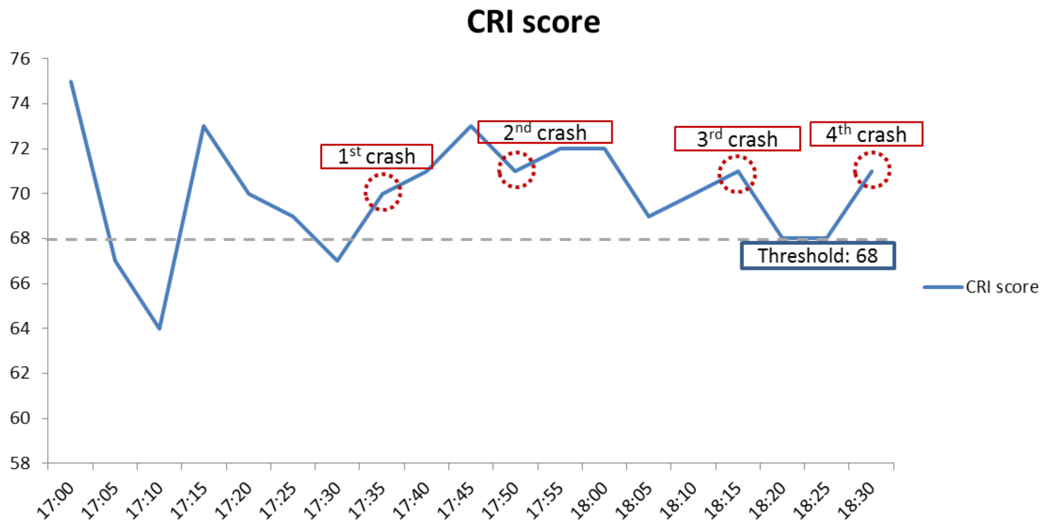

Figure 4.12 Change in CRI Score for Crashes 55,56,57,58

4.8.4 Weaving Segment

Four weaving segments exist in the 13.14-mile stretch, and each segment has crash cases. For example, the highest number of crashes, 19, were seen between upstream detector station 763400 and downstream detector station 763408. Table 4.24 presents three crash cases monitored for crash risk during 5-min intervals, 30 minutes before crashes occurred.

Table 4.24 CRI Scores for the Weaving Segments

Crash num:43	CRI score	Crash num:147	CRI score	Crash num:164	CRI score
2/3/2015 9:00	21	5/27/2015 9:05	19	12/17/2015 15:35	35
2/3/2015 9:05	20	5/27/2015 9:10	20	12/17/2015 15:40	22
2/3/2015 9:10	16	5/27/2015 9:15	19	12/17/2015 15:45	20
2/3/2015 9:15	14	5/27/2015 9:20	22	12/17/2015 15:50	20
2/3/2015 9:20	16	5/27/2015 9:25	23	12/17/2015 15:55	22
2/3/2015 9:25	18	5/27/2015 9:30	17	12/17/2015 16:00	20
2/3/2015 9:30	19	5/27/2015 9:35	13	12/17/2015 16:05	18
2/3/2015 9:35	21	5/27/2015 9:40	16	12/17/2015 16:10	16

All three crash cases did not show high crash risk in any time period before the crashes occurred. All the CRI scores were below the threshold of 27 before the crashes. In Table 4.13, the overall accuracy for weaving segments was 70.8%, which was the lowest among the segment types. The predictive accuracy of prediction of the crash events was 54.7%, and the false positive rate for the weaving segment was the greatest. Hence, the success of the crash risk prediction model for weaving segments highlights the need for additional investigation into other external factors affecting crash risk. Figure 4.13 illustrates the change in CRI scores before crashes occurred.

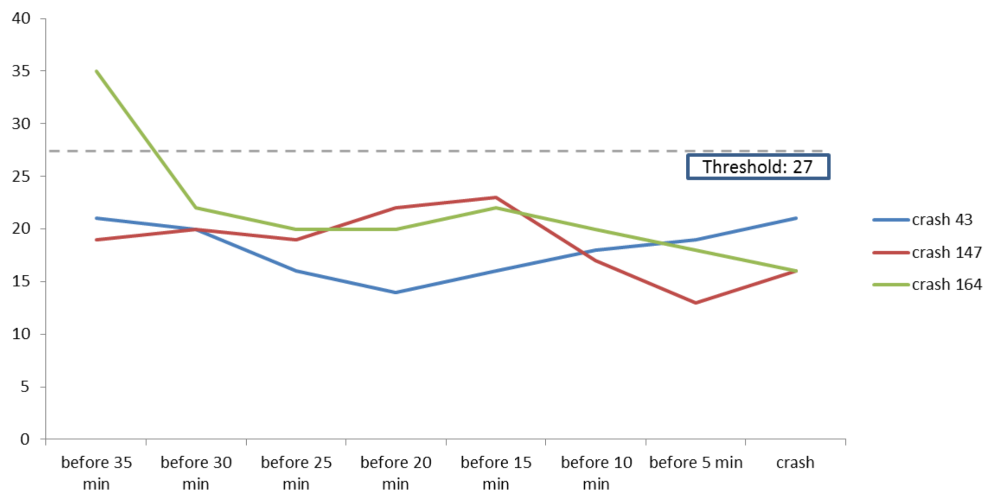

Figure 4.13 Change in CRI Score for the Weaving Segments

A total of 54 crashes were monitored, and high crash risk appeared for on average of 4 minutes before crash occurrences. It should be noted that a secondary crash occurred 25 minutes after the first crash. The first crash occurred at 8:25 and the second crash occurred at 8:50. Table 4.25 shows the change in crash risk between crashes. High crash risks were seen up to 60 minutes before the first crash at 7:25. Traffic conditions became stable for 10 minutes at 7:50, but soon turned back to be unstable and a state of high crash risk remained until the first crash occurred.

Once the first crash occurred, the high crash risk remained for 10 minutes. By the time the crash risk was rising again, the secondary crash had occurred at 8:50. Figure 4.14 illustrates the change in CRI scores before crashes occurred.

Table 4.25 Change in CRI Score for Crash numbers 144, 146

Crash number: 144,146	CRI score
5/27/2015 7:30	37
5/27/2015 7:35	31
5/27/2015 7:40	38
5/27/2015 7:45	60
5/27/2015 7:50	46
5/27/2015 7:55	8
5/27/2015 8:00	20
5/27/2015 8:05	32
5/27/2015 8:10	55
5/27/2015 8:15	55
5/27/2015 8:20	47
5/27/2015 8:25	51
5/27/2015 8:30	54
5/27/2015 8:35	42
5/27/2015 8:40	16
5/27/2015 8:45	21
5/27/2015 8:50	25

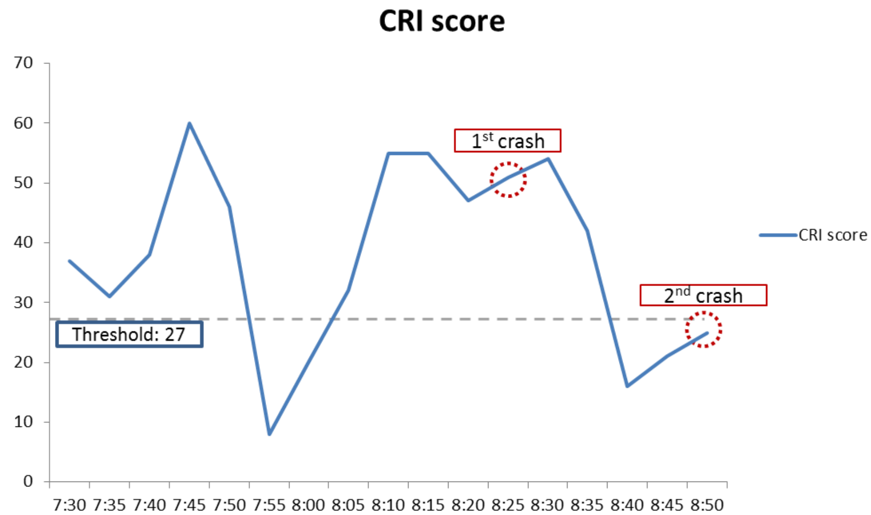

Figure 4.14 Change in CRI Score for Crashes 144,146

4.8.5 Ramp Segment

Twelve ramp segments exist in the 13.14-mile stretch, and each segment has crash cases. For example, the highest number of crashes, 51, occurred between upstream detector station 763392 and downstream detector station 763400. Table 4.26 presents three crash cases which were monitored for crash risk during 5-min intervals, 30 minutes before crashes occurred.

Table 4.26 CRI Scores for the Ramp Segments

Crash num:129	CRI score	Crash num:151	CRI score	Crash num:156	CRI score
12/3/2015 7:00	39	12/21/2015 16:30	41	12/16/2015 6:05	47
12/3/2015 7:05	28	12/21/2015 16:35	39	12/16/2015 6:10	37
12/3/2015 7:10	34	12/21/2015 16:40	47	12/16/2015 6:15	42
12/3/2015 7:15	42	12/21/2015 16:45	46	12/16/2015 6:20	46
12/3/2015 7:20	46	12/21/2015 16:50	49	12/16/2015 6:25	48
12/3/2015 7:25	50	12/21/2015 16:55	45	12/16/2015 6:30	48
12/3/2015 7:30	49	12/21/2015 17:00	50	12/16/2015 6:35	50
12/3/2015 7:35	32	12/21/2015 17:05	34	12/16/2015 6:40	51

For instance, crash number 129 occurred on December 3rd, 7:35. The CRI scores of crash number 129 showed high crash risk for 20 minutes before the crash occurring at 7:35. Crash number 151 showed high crash risk for 30 minutes before the crashing occurring at 17:05. Crash number 156 showed high crash risk for 25 minutes before the crash occurring at 6:40. A total of 177 crashes were monitored for this segment, and high crash risk appeared for on average of 24 minutes before crash occurrences. Figure 4.15 illustrates the change in CRI scores before crashes occurred.

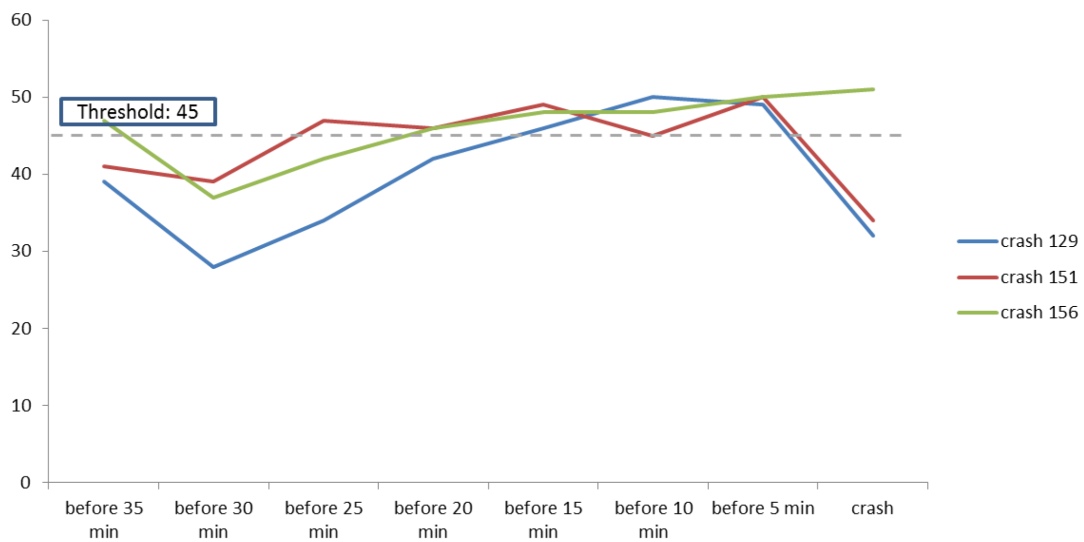

Figure 4.15 Change in CRI Score for the Ramp Segments

Interestingly, three crashes occurred in the same segment at similar time periods. The first crash occurred at 6:05, the second at 6:10, and the third at 6:15. Table 4.27 shows the change in crash risk between crashes. All the time periods prior to and between the crashes showed a high crash risk. Figure 4.16 illustrates the change in CRI scores before crashes occurred.

Table 4.27 Change in CRI Score in Crash Numbers 27, 28, 29

Crash number: 27,28,29	CRI score
1/27/2015 5:40	60
1/27/2015 5:45	64
1/27/2015 5:50	50
1/27/2015 5:55	51
1/27/2015 6:00	54
1/27/2015 6:05	44
1/27/2015 6:10	51
1/27/2015 6:15	44

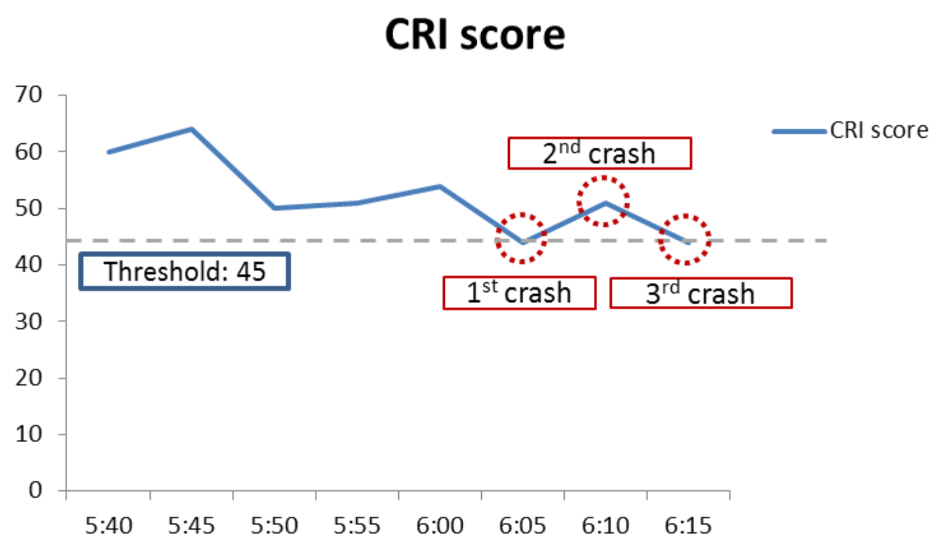

Figure 4.16 Change in CRI Score in Crashes 27, 28, 29

4.8.6 Whole Stretch Monitoring

The above section presented the application of CRI for each segment type such that high crash risk appeared before the crashes occurred and still remained for secondary crash cases.

This section presents monitoring of the change in crash risk on the whole 13.14-mile stretch with respect to traffic conditions of one day randomly picked. The 13.14-mile stretch included seven basic straight segments, one basic curved segment, two basic rolling segments, three weaving segments, and twelve ramp segments. A subject day was randomly chosen and the corresponding five non-crash days of the same time and day of the week from previous weeks before the subject day were also randomly chosen to compute the CRI for the whole stretch. Traffic data on the subject day and averaged traffic data on the five non-crash days were used to calculate CRI scores. The analysis was conducted for morning peak hours (06:00 – 9:00) and afternoon peak hours (16:00 – 19:00), separately.

- Subject day: 04.15.2015, Wednesday, morning peak 06:00 – 09:00 and afternoon peak 16:00 – 19:00.
- Non-crash day: 02.25.2015 (Wednesday), 03.04.2015 (Wednesday), 03.11.2015 (Wednesday), 03.18.2015(Wednesday), 03.25.2015(Wednesday)

Table 4.28 and Table 4.29 present the change in CRI scores for the whole 13.14-mile stretch for both the morning peak and afternoon peak. R, W, S, C, and RO represent ramp, weaving, basic straight, basic curved, and basic rolling segments, respectively. High crash risks are highlighted in red. An actual crash event occurred at 8:50, and that is highlighted in yellow. Consequently, each segment has 38 5-min time slots (12 5-min time slot/hour * 3 hours + extra 2 5-min time slots).

High crash risks tended to manifest in the middle of the stretch in both morning and afternoon peaks except for R2, which is upstream of the stretch. The duration of R2 was almost the whole three hours. Also, the high crash risk had a tendency of moving to downstream as time went on as indicated with the red arrow. On average, each segment had about 13 high crash risk 5-minute slots out of the 38 5-min time slots. As a result, high crash risk segments were judged to be:

- Morning peak: R1-R2(0.54 mile), W3-R7(1.79 miles), R9-S7(2.6 miles), C1-RO2(1.3 miles)

- Afternoon peak: R1(0.27 mile), R4-R5(0.66 miles), W3-R6(1.48 miles), R9-R10(1.1 miles), R12-RO2(1.54 miles)

The number of crashes for morning and afternoon peak in these segments was 70 and 91 which account for 46%, 56%, respectively.

On the other hand, each 5-min slot showed on average ten high crash risks in the 13.14-mile stretch. Therefore, high crash risk time periods were judged to be:

- Morning peak: 6:05-6:30, 7:20-7:25, 7:40-7:55, 8:05-8:10, 8:20-8:30, 8:40-9:05

- Afternoon peak: 16:55-17:05, 17:35-18:00, 18:10-19:05

The number of crashes for morning and afternoon peak in these time periods was 58 and 55 which account for 38.9% and 34%, respectively. During the morning peak, the most frequent crashes occurred on R5 with 39 actual crash events and four high crash risk warnings. Also, the most frequent time period for crashes was 8:45 where 15 events were judged to be high crash risk time periods.

During the afternoon peak, the most frequent crashes occurred on R9 with 35 actual crash events and 20 high crash risk warnings, one of the highest crash risk segments. Also, the most frequent time period for crashes was 19:00 where 17 events that were judged to be high crash risk time periods.

Table 4.28 Crash Risk Monitoring during Morning Peak

Time	R1	R2	R3	W1	S1	S2	S3	R4	R5	W2	W3	S4	R6	R7	R8	S5	R9	R10	R11	S6	S7	R12	C1	RO1	RO2
4/15/2015 6:00	35	43	38	24	36	33	31	34	37	24	22	28	49	46	34	33	44	62	59	32	39	33	42	68	72
4/15/2015 6:05	38	49	40	27	36	27	36	40	27	26	18	36	53	39	34	32	45	36	66	46	42	41	37	73	79
4/15/2015 6:10	27	49	42	19	31	30	20	31	37	22	17	44	45	39	41	35	53	40	55	50	49	48	39	64	69
4/15/2015 6:15	42	53	43	17	28	24	38	38	42	21	11	32	46	37	53	39	42	31	56	37	37	50	35	74	68
4/15/2015 6:20	39	57	41	19	42	51	26	47	48	16	7	46	43	31	34	27	43	41	60	56	43	34	40	79	68
4/15/2015 6:25	38	50	38	20	33	38	31	33	33	16	8	48	46	41	38	41	55	51	74	64	24	37	39	66	77
4/15/2015 6:30	45	59	34	22	52	42	38	36	33	13	21	34	58	35	34	14	62	27	49	43	33	27	37	69	60
4/15/2015 6:35	45	51	35	23	35	26	35	42	41	17	33	26	38	46	41	33	32	20	54	38	21	52	39	79	57
4/15/2015 6:40	43	51	40	21	39	40	33	33	31	12	34	35	52	37	36	25	42	40	48	42	16	41	36	72	77
4/15/2015 6:45	40	52	39	16	36	29	36	43	36	11	34	30	47	47	36	24	36	26	57	50	43	38	32	66	71
4/15/2015 6:50	26	49	36	16	29	33	30	40	33	21	27	37	41	43	40	32	35	45	44	47	33	32	39	72	77
4/15/2015 6:55	35	47	36	21	35	39	18	34	31	19	21	50	42	42	48	38	42	26	57	55	29	36	35	79	78
4/15/2015 7:00	43	56	42	24	26	23	34	41	43	16	15	31	48	36	44	22	40	34	46	54	39	32	33	72	73
4/15/2015 7:05	29	50	34	25	33	37	24	45	51	15	18	35	52	48	52	33	38	34	42	40	34	40	37	74	65
4/15/2015 7:10	52	53	41	26	35	43	27	40	40	15	19	44	43	44	39	30	35	35	50	45	41	34	36	67	64
4/15/2015 7:15	43	54	38	23	43	32	31	34	34	20	14	33	35	40	35	22	44	44	50	64	49	44	37	73	72
4/15/2015 7:20	50	57	40	15	47	46	38	43	35	17	19	47	43	46	39	33	44	51	51	41	41	35	40	70	69
4/15/2015 7:25	44	58	40	12	33	40	29	38	36	18	18	37	56	47	48	59	57	48	49	47	43	49	40	72	76
4/15/2015 7:30	41	55	37	11	34	37	24	38	42	19	24	56	61	58	43	34	41	45	42	48	35	34	38	72	77
4/15/2015 7:35	38	54	33	17	33	24	43	42	40	20	19	64	40	44	39	31	45	39	41	50	25	23	33	72	70
4/15/2015 7:40	41	65	37	18	34	43	39	40	45	14	13	29	46	49	40	36	43	46	55	53	32	49	41	75	69
4/15/2015 7:45	37	59	45	16	31	24	52	40	41	17	17	37	47	38	44	36	46	47	49	48	42	40	36	71	70
4/15/2015 7:50	36	56	41	15	34	51	57	39	27	20	18	38	43	35	33	35	48	48	57	45	31	40	37	74	69
4/15/2015 7:55	56	55	38	10	38	41	17	36	45	17	20	38	41	45	40	44	43	50	61	50	40	19	39	70	72
4/15/2015 8:00	33	50	38	14	33	29	31	39	38	14	22	43	43	33	32	37	44	44	59	47	26	33	38	70	69
4/15/2015 8:05	31	52	40	14	40	40	25	34	36	16	22	34	36	46	49	44	47	44	57	51	42	42	37	77	82
4/15/2015 8:10	27	46	39	11	34	27	24	36	36	15	20	52	45	47	43	29	40	48	59	35	42	45	41	71	79
4/15/2015 8:15	31	50	33	14	37	37	23	35	38	11	26	38	44	36	34	30	47	51	59	40	37	39	43	70	71
4/15/2015 8:20	45	48	34	11	36	38	26	40	39	13	27	41	39	43	50	41	48	39	62	50	20	42	39	81	71
4/15/2015 8:25	46	51	41	2	40	39	34	34	39	20	27	42	51	45	41	33	47	41	66	50	43	39	33	73	70
4/15/2015 8:30	50	53	41	0	37	43	26	35	41	18	29	31	52	38	36	24	46	56	68	56	40	41	33	69	71
4/15/2015 8:35	64	54	37	2	38	29	39	41	44	14	25	43	44	40	52	35	43	29	62	55	35	42	40	67	69
4/15/2015 8:40	49	55	44	3	30	37	52	46	44	14	26	35	46	41	37	29	45	53	75	58	36	40	36	65	69
4/15/2015 8:45	55	59	43	8	28	32	33	46	57	12	34	41	45	40	36	30	49	45	66	47	43	40	38	74	70
4/15/2015 8:50	19	49	40	9	34	30	40	49	40	16	33	42	51	37	48	36	45	39	67	47	39	44	86	68	70
4/15/2015 8:55	44	52	41	8	36	33	30	35	48	16	13	33	48	43	43	33	44	43	83	65	60	42	64	67	78
4/15/2015 9:00	43	51	38	14	41	44	35	41	44	14	19	34	41	41	42	40	54	61	77	43	34	55	61	82	66
4/15/2015 9:05	39	50	42	19	41	38	47	43	35	19	33	35	45	48	44	39	46	47	72	57	41	24	67	77	71
Crash frequency	3	2	6	5	0	9	0	1	39	10	7	0	7	10	2	6	11	4	0	2	13	1	3	2	6

Table 4.29 Crash Risk Monitoring for Afternoon Peak

Time	R1	R2	R3	W1	S1	S2	S3	R4	R5	W2	W3	S4	R6	R7	R8	S5	R9	R10	R11	S6	S7	R12	C1	RO1	RO2
4/15/2015 16:00	46	42	33	28	32	33	37	36	36	14	34	36	41	41	37	33	43	45	37	32	32	23	34	72	70
4/15/2015 16:05	33	41	27	26	36	30	29	14	37	20	36	38	36	38	40	33	42	24	34	30	39	39	46	70	67
4/15/2015 16:10	40	42	34	23	40	33	37	42	41	16	35	38	46	40	41	41	42	48	45	41	41	39	43	70	72
4/15/2015 16:15	45	39	29	20	45	46	38	31	40	17	30	30	35	40	41	32	42	32	35	39	35	36	30	71	72
4/15/2015 16:20	34	42	41	19	38	46	29	34	44	20	31	48	63	43	43	30	44	36	39	38	44	41	55	85	74
4/15/2015 16:25	43	40	35	21	38	35	34	36	36	16	27	45	52	43	25	29	44	40	47	35	28	54	48	91	83
4/15/2015 16:30	40	39	38	19	38	34	33	16	42	16	26	48	63	47	56	48	58	53	44	26	35	42	44	68	69
4/15/2015 16:35	51	42	32	23	35	38	30	46	40	16	26	40	63	48	39	31	50	62	45	37	38	38	28	75	71
4/15/2015 16:40	40	46	13	25	31	16	45	37	33	18	27	32	33	46	27	29	87	44	40	45	79	45	31	72	64
4/15/2015 16:45	39	37	21	29	30	42	44	44	24	17	34	25	20	31	34	30	36	40	34	35	30	49	25	69	69
4/15/2015 16:50	52	38	31	31	33	35	32	49	33	18	41	31	37	40	24	31	37	46	40	28	32	44	51	73	71
4/15/2015 16:55	28	40	33	32	31	27	31	40	46	14	38	30	47	47	32	23	52	59	41	43	39	38	47	71	67
4/15/2015 17:00	50	48	38	33	30	32	31	29	46	9	39	37	34	45	46	31	50	62	38	36	38	38	34	71	74
4/15/2015 17:05	38	43	39	30	26	22	25	40	21	12	31	44	58	37	30	34	41	49	48	35	40	41	61	75	73
4/15/2015 17:10	40	41	46	28	28	20	24	43	28	21	33	46	42	32	33	23	44	56	42	39	31	42	36	79	82
4/15/2015 17:15	43	40	36	20	42	26	23	26	37	23	42	29	31	40	32	24	44	50	38	37	39	57	32	67	68
4/15/2015 17:20	34	41	38	15	36	27	32	37	31	24	35	39	47	39	38	34	44	44	42	32	37	42	39	69	69
4/15/2015 17:25	41	40	32	11	36	33	35	42	36	24	32	41	49	44	39	47	44	41	42	44	37	48	35	71	68
4/15/2015 17:30	50	45	30	7	33	48	32	39	38	24	32	36	42	36	34	32	40	42	35	36	31	44	58	69	73
4/15/2015 17:35	52	47	34	13	26	33	37	30	48	22	30	44	45	40	41	35	47	48	37	37	33	44	42	74	68
4/15/2015 17:40	50	48	40	18	36	40	38	51	49	22	33	43	48	38	35	32	48	48	39	39	33	41	32	71	69
4/15/2015 17:45	51	40	47	24	28	33	32	52	23	28	37	47	41	40	35	28	48	63	47	46	32	44	41	75	68
4/15/2015 17:50	40	42	35	26	36	39	31	33	47	28	28	43	41	40	53	35	51	49	38	29	31	37	50	69	68
4/15/2015 17:55	29	39	39	29	25	29	31	47	45	19	24	45	33	38	46	34	59	57	47	60	36	50	44	70	73
4/15/2015 18:00	40	40	34	29	32	34	40	42	23	22	29	42	36	43	52	42	55	44	30	31	39	49	30	72	70
4/15/2015 18:05	41	40	29	28	25	29	39	40	36	20	24	34	28	38	38	31	50	64	46	39	31	43	43	73	70
4/15/2015 18:10	39	38	38	24	27	38	24	51	49	16	28	42	52	40	39	27	48	39	36	40	34	43	33	71	73
4/15/2015 18:15	36	39	37	23	33	23	42	28	47	18	30	39	56	43	52	30	49	46	40	46	36	54	32	70	69
4/15/2015 18:20	46	41	37	21	34	35	38	35	47	18	24	37	47	42	51	30	36	55	45	40	32	54	42	69	72
4/15/2015 18:25	27	40	28	23	34	23	36	52	18	23	26	33	58	42	43	23	54	52	40	31	35	58	57	74	76
4/15/2015 18:30	31	38	34	21	19	18	25	27	27	21	41	42	46	36	39	31	52	60	39	45	34	48	34	69	70
4/15/2015 18:35	42	40	24	20	29	42	43	54	41	30	14	42	40	36	23	18	41	57	37	36	39	49	51	73	77
4/15/2015 18:40	52	47	31	16	45	40	32	49	41	30	-19	48	65	50	49	29	49	54	40	34	36	48	39	77	73
4/15/2015 18:45	35	41	35	10	39	25	29	35	27	21	-2	68	65	48	39	31	47	53	46	32	30	48	44	72	78
4/15/2015 18:50	44	39	31	15	21	38	9	29	17	16	28	22	44	44	38	22	50	52	40	31	40	44	39	75	79
4/15/2015 18:55	50	49	38	15	33	37	42	49	42	15	36	27	30	33	27	17	35	49	37	29	36	48	41	69	71
4/15/2015 19:00	55	48	44	10	46	61	32	44	36	16	28	48	60	51	50	42	48	45	45	36	34	53	50	70	71
4/15/2015 19:05	40	40	37	16	41	46	22	46	29	19	24	37	66	44	32	35	44	45	44	34	39	49	32	72	71
Crash frequency	0	0	13	8	0	3	2	2	12	3	2	1	0	4	0	7	35	12	5	5	21	8	13	0	6

4.9 Updating-temporal transferability

As mentioned in Section 2.3, the model parameters do not remain stable over time or space. Thus, a crash risk prediction model cannot be directly transferred from one freeway to another due to the variability in traffic conditions, driver populations, and geometric characteristics. Consequently, the crash risk prediction model developed for one freeway produces a low predictive performance on other freeways. However, once a model is well specified, updating would be more cost-effective than developing a new model. From the lessons in previous studies, this study does not consider the spatial updating because of the very poor predictive performance of the spatial updating. In this study, the Bayesian random intercept regression models for the I-110N freeway in 2015 are updated. Bayesian updating approach is used to update the models for the I-110N freeway in 2016. This approach can update an old model as new data become available. When updating the crash risk prediction models, the estimation results of the models developed by 2015 data are used as the informative prior distributions and are incorporated into 2016 data in a new updated posterior distribution. Finally, the predictive performances of the updated models are evaluated based on sensitivity depending on different false alarm rates.

4.9.1 Bayesian Random Intercept Logistic Regression Models in 2016

Before updating the 2015 Bayesian random logistic regression models, the proposed generalized procedure was conducted to identify significant contributing factors on the I-110N freeway in 2016. The purpose of this is to compare the predictive performance of the new 2016 Bayesian random intercept logistic regression models with updated 2015 Bayesian random intercept logistic regression models.

There are 223 crashes in 2016 including 60 basic straight segment crashes, 12 basic rolling segment crashes, 7 basic curved segment crashes, 24 weaving segment crashes, and 120 ramp segment crashes. The whole dataset was split into training and validation datasets. For training dataset, 70% of the whole dataset had a total of 156 crashes including 42 basic straight segment crashes, 5 basic curved segment crashes, 8 basic rolling segment crashes, 17 weaving segment crashes, and 84 ramp segment crashes. The training dataset was used to develop Bayesian random intercept logistic regression models. The remaining 30% of the whole dataset which is validation dataset including 18 basic straight segment crashes, 2 basic curved segment crashes, 4 basic rolling segment crashes, 7 weaving segment crashes, and 36 ramp segment crashes was used to compute crash risk index and to validate the performance of the Bayesian random intercept logistic regression models. Table 4.30 presents the identified contributing factors in 2016.

Table 4.30 The Contributing Factors in 2015 and 2016

Segment type	Contributing Factor	
	2015	2016
Basic Straight Segment	• ADFUD • ADSUD • CVSD • OAFRU • OAFRD • SFU • VISIBILITY • LIGHT CONDITION	• ADFUD • ADOUD • CVSD • ADSLU • ADFLU • OAFRD • VISIBILITY • LIGHT CONDITION
Basic Curved Segment	• CVFU • ADCVSUD • OAFRU • SSD • PAVEMENT • LIGHT CONDITION	• CVFU • ADSUD • OAFRU • ATU • PAVEMENT • LIGHT CONDITION
Basic Rolling Segment	• CVFD • OAFRU	• CVFD • OAFRU • SSD
Weaving Segment	• ADSUD • ATD • CVFU • CVSD • PAVEMENT	• ADSUD • ATD • CVFU • ATU • OAFRD • PAVEMENT
Ramp Segment	• ADFLD • ADSLU • OAFRU • SFD • SFU • SSD • PAVEMENT	• ADFLD • ADSLU • OAFRU • ATU • SSD • PAVEMENT

The results show the changes in contributing factors. Some factors that are significant in 2015 turn out to be insignificant in 2016 and some new factors are selected in 2016. Thus, the traffic flow conditions on the selected I-110 northbound section in 2015 and 2016 were compared. Table 4.31 shows the changes in traffic variables. As shown in Table 4.31, the average flow rate grew by 4.96%, and the average occupancy increased by 8.48% and the average speed decreased by

4.87%. There was no change in geometric characteristics. The difference in traffic patterns indicates that the contributing factors might be distinct over time.

Therefore, new Bayesian random intercept logistic regression models in 2016 are developed and compared with 2015 models as presented in Table 4.32 – Table 4.36.

Table 4.31 The Change in Traffic Variables on I-110 northbound in 2015 and 2016

Traffic variable	I-110N, 2015	I-110N, 2016	Percent change between 2015 and 2016
Average flow (veh/h/lane)	1517	1592	4.96%
Average occupancy (%)	33	36	8.48%
Average speed (mph)	49	46	-4.87%
Average truck (veh/h)	195	212	9.11%

Table 4.32 Estimation Results of Bayesian Random Intercept Logistic Regression Model on Basic Straight Segments in 2016

Variable	Model 1(I-110N, 2015)				Model 2 (I-110N, 2016)			
	Mean	(2.5%	97.5%)[b]	OR	Mean	(2.5%	97.5%)	OR
Intercept	-4.037	-5.129	-3.824	-	-4.725	-5.235	-4.147	
ADFUD	-0.014	-0.022	-0.007	0.986	0.007	0.001	0.013	1.007
ADOUD	-[a]	-	-	-	-0.018	-0.070	0.034	0.983
ADSLU	-	-	-	-	0.036	-0.100	0.175	1.039
ADFLU	-	-	-	-	0.084	0.075	0.092	1.088
ADSUD	0.003	-0.038	0.044	1.003	-	-	-	-
CVSD	0.003	-0.059	0.065	1.003	0.052	0.027	0.071	1.053
OAFRU	-0.003	-0.064	0.061	0.998	-	-	-	-
OAFRD	-0.003	-0.064	0.059	0.998	-0.012	-0.207	1.083	0.993
SFU	0.035	0.021	0.051	1.036	-	-	-	-
VISIBILITY	-0.026	-0.081	0.030	0.975	-0.090	-0.091	-0.087	0.914
LIGHT	0.038	0.019	0.053	1.039	0.052	0.048	0.063	1.053

a This variable is insignificant in the model
b The 95% credible interval for the parameter estimates

Table 4.33 Estimation Results of Bayesian Random Intercept Logistic Regression Model on Basic Curved Segments in 2016

Variable	Model 1(I-110N, 2015)				Model 2 (I-110N, 2016)			
	Mean	(2.5%	97.5%)b	OR	Mean	(2.5%	97.5%)	OR
Intercept	-4.794	-5.102	-4.414	-	-4.228	-4.768	-4.173	-
CVFU	-0.027	-0.638	0.594	1.023	-0.004	-0.200	0.193	1.001
DCVSUD	0.027	-0.592	0.647	1.079	-	-	-	-
OAFRU	-0.234	-0.802	0.345	0.826	-0.013	-0.206	0.182	0.992
SSD	0.129	0.006	0.267	1.140	-	-	-	-
ATU	-	-	-	-	0.074	-0.004	0.168	1.089
ADSUD	-	-	-	-	-0.006	-0.174	0.164	0.998
PAVEMENT	0.014	0.008	0.025	1.014	0.028	0.021	0.040	1.029
LIGHT	0.052	0.034	0.079	1.053	0.083	0.076	0.090	1.087

a This variable is insignificant in the model
b The 95% credible interval for the parameter estimates

Table 4.34 Estimation Results of Bayesian Random Intercept Logistic Regression Model on Basic Rolling Segments in 2016

Variable	Model 1(I-110N, 2015)				Model 2 (I-110N, 2016)			
	Mean	(2.5%	97.5%)b	OR	Mean	(2.5%	97.5%)	OR
Intercept	-3.852	-4.278	-3.529	-	-3.247	-3.879	-2.945	-
CVFD	0.107	-0.506	0.732	1.170	0.001	-0.194	0.197	1.006
OAFRU	0.007	-0.479	0.492	1.039	0.022	-0.171	0.213	1.027
SSD	-	-	-	-	0.115	0.095	0.140	1.122

a This variable is insignificant in the model
b The 95% credible interval for the parameter estimates

Table 4.35 Estimation Results of Bayesian Random Intercept Logistic Regression Model on Weaving Segments in 2016

Variable	Model 1(I-110N, 2015)				Model 2 (I-110N, 2016)			
	Mean	(2.5%	97.5%)b	OR	Mean	(2.5%	97.5%)	OR
Intercept	-4.012	-4.499	-3.825	-	-3.712	-4.182	-3.412	-
ADSUD	0.064	0.014	0.115	1.066	0.079	0.071	0.082	1.082
ATD	0.080	0.044	0.122	1.083	0.036	0.004	0.071	0.999
ATU	-	-	-	-	0.024	0.020	0.071	1.024
CVFU	0.001	-0.060	0.064	1.002	0.006	0.201	0.190	1.037
CVSD	0.004	-0.057	0.065	1.004	-	-	-	-
OAFRD	-	-	-	-	0.038	0.231	0.155	0.967
PAVEMENT	0.033	0.019	0.059	1.034	0.041	0.036	0.053	1.042

a This variable is insignificant in the model

Table 4.36 Estimation Results of Bayesian Random Intercept Logistic Regression Model on Ramp Segments in 2016

Variable	Model 1(I-110N, 2015)				Model 2 (I-110N, 2016)			
	Mean	(2.5%	97.5%)b	OR	Mean	(2.5%	97.5%)	OR
Intercept	-5.111	-5.728	-4.842	-	-5.782	-6.136	-5.234	-
ADFLD	-0.070	-0.102	-0.040	0.932	-0.052	-0.094	-0.022	0.949
ADSLU	-0.010	-0.079	0.056	0.991	-0.049	-0.137	0.037	0.953
OAFRU	0.033	-0.034	0.117	1.035	0.016	-0.172	0.206	1.021
SFD	0.005	-0.003	0.013	1.005	-	-	-	-
SFU	0.008	0.003	0.013	1.008	-	-	-	-
SSD	0.046	0.017	0.079	1.047	0.113	0.092	0.131	1.120
ATU	-	-	-	-	0.012	-0.009	0.034	1.013
PAVEMENT	0.065	0.038	0.089	1.067	0.083	0.071	0.098	1.087

a This variable is insignificant in the model
b The 95% credible interval for the parameter estimates

Model 1 and Model 2 represent the crash risk prediction models for I-110N freeway in 2015 and 2016, respectively. These results indicate that the impact of contributing factors for certain time period is not maintained and the impact can be zero for other time periods. For instance, the factor OAFRU on ramp segments in 2015 and 2016 has the odds ratios of 1.035 and 1.021, respectively. The OAFRU had an impact of an increase in crash risk by 3.5% in 2015, but the impact is changed to 2.1% in 2016. Also, the factor ATU didn't turn out to be a significant factor in 2015, but it has an impact of 1.3% increase in crash risk in 2016.

On the other hands, Bayesian updating approach is effective in improving temporal transferability even when new data are limited. When limited new data are available, updating an existing model is better than developing a model using the limited new data. Also, developing a new model in the next year may take longer to get high predictive performance since it would take time for data to be accumulated. This chapter shows the updated 2015 crash risk models, assuming that we have limited amount of data for 2016 (25%, 50%, and 90% of the whole 2016 dataset). It is expected that the predictive performance of the updated models increases with an increase in the sample size.

The estimation results of the 2015 models developed by 2015 dataset were used as the informative prior distribution and the new dataset of 2016 were incorporated in a new updated posterior distribution. Temporal updating was tested by evaluating the predictive performance. For evaluation of the predictive performance, a dataset that was not used in the updated 2015 crash risk models was used as scoring dataset. Table 4.37 to Table 4.39 summarize the predictive performance of updated 2015 models in 2016. For comparison, the prediction performances of the new developed Bayesian random intercept regression models in 2016 without informative prior data of 2015 and with informative prior data of 2015 are evaluated and are compared with the updated 2015 models with the various limited data of 2016 as shown in Table 4.37 to Table 4.39.

Table 4.37 Predictive Performance of Updated 2015 Models on Basic Straight Segments in 2016

False alarm rates	Sensitivity (%) (True Positive Rate)			The sensitivity of 2015 crash risk models updated by different sub-samples (%)		
	New 2016 model with no 2015 data	New 2016 model with 2015 data	2015 models in 2016	25%	50%	90%
0.05	68.3	71.2	31.5	35	46.7	60
0.1	73.3	74.5	43.8	45	49.2	63.3
0.15	75	77.7	48.8	50	53.5	69.2
0.2	78.3	80.9	52.8	51.7	59.1	70
0.25	83.3	85.2	54.1	53	62	71.2

Table 4.38 Predictive Performance of Updated 2015 Models on Weaving Segments in 2016

False alarm rates	Sensitivity (%) (True Positive Rate)			The sensitivity of 2015 crash risk models updated by different sub-samples (%)		
	New 2016 model with no 2015 data	New 2016 model with 2015 data	2015 models in 2016	25%	50%	90%
0.05	38.7	41.4	14.8	16.7	31.3	45.8
0.1	55.2	57.8	29.7	33.0	41.7	61.5
0.15	58.3	63.4	38.1	38.8	42.5	68.2
0.2	62.5	69.3	43.2	44.1	48.5	70.8
0.25	68.1	75.2	49.1	50.9	54.3	70.8

Table 4.39 Predictive Performance of Updated 2015 Models on Ramp Segments in 2016

False alarm rates	Sensitivity (%) (True Positive Rate)			The sensitivity of 2015 crash risk models updated by different sub-samples (%)		
	New 2016 model with no 2015 data	New 2016 model with 2015 data	2015 models in 2016	25%	50%	90%
0.05	30.8	34.5	17.8	19.2	27.1	30.1
0.1	57.5	62.8	37.1	38.2	45.8	55.2
0.15	65	70.2	47.9	49.5	52.9	63.1
0.2	65.8	74.9	50	51.7	59.8	66.8
0.25	68.3	79.2	55.1	55.9	61	70.3

It should be noted that the number of 2016 crash data on basic curved segments and basic rolling segments were not large enough to update the 2015 crash risk models so these two segment types are excluded in the analysis.

The predictive performance of the newly developed 2016 models is noticeably better than that of updated 2015 crash risk models. Also, the developed 2016 models with the informative prior distribution of the year 2015, produced the better predictive performance. As expected, the Bayesian framework that adds a prior distribution of each parameter could make a model better performance.

However, updated 2015 models provide better predictive performance than 2015 models in 2016, even for the minimum sample size that only contains 25% samples of the 2016 I-110N samples. The updated 2015 models with 25% sample size showed even better sensitivity (true positive rate) that it achieved over 50% at 0.15 false positive rate on basic straight segments. When the sample size is greater, the predictive performance is close to the newly developed 2016 models. Thus, this result indicates that the Bayesian updating approach is effective in improving the temporal transferability of the crash risk models with low data available. This study tried to update the existing models with the percentages of the whole 2016 data. In real world, it is expected that traffic operators can make a decision of how often an existing model is updated. It is not beneficial to update the models in real time since crash is a random event, but the update can be carried out monthly. For example, an existing model could be updated monthly once a month crash and traffic data is accumulated.

As a result, the outcomes of this analysis would be valuable for freeway traffic operators in how to timely maintain the use of crash risk prediction models. This approach is expected to be used to support the update of existing crash risk prediction models for traffic safety enhancement on freeways.

Chapter 5 Application of a New Variable Speed Limits (VSL) Control

5.1 *Introduction*

This chapter presents the feasibility of utilizing a Variable Speed Limits (VSL) control to improve safety on freeways once high crash risk computed by the crash risk indices is detected. We believe that proactive intervention strategies would be required to alleviate crash risk on freeways. In our experiments, real-time VSL was applied to a 2.6-mile segment on the northbound direction of the I-110 freeway in California in 2015. The details of the results are presented in the remaining sections.

5.2 *Variable Speed limits (VSL) Strategy*

A Variable Speed Limits (VSL) system adopts dynamic sign indicating speed limit that aims at reducing the traveling speed so that it achieves speed homogeneity between upstream flow and downstream flow. In the abundant VSL literature, system objectives mainly fall into the aspects of traffic safety improvement or freeway operation enhancement.

From the operation enhancement perspective, a VSL control can enhance operational efficiency on recurrently congested roadways. For instance, Chang et al. (2011) installed VSLs integrated with travel time information on recurrently congested segments in Maryland which improves travel time and throughputs by 10-25%. A study on the I-495 Capital Beltway (2009) revealed that VSL could postpone the formation of bottleneck congestion. Hadiuzzaman and Tony (2012) proposed Cell Transmission Model (CTM) based VSL control, and the VISSIM simulation results showed a 7% and 15% improvement in the flow rate and travel time, respectively. Yang et al. (2013) proposed a VSL control model adopting the concept of Kalman Filter. The proposed

VSL controls were simulated with different compliance rates in VISSIM. They found the reduction in travel time over recurrent bottleneck locations by 3%-16% compared to no VSL scenario.

On the other hand, VSL is also utilized to enhance traffic safety by reducing crash risk. VSL is initially designed to reduce the speed difference on some hazardous segments. Less variability leads to fewer crashes, fewer short headways, and lower mean speeds according to Ha et al. (2003). Smulders (1990) agreed that fewer crashes occur when speeds are lowered, and fewer short headways are observed. A study in Finland by Rämä (1999) again showed that VSL leads to lower speeds and less variability. The effect was attributed not only to smoothing of traffic flow through longer following distances but also through a reduction in the number of lane changes during congestion. Aty et al. (2008) found proper VSL strategy such as speed change implementation, speed zone threshold, speed change distance, and speed change time period reduce rear-end crash risk and lane-change crash risk with respect to different loading scenarios. Jo et al. (2012) proposed a new VSL algorithm based on the association of multiple stations on a freeway and confirmed that the speed variances were decreased and the speed differences between stations were also reduced by 14.2% and 20.1%, respectively. Van den Hoogen and Smulders (1994) performed an experiment with the application of variable speed control on motorways in the Netherlands. From the experiment, they found that the differences in volume, speed, and occupancy between and within lanes became smaller and variations also decreased when variable speed control was implemented. Rämä (1999) observed that the variable speed limits reduced mean speed and standard deviation of speed and increased the extent of speed reduction. Lee et al. (2006) demonstrated the potential safety benefits of VSL by using a real-time crash prediction model integrated with a microscopic traffic simulation model. The study found that VSL can reduce average total crash potential by 5-17%. In Yu et al. (2014) study, safety impacts of the VSL system were quantified as crash risk improvements and speed homogeneity improvements. The proposed VSL system demonstrated that the traffic safety improved by decreasing crash risk and enhancing speed homogeneity under the high and moderate compliance levels. Hasanpour et al. (2017) used an optimization decision tree for VSL and showed that the queue length was decreased by more than 20%. Also, a smoothing was achieved regarding speed changes and the number of stops and the stop time were reduced resulting in increased safety.

From the literature review, one can observe that proper control of traffic speed can contribute to both a reduction in crashes and improved efficiency of freeway operations. Most of VSL studies adopted an experimental design approach to identify the best control strategies. A certain number of different control strategies are simulated with microscopic simulation experiments and compared. The experimental design way requires extensive simulation work, and the results are not transferable between different facilities. The proper speed limit on one freeway can be less effective on other freeways. Rather than making an experimental design, a VSL control reflecting real-time traffic flow characteristics should be designed.

Furthermore, many advanced studies on real-time crash risk prediction models only emphasize the utilization of the crash risk prediction models as an evaluation measure of traffic safety and the studies have utilized them as a countermeasure for crash prevention rarely. Among many ways of real-time countermeasures, this study proposes a dynamic VSL control to reduce the resulting crash risk quantified by the CRI developed by crash risk prediction models under different five segment types.

Many field studies showed that VSL influences traffic flow characteristics such as speed and flow difference between upstream flow and downstream flow and between adjacent lanes, mean speed and speed variance. These studies found that VSL stabilizes traffic flow and reduces congestion. Through properly displayed and dynamically changed speed limit based on traffic conditions, it is believed that VSL can smooth the transition between upstream flow and downstream flow and reduce the crash risk impending crash occurrence. This chapter investigates the benefits of variable speed limit (VSL) implementation for real-time crash risk reduction.

5.3 <u>VSL Control Strategy</u>

In implementing VSL, we need to include logic that addresses the following four strategy control factors:

1. When should the speed limits be changed?
2. How long should the speed limits last?
3. How are the speed limits calculated?
4. How much can the speed limits be changed once?

To find the optimal solution, the impacts of these four factors on crash risk need to be considered. First, the proposed VSL works based on high crash risk computed by CRIs. In Chapter 4, we monitored crash risk in the northbound direction of the I-110 freeway in California, and high crash risk is determined on each segment with the thresholds of five different segment types. The VSL control is implemented once three consecutive high crash risks are detected. In other words, if a segment presents a high crash risk for 15 minutes, a new speed limit is determined and posted for the following 5 minutes. The reason is that more frequent change in speed limits can confuse drivers and drivers are less likely to comply with the changed speed limits.

Second, unlike experimental design for durations of intervention, this VSL remains in effect until crash risks drop below the thresholds for three consecutive time periods. In other words, if the crash risk is below the thresholds for 15 minutes, the speed limit reverts to the default speed limit. This restriction can prevent the frequent implementation of VSL.

Third, a new posted speed limit is set equal to the average speed observed at an upstream detector station and a downstream detector station. This average speed, defined as transition speed, helps avoid abrupt changes in speed by requiring drivers to make more gradual speed changes.

The new speed limit using the concept of transition speed is calculated as:

$$\mathrm{SL}(x_i, \mathrm{t}+1) = \mathrm{S}(x_i, t) = \frac{S(x_{i-1},t)+S(x_{i+1},t)}{2} \tag{5.1}$$

where $\mathrm{SL}(x_i, t+1)$ is the speed limit that will be imposed on the segment, from detector station x_i to detector station x_{i+1}, for the next time interval t + 1, $\mathrm{S}(x_i, t)$ is the transition speed at the current detector station x_i at the current time interval t, $S(x_{i-1}, t)$ is the average speed upstream detector station of current detector station x_i computed over the time period from t-1 to the current time t, and $S(x_{i+1}, t)$ is the average speed at downstream detector station of current detector station x_i computed over the time period from t-1 to the current time t.

Assume that the speed at the upstream detector, $S(x_{i-1}, t)$, is much higher than the speed at the downstream detector station, $S(x_{i+1}, t)$ and speed limit changes are displayed through the VMS in the middle of x_{i-1} and x_i. Thus, it is required to reduce the speeds of vehicles approaching the downstream detector to $S(x_{i+1}, t)$. If the speed limit set equal to the average speed of the downstream station of current detector station, vehicles are forced to decelerate speeds rapidly before they reach the current detector station x_i as the dotted line shown in Figure 5.1. On the other hand, the proposed transition speed allows the vehicles to decelerate gradually over a longer distance as the solid line in Figure 5.1 so that it can prevent abrupt speed change for vehicles approaching the detector station x_i . Since high deceleration is highly likely to increase crash risk, it is believed that the transition speed can avoid high deceleration rates and reduce crash risk.

In this study, we assume the posted speed limits should be integer multiples of 5mph. For instance, if the speed limit computed by Equation 5.1 is 43.7mph, the speed limit of 45mph should be posted.

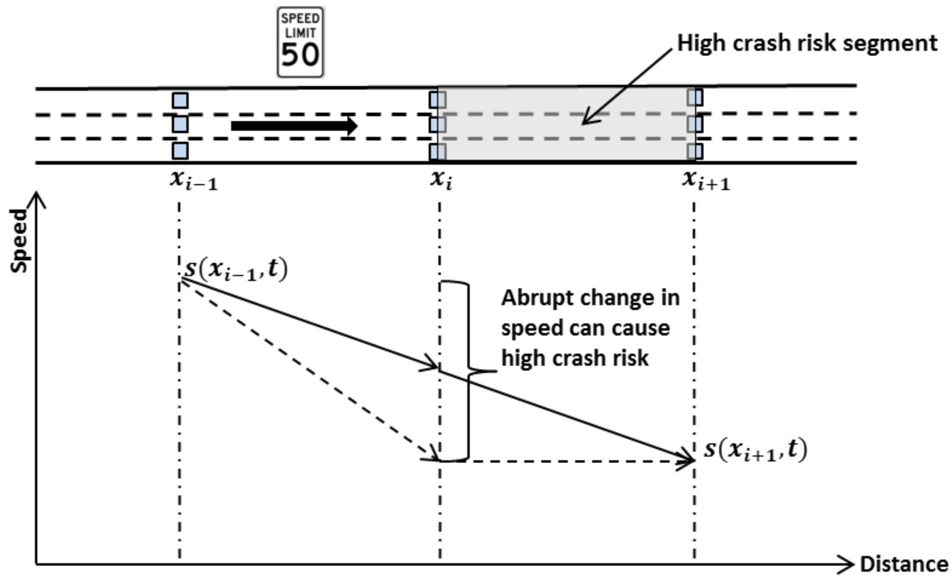

Figure 5.1 Comparison of Speed Control Strategies

Fourth, change in speed limit is possibly at most 15 mph once from the current posted speed limit at each time when the speed limit is changed to avoid abrupt deceleration. For example, if the new speed limit computed is 50 mph on the segment with a current 70 mph speed limit, 60 mph should be posted in the next time interval, and 50 mph should be posted in the next time interval later. The minimum speed limit that can be applied is 40 mph because below 40 mph can cause longer travel time due to slow traffic flow. Figure 5.2 presents the flowchart of VSL control logic.

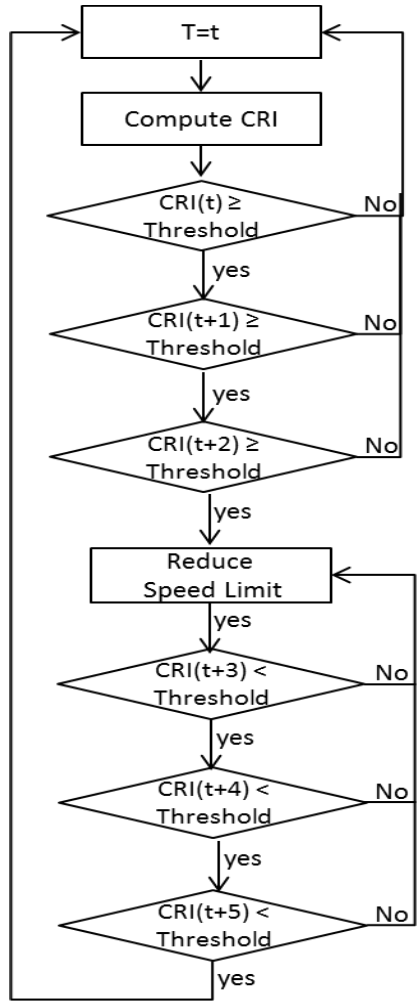

Figure 5.2 Flowchart of VSL Control Logic

5.4 Case Study

The above-mentioned VSL control strategy is tested on a 2.6-mile stretch of a sample I-110N freeway segment. As shown Figure 5.3, the tested area starts from milepost 20.53 and ends at milepost 23.13 where six detector stations are installed and thus crash risk improvement on the five segments are tested. Especially, it was observed that a ramp segment, the detector station 50 to the detector station 51, and a basic straight segment, the detector station 51 to the detector station 53, are the most frequent high crash risks segments during the morning peak, 06:00 AM to 09:00 AM.

Figure 5.3 A 2.6-mile Stretch of a Sample Freeway Segment on I-110N in CA

The detector stations collect the traffic flow information necessary for the calculation of CRI, and VMSs display the new speed limits to drivers on the basis of the computed CRI. Whenever the VSL control strategy detects the need of change in speed limits, VMSs indicate the sign of the reduced speed limits so that drivers approaching high crash risk segments reduce their speed before they pass the segments.

This study uses the VISSIM microscopic simulator to evaluate the changes in crash risk as a result of VSL control strategy implementation. An advantage of VSL is to adjust dynamically sets of speed limits properly located along a target segment to smooth the speed transition between upstream flow and downstream flow. The weekday morning peak hours (6-9 AM) on 4/15, 2015 are modeled. To accurately reflect the real traffic conditions, the network in VISSIM should be calibrated. In many previous studies simulated by VISSIM, the networks were calibrated by the adjustment of vehicle-following behavior parameters on freeways: CC0 through CC9 which were introduced by Gomes et al. (2004). In this study, CC0, CC1, CC4, CC5, and Waiting Time before Diffusion are modified, and the calibration is evaluated by GEH statistics. The modified CC parameters and Waiting Time before Diffusion for calibration in this study showed similar values as Gomes et al. (2004) and Jo et al. (2012). GEH is a value calculated with traffic volumes at the 5-min interval captured from the simulated data and the real traffic data as shown in Equation 5.2.

$$\text{GEH} = \sqrt{\frac{2(F_{real}-F_{sim})^2}{(F_{real}+F_{sim})}} \tag{5.2}$$

where F_{real} is the observed real flow and F_{sim} is the simulated flow from the simulation network. According to the Federal Highway Administration (FHWA), if more than 85% of the measurement locations' GEH values are less than 5, then the simulated flow would accurately reflect the real-field traffic flow (FHWA, 2004). Table 5.1 shows the GEH statistics for the six detector stations for the 3-h simulation period; however, the first half hour was used as a warm-up period, and no statistics were collected during that period. 97.2% of the GEH values are within the error of 5. The calibrated flows are also shown in Figure 5.4. It can be concluded that the network setup in VISSIM can accurately reflect the real traffic situations.

Table 5.1 GEH Statistics for the Six Calibrated Detector Stations

Detector Station(Milepost)	N	Mean	Std.dev	Minimum	Maximum
47(20.53)	30	1.57	1.25	0.05	4.33
49(21.29)	30	1.63	1.28	0.25	4.67
50(21.63)	30	2.30	1.51	0.05	5.52
51(22.03)	30	1.70	1.46	0.10	6.50
53(22.04)	30	2.58	1.48	0.20	5.27
55(23.13)	30	2.22	1.54	0.20	6.55

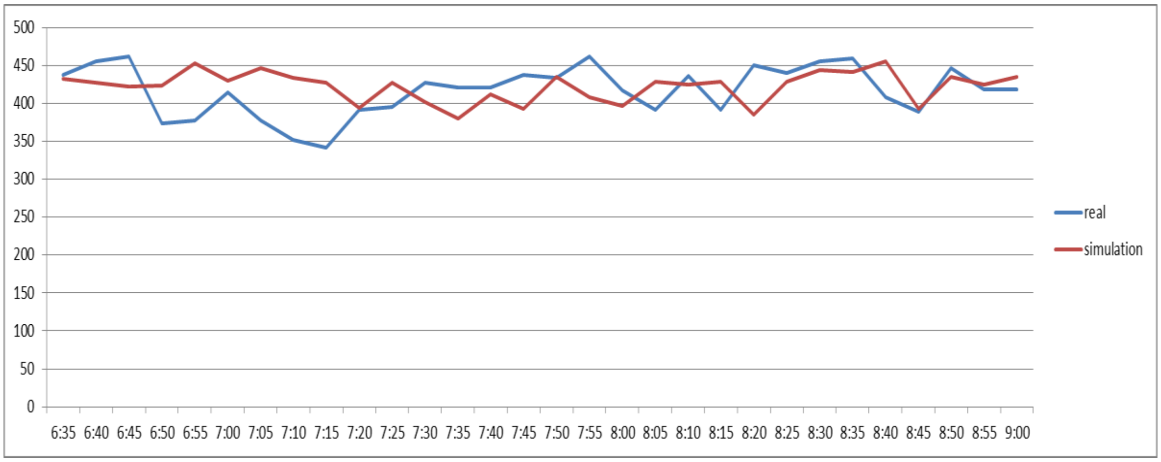

Detector Station 47

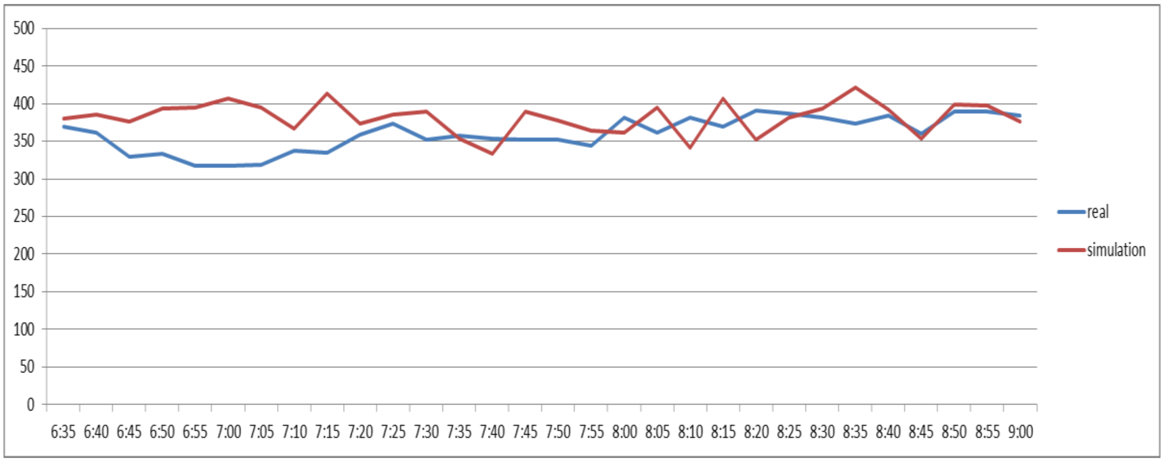

Detector Station 49

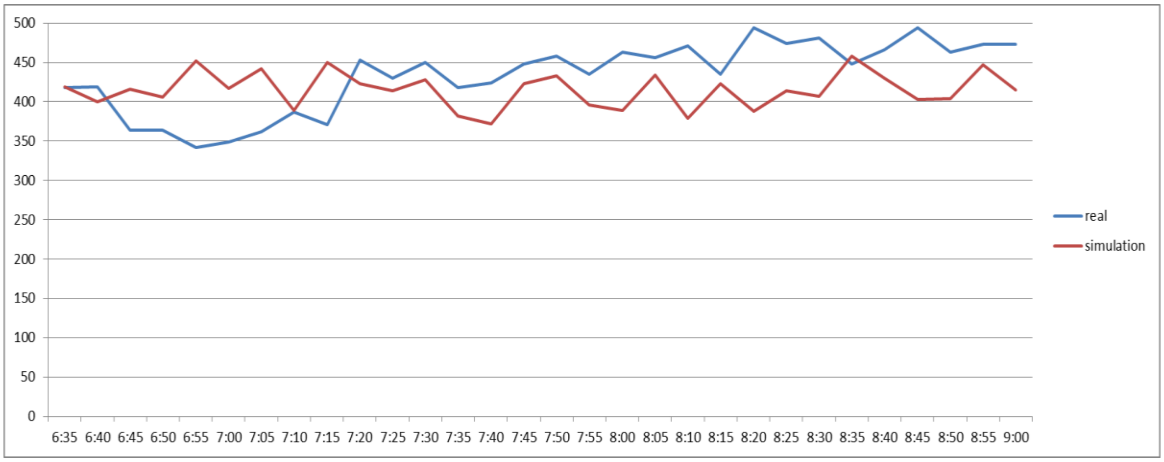

Detector Station 50

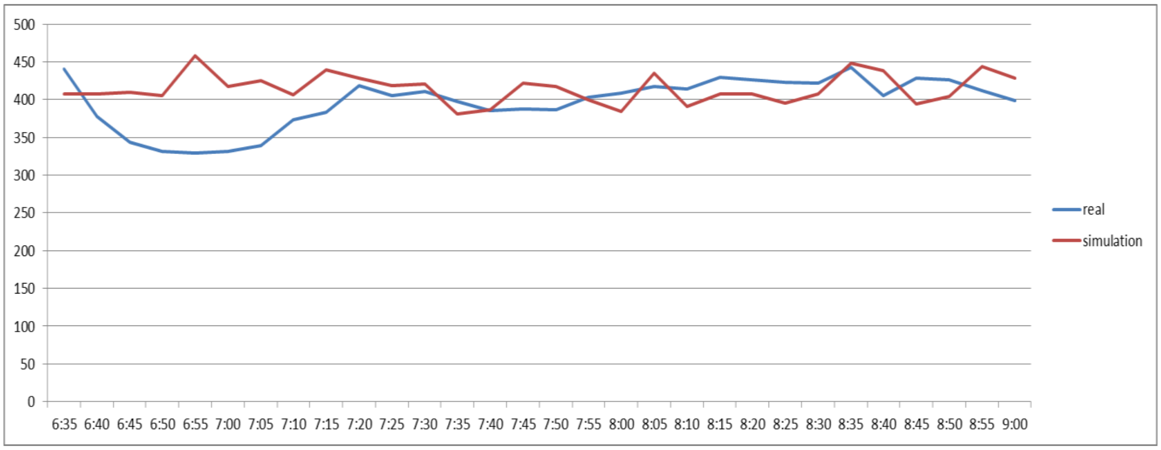

Detector Station 51

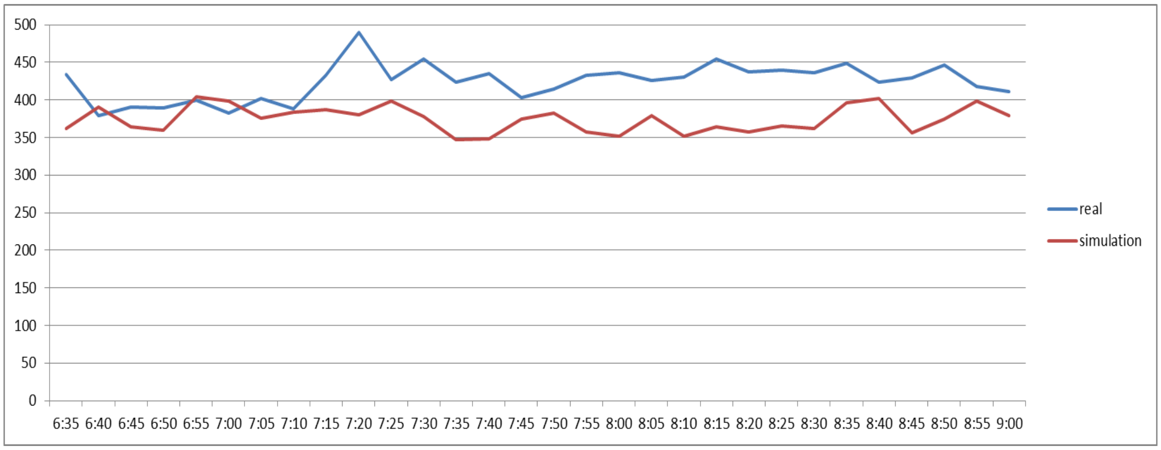

Detector Station 53

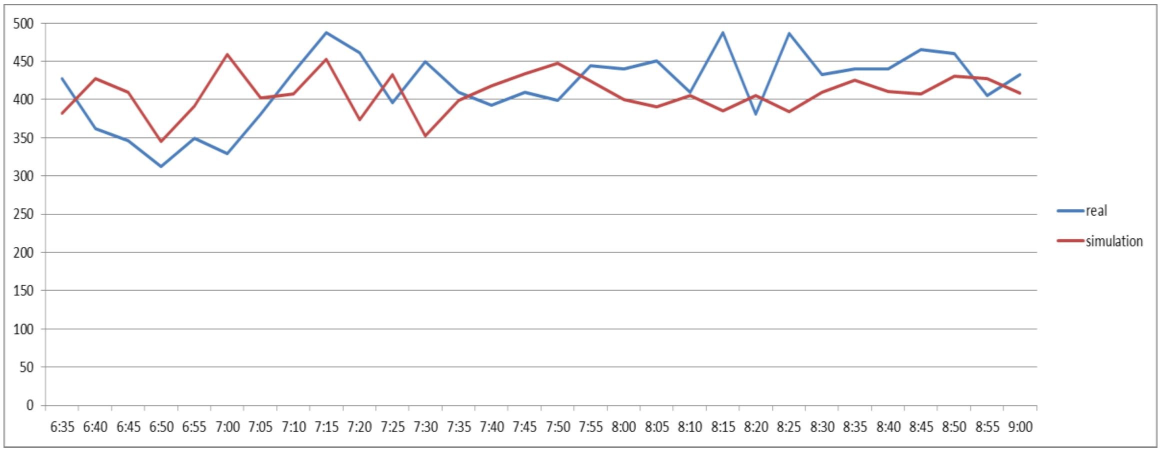

Detector Station 55

Figure 5.4 Calibrated Flow at Detector Stations

To validate the simulation network, CRI is computed with traffic flow parameters extracted from each detector station in VISSIM simulation network at 5-min interval to detect high crash risk 5-min intervals and compared the CRI computed with real traffic data as shown in Table 5.2 and Table 5.3. The number of high crash risk 5-min intervals in VISSIM network are close to that of in the real world. In Table 5.3, pink cells are the indication of high crash risk. After the calibration, the number of the time periods presenting high crash risk was closely matched with real data. It is demonstrated that the VISSIM network is satisfactorily validated.

Table 5.2 Comparison of the Number of Time-Cells of High Crash Risk for Each Segment

	47-49	49-50	50-51	51-53	53-55
Real data	12	14	26	27	13
Before Calibration (matched time-cells)	6(2)	9(5)	20(18)	18(16)	9(4)
After Calibration (matched time-cells)	17(10)	17(13)	26(24)	23(22)	13(9)

Table 5.3 Comparison of Calculation of High Crash Risk in the Simulation Network

Observed High Crash Risk					
Time	47-49	49-50	50-51	51-53	53-55
6:35	32	20	54	38	21
6:40	42	40	48	42	16
6:45	36	26	57	50	43
6:50	35	45	44	47	33
6:55	42	26	57	55	29
7:00	40	34	46	54	39
7:05	38	34	42	40	34
7:10	35	35	50	45	41
7:15	44	44	50	64	49
7:20	44	51	51	41	41
7:25	57	48	49	47	43
7:30	41	45	42	48	35
7:35	45	39	41	50	25
7:40	43	46	55	53	32
7:45	46	47	49	48	42
7:50	48	48	57	45	31
7:55	43	50	61	50	40
8:00	44	44	59	47	26
8:05	47	44	57	51	42
8:10	40	48	59	35	42
8:15	47	51	59	40	37
8:20	48	39	62	50	20
8:25	47	41	66	50	43
8:30	46	56	68	56	40
8:35	43	29	62	55	35
8:40	45	53	75	58	36
8:45	49	45	66	47	43
8:50	45	39	67	47	39
8:55	44	43	83	65	60
9:00	54	61	77	43	34

Simulated High Crash Risk before Calibration					
Time	47-49	49-50	50-51	51-53	53-55
6:35	28	41	45	42	39
6:40	27	55	50	39	40
6:45	32	30	51	31	38
6:50	38	44	42	40	25
6:55	39	39	55	41	47
7:00	40	21	40	43	49
7:05	22	26	45	40	24
7:10	27	50	46	37	22
7:15	41	60	26	45	21
7:20	39	41	50	40	38
7:25	45	33	58	32	22
7:30	40	48	49	50	39
7:35	48	50	26	33	39
7:40	49	41	32	55	40
7:45	32	38	49	45	40
7:50	41	36	51	48	27
7:55	40	32	53	48	39
8:00	49	31	45	41	22
8:05	48	11	31	28	38
8:10	50	28	39	27	41
8:15	41	45	47	45	24
8:20	39	30	52	26	27
8:25	40	45	49	39	32
8:30	41	50	50	30	40
8:35	35	30	52	45	39
8:40	25	35	42	50	47
8:45	29	27	50	21	40
8:50	35	40	46	23	38
8:55	29	44	34	48	38
9:00	34	50	44	40	38

Simulated High Crash Risk after Calibration					
Time	47-49	49-50	50-51	51-53	53-55
6:35	41	30	54	38	38
6:40	45	41	48	38	42
6:45	37	28	57	38	43
6:50	38	40	48	48	45
6:55	44	37	57	51	37
7:00	42	38	46	53	39
7:05	40	36	50	39	34
7:10	50	40	53	57	47
7:15	45	45	58	55	41
7:20	40	53	51	48	37
7:25	51	50	49	39	32
7:30	45	46	44	50	31
7:35	46	49	36	53	29
7:40	43	50	52	49	38
7:45	42	48	49	41	40
7:50	48	46	41	48	37
7:55	44	52	43	49	39
8:00	44	46	50	57	26
8:05	41	48	51	53	41
8:10	40	48	59	47	43
8:15	46	51	57	39	38
8:20	48	34	62	33	25
8:25	50	40	69	58	42
8:30	51	52	70	40	39
8:35	55	31	62	55	38
8:40	45	55	73	59	37
8:45	49	47	50	51	41
8:50	45	40	56	53	40
8:55	49	43	75	68	64
9:00	54	68	77	42	48

In the real world, the drivers compliance with various speed limits is obviously limited. This has been proved in a field experiment. Soriguera and Sala (2014) empirically found that dynamic speed limits only affect drivers' behavior with speed enforcement. Also, Yu et al. (2014) found in a simulation that many drivers tended to ignore the lower speed limit. According to the compliance analysis on M25 in England, the compliance with the posted speed limit of 40 and 50 was between 10 % and 20 %. The analysis thus has provided insight into an element of driver behavior that it highlights the tendency for drivers to comply less with the low speed limits (40 to 50 mph). Riggins et al. (2016) evaluated the compliance as the difference between displayed speed limits and the measured speed of traffic on Oregon Route 217 (OR-217), a 7-mile stretch of freeway in Oregon. They observed that the mean compliance value was +9 mph with a standard deviation of 8 mph. A total of 88% of the observations were above the posted speed limit. 23% of the observations fell within ±5 mph, while 53% fell within ±10 mph.

Therefore, speed distributions under various speed limits and the speed distributions with three compliance levels: high compliance level, moderate compliance level, and low compliance level are needed to be defined. The speed distributions under various speed limits following normal distribution are presented in Table 5.4.

Table 5.4 Speed Distributions under Various Speed Limits

	Low compliance		moderate compliance		high compliance	
speed limits	mean	(lower, upper)	mean	(lower, upper)	mean	(lower, upper)
60	72	(62,82)	65	(59,71)	61	(57,65)
55	66	(56,76)	60	(54,66)	55	(51,59)
50	61	(51,71)	55	(49,61)	49	(43,55)
45	55	(45,65)	50	(44,56)	45	(39,51)
40	50	(40,60)	45	(39,51)	39	(35,43)
35	44	(34,54)	40	(34,46)	35	(31,39)

The VISSIM simulation applies a different proportion of compliance rates based on the empirical findings in previous studies; 50% low compliance rate, 30% moderate compliance, and 20% compliance rate in VISSIM. For comparison, two cases of 100% low compliance rate and 100% high compliance rate are also tested in VISSIM simulation.

To eliminate the random effect of the results, five simulations were conducted for the VSL control strategy and the average crash risk on each segment is calculated from the simulation runs. 5-minute average crash risks and travel times are utilized as evaluation measures for traffic safety and resulting traffic operation efficiency.

5.5 *Simulation Results*

5.5.1 Crash Risk Improvement

A 3-h simulation, with a 30-min warm-up period, was used to evaluate the VSL control for the five segments. To see the change in crash risk over time, the CRIs were computed on each segment:47-49, 49-50, 50-51, 51-53, 53-55 at every 5-min interval right after the warm-up period. The VSL control implemented in a segment where three consecutive high crash risks are observed. For instance, on 50-51 segment, three consecutive high crash risks were observed from 6:35 AM through 6:45 AM and new speed limit which is 40 mph was displayed at 6:45:01 for 25 minutes since the CRI from 6:55 to 7:10 dropped below the predetermined thresholds. Afterwards, the speed limit reverted to the default speed limit which is 70 mph. Another VSL control was implemented at 8:00:01 for 45 minutes with the speed limit of 40 mph. Hence, the VSL control was implemented on 50-51 segment and 51-53 segment as shown in Table 5.5. On 50-51 segment, the VSL was implemented for 70 minutes, 6:45 – 7:10 and 8:00 – 8:45 and on 51-53 segment, the VSL was implemented for 85 minutes, 6:50 -7:25 and 8:10 – 9:00. For the comparison, Table 5.5 also presents the results of two additional compliance rates. The two cases had obviously different results that the duration of VSL implementation got shorter at 100% high compliance rate and the VSL was implemented for 55 minutes on 50-51 segment and for 55 minutes on 51-53 segment. The duration of VSL implementation got longer at 100% low compliance rate and the VSL was implemented for 105 minutes on 50-51 segment and for 125 minutes on 51-53 segment. These results suggest that the effectiveness of VSL can be optimal by making drivers comply with the low speed limit by enforcement.

Table 5.5 Percentages of the Implemented Duration

	50-51 segment	51-53 segment
Speed limit (mph)	40mph	50mph
Low:Moderate:High = 50:30:20	46.7%	56.7%
100% low compliance	70.0%	83.3%
100% high compliance	33.3%	30.0%

Table 5.6 displays the change in crash risk on the five segments. Among 150 5-min time periods (30 5-min time periods * 5 segments), 92 5-min time periods showed high crash risk before VSL implementation, but it reduced to 59 5-min time periods after VLS implementation. Table 5.7 indicates the changed numbers of high crash risk 5-min time periods on each segment. Table 5.7 also indicates the results of the two cases. The effectiveness of VSL at 100% low compliance turned out to be less than other two cases, but the case of 100% high compliance rate had the best performance in that the number of time periods of high crash risk got reduced to 37 5-min time periods.

Table 5.6 Change in crash risk after VSL implementation

Before VSL Implementation							After VSL Implementation					
Time	47-49	49-50	50-51	51-53	53-55		Time	47-49	49-50	50-51	51-53	53-55
6:35	32	20	54	38	21		6:35	32	20	54	38	21
6:40	42	40	48	42	16		6:40	41	40	48	42	16
6:45	36	26	57	50	43		6:45	36	26	57	50	40
6:50	35	45	44	47	33		6:50	35	43	41	47	30
6:55	42	26	57	55	29		6:55	42	26	52	43	30
7:00	40	34	46	54	39		7:00	39	35	40	41	37
7:05	38	34	42	40	34		7:05	38	35	37	39	35
7:10	35	35	50	45	41		7:10	34	34	44	40	36
7:15	44	44	50	64	49		7:15	44	42	45	39	37
7:20	44	51	51	41	41		7:20	44	45	43	38	39
7:25	57	48	49	47	43		7:25	56	44	47	39	42
7:30	41	45	42	48	35		7:30	40	43	40	43	34
7:35	45	39	41	50	25		7:35	44	39	41	40	32
7:40	43	46	55	53	32		7:40	41	47	50	39	34
7:45	46	47	49	48	42		7:45	46	48	44	40	38
7:50	48	48	57	45	31		7:50	48	42	51	40	40
7:55	43	50	61	50	40		7:55	43	48	54	39	39
8:00	44	44	59	47	26		8:00	43	43	57	42	25
8:05	47	44	57	51	42		8:05	47	43	44	48	38
8:10	40	48	59	35	42		8:10	39	46	46	40	30
8:15	47	51	59	40	37		8:15	46	48	46	40	38
8:20	48	39	62	50	20		8:20	48	37	44	40	24
8:25	47	41	66	50	43		8:25	47	41	48	39	39
8:30	46	56	68	56	40		8:30	46	50	49	39	38
8:35	43	29	62	55	35		8:35	43	28	42	45	35
8:40	45	53	75	58	36		8:40	45	40	44	42	30
8:45	49	45	66	47	43		8:45	48	45	43	38	30
8:50	45	39	67	47	39		8:50	44	40	46	43	34
8:55	44	43	83	65	60		8:55	44	44	68	42	40
9:00	54	61	77	43	34		9:00	55	61	60	36	37

Table 5.7 High Crash Risk 5-min Time Cells after VSL Implementation

	47-49	49-50	50-51	51-53	53-55
Before VSL	12	14	26	27	13
After VSL					
Low:Moderate:High = 50:30:20	10	9	17	19	4
100% low compliance	10	12	22	23	8
100% high compliance	6	5	11	12	3

Safety effects of the VSL control are quantified as crash risk improvements. Figure 5.5 displays the crash risks improvements (positive means traffic safety improved) for each segment under 50% low compliance rate, 30% moderate compliance, and 20% high compliance rate we assumed in this study. It shows the crash risk differences of the VSL cases compared to the non-VSL control cases. Positive values of crash risk improvements indicate enhanced traffic safety with VSL; while negative crash risk differences mean worse traffic safety situations. In the simulations, two segments of 50-51 and 51-53 were the VSL controlled segments. It was observed that the simulated whole 2.6-mile segment generally has improved traffic safety by a decrease in crash risk and the VSL targeted segments achieved the most traffic safety benefits and the upstream of the targeted segments also had positive crash risk improvement.

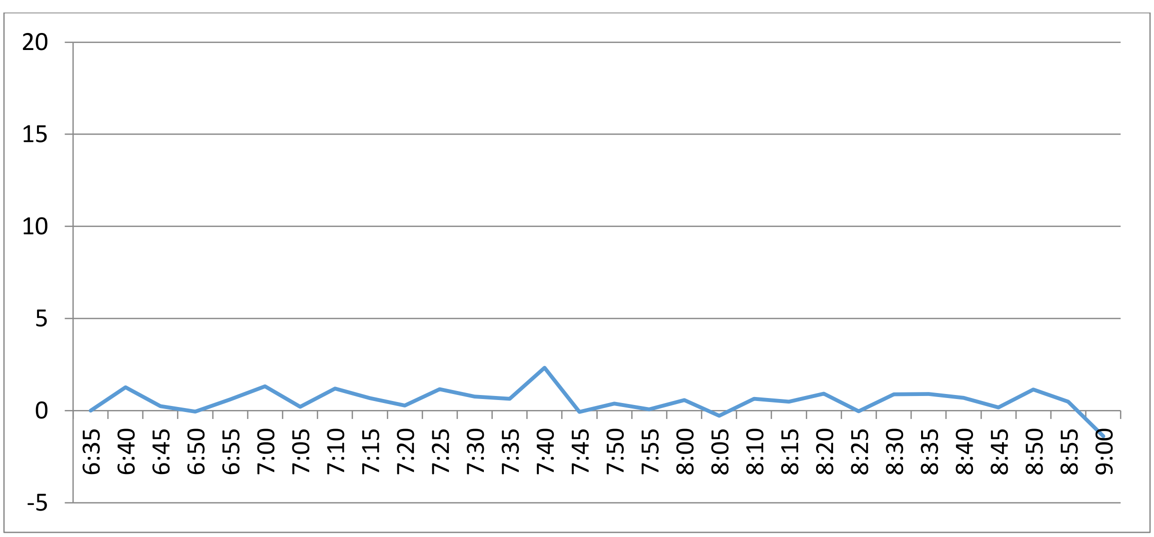

47-49 segment

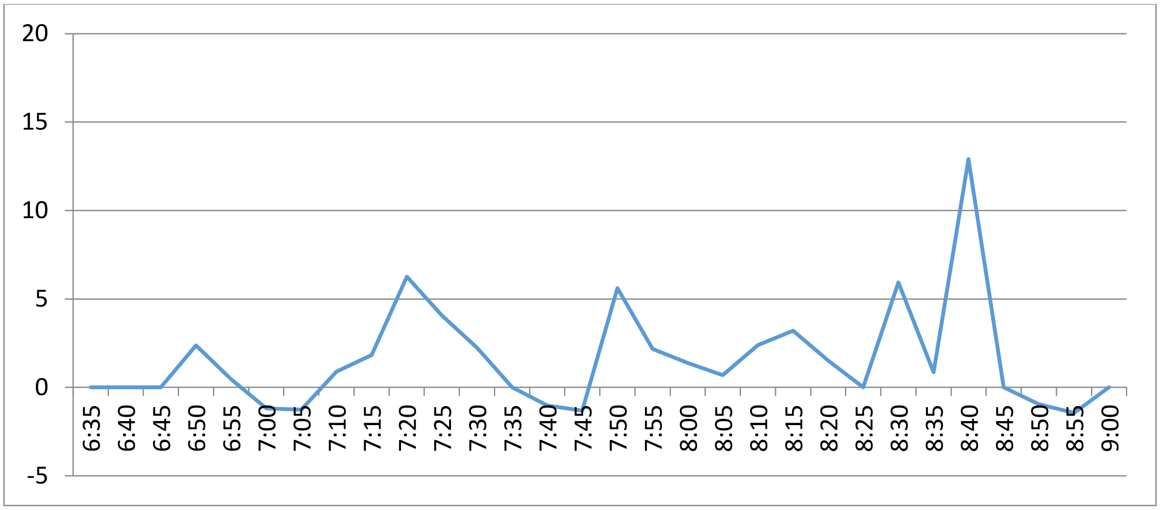

49-50 segment

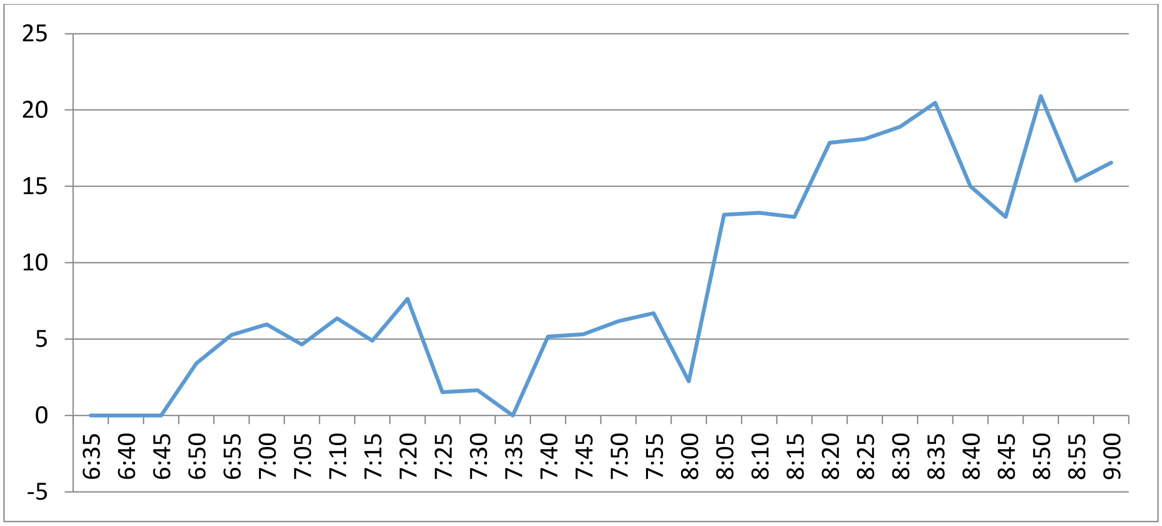

50-51 segment

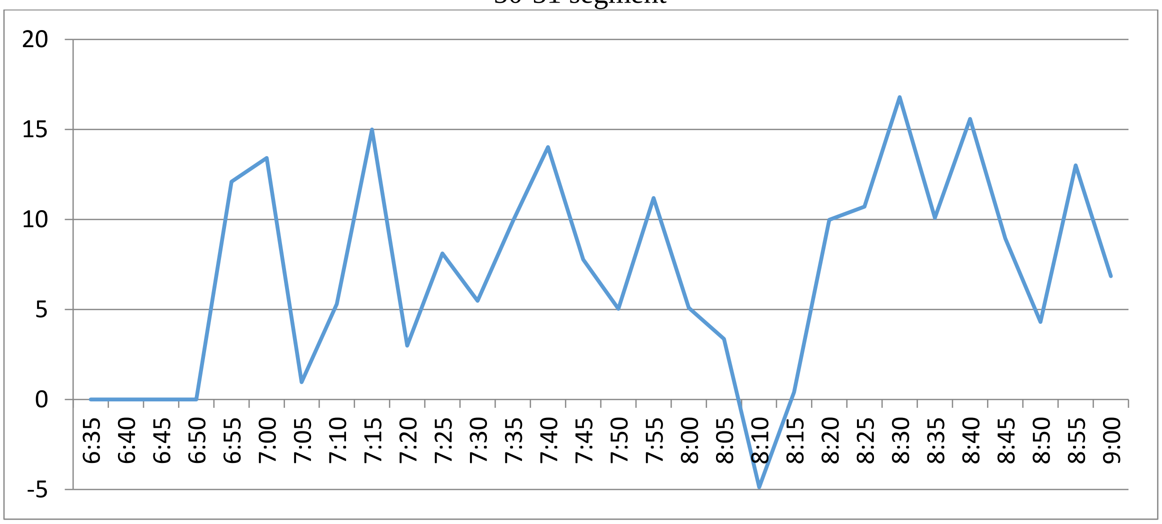

51-53 segment

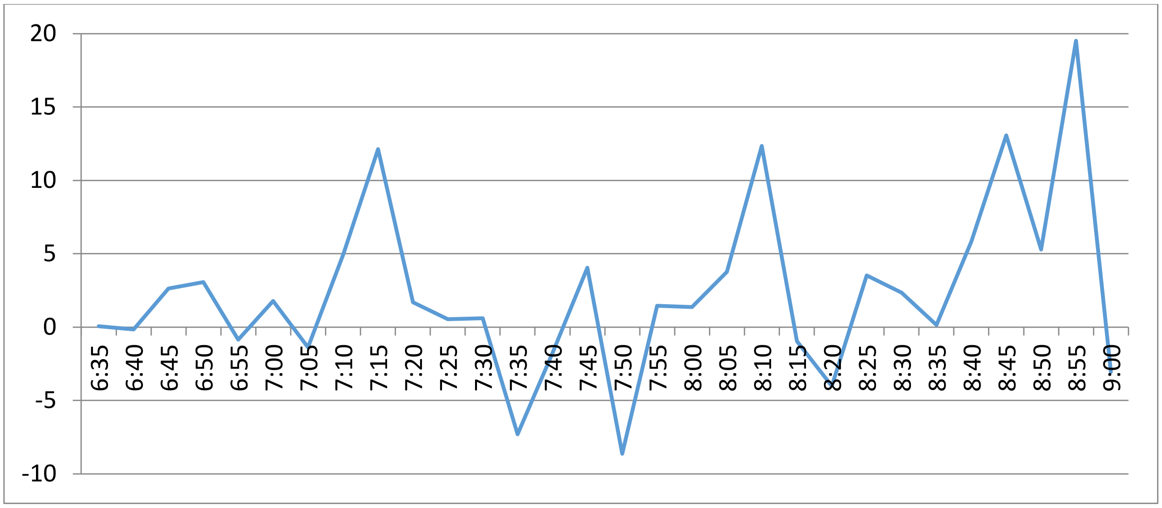

53-55 segment

Figure 5.5 Crash Risk Improvements for Each Segment

A concern with the application of VSL is crash risk migration. If the VSL would lower crash risk in one segment it might increase it at others. The figures indicate that crash risk improvements in both upstream and downstream segments of the VSL targeted segments have been achieved, therefore, crash risk migration is prevented.

5.5.2 Travel Time

If the posted speed limit is too low to enhance the traffic safety or to cover large areas, the increase in travel time is unavoidable. The VSL effect on travel time could be less effective than traffic safety enhancement, but many studies showed a positive result in a reduction in travel time using VSL. Figure 5.6 shows the travel times between detector station 47 and detector station 55 using VSL and not using VSL. There is no big travel time difference between VSL and no VSL, but as it turned out be reduction in travel time was achieved as well.

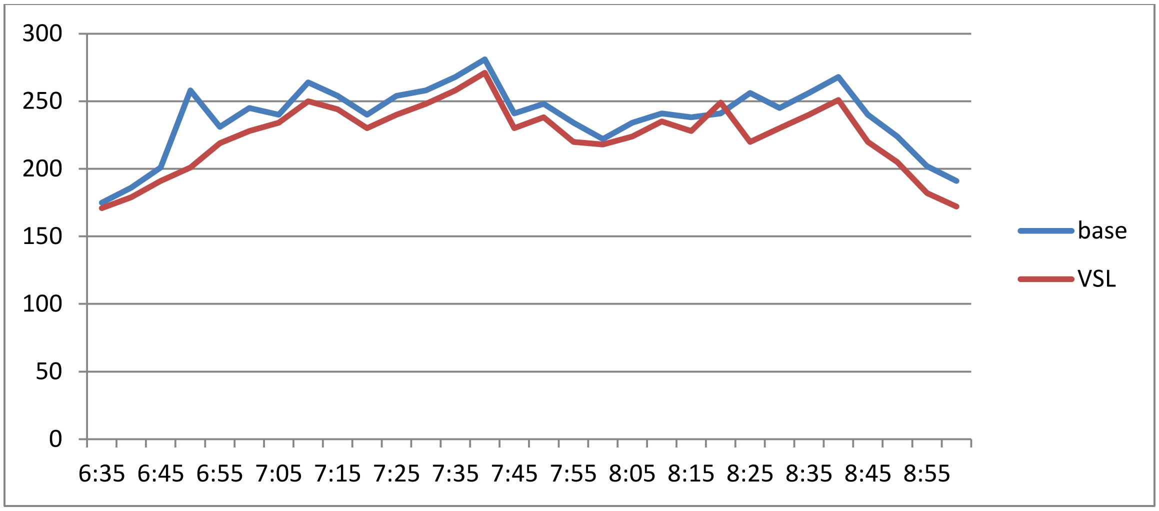

Figure 5.6 Comparison of travel times using VSL and no VSL

5.6 Closure

This chapter proposed a VSL control using the transition speed which is defined as the average speed of upstream and downstream detector stations of the targeted segment. The VSL is to be implemented once high crash risks are detected for 15 minutes and is withdrawn once the calculated crash risk drops below the thresholds. The effect of the proposed VSL control on traffic safety improvement was investigated in VISSIM simulation. It was evident that the whole segment achieved a reduction in crash risk and in travel times. It was demonstrated that the CRI can be utilized for the evaluation of traffic safety and the proposed VSL control strategy has positive impact on decreasing crash risk and travel time as well. However, further investigation into driver compliance is needed to maximize the full potential of the VSL control.

Chapter 6 Conclusions and Future Research

6.1 Research Summary and Contributions

To explicitly identify the relationship between crash risk and potential contributing factors and to enhance traffic safety on freeways, this research has focused on the development of a crash risk index (CRI) and proposed a Variable Speed Limits (VSL) control. Based on the deficiencies of the collection of potential contributing factors and limitations of existing crash risk indices, this research has made contributions mainly in the following four avenues:

- Examination of all traffic parameters that have been proved to be influential in a change in crash risk combined with environmental characteristics with respect to five different segment types;
- Establishment of a concrete generalized framework that can be employed on freeways aiming at monitoring changes in crash risk;
- Development of crash risk indices that quantify the crash risk in real time coming from any impending rear-end or sideswipe crashes for a segment; and
- Proposing a Variable Speed Limits (VSL) control aiming to reduce the crash risk that is quantified by the crash risk indices that are developed for traffic safety improvement on freeways.

A brief summary of research finding in those regards is presented below.

Comprehensive Analysis for Capturing the Interrelation between Crash Risk and Potential Factors

Since it has been confirmed that the contributing factors identified are distinct with respect to crash types, crash severity, and geometric characteristics, it is necessary to identify accurately the contributing factors affecting crash risk. To that end, it is necessary to examine all the contributing factors together that have been proved to have an impact on the crash risk in the existing studies. Chapter 2 introduced the different contributing factors identified in the literature and Chapter 3 presented the candidate contributing factors that should be collected. The findings indicate that hazardous traffic conditions are caused by different traffic parameters combined with other environmental characteristics under five different segment types and that the intensity of a contributing factor can be different in different segment types.

Establishment of a Concrete Traffic Safety Management System for Freeways

Chapter 3 has established a generalized framework that can be employed for freeway traffic safety improvement. It provides a collection of candidate contributing factors, methods for identification of contributing factors under five different segment types, building crash risk prediction models using Bayesian random intercept logistic regression, developing a crash risk index, and updating the crash risk prediction models. It also proposed a variable speed limits (VSL) control and the effectiveness of it has been validated based on the computed crash risk with the crash risk indices. If this whole framework is utilized on a freeway, it will help traffic operators to identify hazardous traffic conditions better and to implement proactive interventions to alleviate crash risk in the right location at the right time.

Development of Crash Risk Indices that Enable Traffic Operators to Monitor Crash Risk in a Quantitative Way in Real Time

To overcome the limitations of the existing crash risk indices, Chapter 3 proposed a crash risk index that quantify the crash risk from impending rear-end and sideswipe crashes and Chapter 4 presented its application in monitoring crash risk in real time. The results of monitoring demonstrated that the crash risk indices result in high crash risk prior to crash occurrence. This contributes to identify hazardous traffic conditions ahead of crash occurrence, and make preemptive countermeasures possible.

Proposing a Variable Speed Limits (VSL) Control Aiming to Reduce Crash Risk

Most of VSL studies adopted an experimental design approach to find the optimal strategy. A certain number of different control strategies are simulated with microscopic simulation experiments and compared. The experimental design way requires extensive simulation work, and the results are not transferable between different facilities. The proper speed limit on one freeway can be less effective on other freeways. To overcome this limitation, Chapter 5 proposed a dynamic VSL control reflecting real-time traffic flow characteristics. The dynamic speed limit is set equal to the average speed observed at an upstream detector station and a downstream detector station from the current detector station defined as transition speed. The VSL control was implemented based on the CRIs. The results indicated that the proposed VSL control reduces the high crash risk below thresholds and achieves a reduction in travel time as well. Furthermore, the high crash risk migration could also be prevented.

Although this research has made contributions based on the deficiencies of the collection of potential contributing factors and limitations of existing crash risk indices, this research has some limitations:

- This research has been conducted assuming that the detector data is accurate. The predictive performance of the CRIs depends on the quality of data that is obtained from detectors. As a result, the predictive performance of the CRIs could be less accurate with low quality of data.

- In the development of a CRI, we only considered a linear relationship between crash risk and contributing factors. Hence, we have not considered any nonlinear relationship between the crash risk and its contributing factors.
- This research has not focused on factors that affect the severity of crashes when they happen. Rather, it only considered that factors that influence the crash risk itself.

6.2 Future Research

In spite of the contributions made in this research, several key issues remain to be investigated to enhance the real-time crash risk prediction models and to develop better proactive intervention strategies. Examples of these research issues are summarized below.

Developing CRIs for Different Levels of Crash Severity

This study developed a crash risk index for detection of high crash risk time periods for rear-end and sideswipe crashes. An application of a CRI can be extended to develop crash risk indexes for crashes with different levels of severity. Previous studies have found that the contributing factors such as traffic parameters, environmental factors, and geometric characteristics are apparently different for crashes that result is fatality, injury, and property damage. Thus, the development of the CRIs can be extended to detect high crash risk under different severity levels.

Exploring Nonlinear Relationship Between Crash Risk and Its Contributing Factors

This study has been conducted assuming linear relationship between crash risk and its contributing factors. Due to the complicated nature of crashes, however, it is also important to consider any nonlinearities that may exist in the relationship between the crash risk and its contributing factors. Under linearity, the amount of change in the mean value of crash risk associated with a unit increase in a contributing factor, holding all other factors constant, is the same regardless of the level of the contributing factor. In other words, the effect of a one-unit increase in the contributing factor does not depend on the value of the contributing factor. Under nonlinear relationship, however, the effect of the contributing factor on crash risk depends on the value of the contributing factor; in effect, the contributing factor somehow interacts with itself. The interaction may be multiplicative. Thus, a future study needs to explore nonlinear relationship between crash risk and its contributing factors.

Decision of New Speed Limits Using CRI Thresholds

This study has determined the new speed limits based on the transition speed using the average speeds of upstream detector stations and downstream detectors stations. This is advantageous to reflect real-time traffic condition, but it is not the best strategy for the purpose of reducing the high crash risk estimated by the CRIs. One way to reflect directly the real-time crash risk level is the use of the thresholds judging high crash risk. It is expected that new speed limit based on thresholds could affect change in crash risk in a direct way.

Investigation for the Impacts of Other External Factors on Change in Crash Risk

This research has investigated the candidate factors affecting crash risk based on a matched case-controlled method. The matched case-controlled design controls for the impact of some confounding factors, such as the time and the locations of crashes, at the stage of selecting controls. Due to this reason, there are some limitations on the investigation for some factors such as sun glare, number of lanes, and lane width. The impacts of those factors on crash occurrence have already been studied, but the study on how these factors affect the change in crash risk has not been studied. Thus, it is desirable that an innovative method that incorporates them in crash risk prediction models is developed.

Choice of Threshold Indicating High Crash Risk

This research utilized the Youden index when selecting thresholds that indicate high crash risk so that a hazardous traffic condition is decided based on high crash risk and the following VSL control is also implemented aiming to eliminate the high crash risk on the targeted segment. Hence, the choice of the threshold is quite an important step in this research. This research has selected the thresholds with respect to five different segment types, but the threshold would vary from a freeway to another and by location, time of day, and the day of the week on the same freeway. Thus, Calibration of the threshold values depending on the time of day, the day of the week, and locations is needed to be studied.

Lane-Restriction Control

This research proposed a variable speed limits (VSL) control to improve traffic safety on freeways. The results showed crash risk improvement and reduction in travel time. Along with a VSL control, the Lane Operation Restriction (LOR) control is one of the promising interventions to reduce crash risk by decreasing the number of lane-changes. However, the LOR control studies have been mostly limited to the truck-lane restriction and specific facilities such as bridges and on-ramp junctions. Also, there are few studies on the application of VSL control combined with LOR control. As connected automated vehicle technology is rapidly developing in recent years, it is expected for vehicles to comply with traffic intervention controls. Hence, A study on the application of LOR control combined with the VSL control can enhance traffic safety.

References

Abdel-Aty, M., Pande, A., Lee C., Gayah, V., and Santos, C.D., “Crash risk assessment using intelligent transportation systems data and real-time intervention strategies to improve safety on freeways,” Journal of Intelligent Transportation Systems, Vol. 11(3), pp. 107-120, 2007.

Abdel-Aty, M., Dilmore, J., Hsia, L., “Applying variable speed limits and the potential for crash migration.” Transportation Research Record 1953, Transportation Research Board, Washington D.C., pp. 21-30, 2006.

Ahn, S., Laval, J., and Cassidy, M.J., “Effects of merging and diverging on freeway traffic oscillations,” Transportation Research Record 2188, Transportation Research Board, Washington D.C., pp. 1-8, 2010.

Ahn, S., Cassidy, M.J., “Freeway traffic oscillations and lane-change maneuvers,” presented at the conference of Transportation and Traffic Theory, 2007.

Abdel-Aty, M., Uddin, N., Pande, A., Abdalla, F.M., and Hsia, L., “Predicting freeway crashes from loop detector data by matched case-control logistic regression,” Transportation Research Record 1897, Transportation Research Board, Washington D.C., pp. 88-95, 2004.

Ahmed, M., Abdel-Aty, M., & Yu, R., “Assessment of interaction between crash occurrence, mountainous freeway geometry, real-time weather, and AVI traffic data,” presented at the 91st annual meeting of the Transportation Research Board, Washington D.C., 2012.

Abdel-Aty, M., Pande, A., Lee, C., Gayah, V., Santos, C.D., “Crash risk assessment using intelligent transportation systems data and real time intervention strategies to improve safety on freeways.” Journal of Intelligent Transportation Systems, Vol. 11(3), pp. 107-120, 2007.

Abdel-Aty, M., Cunningham, R.J., Gayah, V.V., Hsia, L., "Dynamic variable speed limit strategies for real-time crash risk reduction on freeways." Transportation Research Record 2078, Transportation Research Board, Washington D.C., pp. 108-116, 2008.

Abdel-Aty, M., Dilmore, J., Dhindsa, A., "Evaluation of variable speed limits for real-time freeway safety improvement." Accident Analysis and Prevention, Vol. 38, pp. 335-345, 2006.

Breiman, L., "Random forests," Machine Learning, Vol. 45(1), pp. 5-32, 2001.

Bertness, J., "Rain-related impact on selected transportation activities and utility services in the Chicago area," Journal of Applied Meteorology and Climatology, Vol. 19(5), pp. 545-556, 1980.

Brackstone, M., McDonald, M., and Wu, J., "Lane changing on the motorway: factors affecting its occurrence, and their implications. Presented at Road Transport Information and Control Conference, pp. 160–164, 1998.

Bhowmick, A., Qiu, T.Z., Hadiuzzaman, M., "Driver compliance analysis of variable speed limit based freeway traffic control." 11th International Conference of Chinese Transportation Professionals, 2011.

Chen, Y., Persaud, B., and Sacchi, E., "Improving transferability of safety performance functions by Bayesian model averaging," Presented at the 90th annual meeting of the Transportation Research Board, Washington, DC, 2011.

Christoforou, Z., Cohen, S., and Karlaftis, M.G., "Identifying crash type propensity using real-time traffic data on freeways," Journal of safety research, Vol. 42(1), pp. 43–50, 2011.

Chovan, J.D., Tijerina, L., Alexander, G., and Hendricks, D.L., "Examination of lane change crashes and potential IVHS countermeasures," Department of Transportation, Report DOT-VNTSC-THRSA-93-2, NHTSA, 1994.

Chang, G.L., Park, S.Y., Paracha, J., “Intelligent transportation system field demonstration: integration of variable speed limit control and travel time estimation for a recurrently congested highway.” Transportation Research Record 2243, Transportation Research Board, Washington D.C., pp. 55-66, 2011.

Chen, D., Ahn, S., Hegyi, A., “Variable speed limit control for steady and oscillatory queues at fixed freeway bottlenecks.” Transportation Research Part B, Vol. 70, pp. 340-358, 2014.

Eisenberg, D., Warner, K., “Effects of snowfalls on motor vehicle collisions, injuries and fatalities,” American Journal of Public Health, Vol. 95(1), pp. 120-124, 2005.

Fridstrom, I., Ifver, J., Ingebrigtsen, S., Kulmala, R., and Thomasen, L., “Measuring the contribution of randomness, exposure, weather, and daylight to the variation in road accident counts,” Accident Analysis and Prevention, Vol. 27(1), pp. 1-20, 1995.

Golob, T.F., Recker, W.W., and Alvarez, V.M., “A tool to evaluate the safety effects of changes in freeway traffic flow,” presented at the 82nd annual meeting of the Transportation Research Board, Washington D.C., 2003.

Golob, T., Recker, W., “Relationships among urban freeway accidents, traffic flow, weather, and lighting conditions,” Journal of Transportation Engineering, Vol. 129(4), pp. 342-353, 2003.

Gomes, G., May, A., Horowitz, R., “Congested freeway microsimulation model using VISSIM.” Transportation Research Record 1876, Transportation Research Board, Washington D.C., pp. 71-81, 2004.

Hossain, M., Muromachi, Y., “Understanding crash mechanism on urban expressways using high-resolution traffic data,” Accident Analysis and Prevention, Vol. 57, pp. 17-29, 2013.

Hossain, M., Muromachi, Y., “Understanding crash mechanisms and selecting interventions to mitigate real-time hazards on urban expressways,” Transportation Research Record 2213, Transportation Research Board, Washington D.C., pp. 53-62, 2011.

Hourdos, J.N., Garg, Vishnu, Michalopoulos, P.G., and Davis, G.A., “Real-time detection of crash-prone conditions at freeway high-crash location,” Transportation Research Record 1968, Transportation Research Board, Washington D.C., pp. 83-91, 2006.

Hassan, H.M., Abdel-Aty, M.A., “Predicting reduced visibility related crashes on freeways using real-time traffic flow data,” Journal of Safety Research, Vol. 45, pp. 29-36, 2013.

Highway Capacity Manual, Transportation Research Board, Washington, D.C., 2010.

Hossain, M., Muromachi, Y., “A real-time crash prediction model for the ramp vicinities of urban expressways,” IATSS Research, Vol. 37(1), pp. 68-79, 2013a.

Hossain, M., Muromachi, Y., “A Bayesian network based framework for real-time crash prediction on the basic freeway segments of urban expressways,” Accident Analysis and Prevention, Vol. 45, pp. 373-381, 2012.

Hadayeghi, A., Shalaby, A.S., Persaud, B.N., and Cheung, C., “Temporal transferability and updating of zonal level accident prediction models,” Accident Analysis and Prevention, Vol. 38, pp. 579-589, 2006.

Hadiuzzaman, M., Qiu, T.Z., “Cell transmission model based variable speed limit control for freeways.” Canadian Journal of Civil Engineering, Vol. 40(1), pp. 46-56, 2013.

Hoogen, E.V.D., Smulders, S., “Control by variable speed signs: results of the Dutch experiment.” Road Traffic Monitoring and Control, Conference Publication No. 391, pp. 26-28, 1994.

Hasanpour, M.Z., Ahadi, M.R., Moghadam, A.S., Behzadi, G.A., “Variable speed limits: strategies to improve safety and traffic parameters for a bottleneck.” Engineering, Technology & Applied Science Research, Vol. 7, pp. 1535-1539, 2017.

Jo, Y., Choi, H., Jeon, S., Jung, I., “Variable speed limit to improve safety near traffic congestion on urban freeways.” IEEE International Conference on Information Science and Technology, Hubei, China, 2012.

Keay, K., Simmonds, I., "The association of rainfall and other weather variables with road traffic volume in Melbourne Australia," Accident Analysis and Prevention, Vol. 37(1), pp. 109-124, 2005.

Khattak, A., Knapp, K., "Interstate highway crash injuries during winter snow and nonsnow events," Transportation Research Record 1746, Transportation Research Board, Washington D.C., pp. 30-36, 1998.

Kim, D.G., Lee, Y., Washington, S., and Choi, K., "Modeling crash outcome probabilities at rural intersections: application of hierarchical binomial logistic models," Accident Analysis and Prevention, Vol. 39, pp. 125-134, 2007.

Khondaker, B., Kattan, L., "Variable speed limit: A microscopic analysis in a connected vehicle environment." Transportation Research Part C, Vol. 58, pp. 146-159, 2015.

Lin, Lei, Wang, Q., and Sadek, A.W., "A novel variable selection method based on frequent pattern tree for real-time traffic accident risk prediction," Transportation Research Part C, Vol. 55, pp. 444-459, 2015.

Leur, P.D., Sayed, T, "Development of a road safety risk index," Transportation Research Record 1784, Paper No. 02-2814, 2002.

Lee, C., Abdel-Aty, M., and Hsia, L., "Potential real-time indicators of sideswipe crashes on freeways," Transportation Research Record 1953, Transportation Research Board, Washington D.C., pp. 41-49, 2006.

Lee, C., Saccomanno, F., and Hellinga, B., "Analysis of crash precursors on instrumented freeways," Transportation Research Record 1784, Transportation Research Board, Washington D.C., Paper No. 02-3790, 2002.

Lee, C., Park, P.Y., and Abdel-Aty, M., "Lane-by-lane analysis of crash occurrence based on driver's lane-changing and car-following behavior," Journal of Transportation Safety & Security, Vol. 3, pp. 108-122, 2011.

Lee, C., Hellinga, B., Saccomanno, F., "Assessing safety benefits of variable speed limits" Transportation Research Record 1897, Transportation Research Board, Washington D.C., pp. 183-190, 2004.

Li, Z., Chung, K, and Cassidy, M.J., "Collisions in freeway traffic influence of downstream queues and interim means to address them," Transportation Research Record 2396, Transportation Research Board, Washington D.C., pp. 1-9, 2013.

Li, Z., Ahn, S., Chung, K, Ragland, D.R., Wang, W., and Yu, J., "Surrogate safety measure for evaluating rear-end collision risk related to kinematic waves near freeway recurrent bottlenecks," Accident Analysis and Prevention, Vol. 64, pp. 52-61, 2014.

Li Y., Bai, Y., "Development of crash-severity-index models for the measurement of work zone risk levels," Accident Analysis and Prevention, Vol. 40, pp. 1724-1731, 2008.

Lee, C., Abdel-Aty, M., "Temporal variations in traffic flow and ramp-related crash risk," presented at the 9th international conference of applications of advanced technology in transportation, 2006.

Lu, X.Y., Qiu, T.Z., Varaiya, P., Horowitz, R., Shladover, S.E., "Combining variable speed limits with ramp metering for freeway traffic control." American Control Conference, Baltimore, USA, 2010.

Lee, C., Hellinga, B., Saccomanno, F., "Evaluation of variable speed limits to improve traffic safety." Transportation Research Part C, Vol. 14, pp. 213-228, 2006.

Madanat, S., Liu, P.C., "A prototype system for real-time incident likelihood prediction." ITS-Idea program project final report, Transportation research board, National research council, Washington, D.C., 1995.

Maciejewski, M., "A comparison of microscopic traffic flow simulation systems for an urban area." Transport Problems. Vol. 5, Issue 4, 2010.

Oh, J., Oh, C., Ritchie, S.G., and Chang, M., "Real-time estimation of accident likelihood for safety enhancement," Journal of Transportation Engineering, Vol. 131(5), pp. 358-363, 2005.

Oh, C., Park, S., and Ritchie, S.G., "A method for identifying rear-end collision risks using inductive loop detectors," Accident Analysis and Prevention, Vol. 38, pp. 295-301, 2006.

Oh, C., O, J., and Min J., "Real-time detection of hazardous traffic events on freeways- methodology and prototypical implementation," Transportation Research Record 2129, Transportation Research Board, Washington D.C., pp. 35-44, 2009.

Oh, C., Kim, T., "Estimation of rear-end crash potential using vehicle trajectory data," Accident Analysis and Prevention, Vol. 42(6), pp. 1888–1893, 2010.

Ozbay, K., Yang, H., Bartin, B., and Mudigonda, S., "Derivation and validation of new simulation-based surrogate safety measure. Transportation Research Record 2083, Transportation Research Board, Washington D.C., pp. 105-113, 2008.

Oh, C., Oh, J.S., Ritchie, S.G., and Chang, M., "Real-time estimation of freeway accident likelihood," presented at 80th annual meeting of the Transportation Research Board, Washington, DC, 2001.

Pande, A., Abdel-Aty, M., "Assessment of freeway parameters leading to lane-change related collisions," Accident Analysis and Prevention, Vol. 38, pp. 936-948, 2007.

Park, S., Ritchie, S.G., "Exploring the relationship among freeway speed variance, lane changing, and vehicle heterogeneity," presented at 83rd annual meeting of the Transportation Research Board, Washington, D.C., 2004.

Pande, A., Abdel-Aty, M., "A freeway safety strategy for advanced proactive traffic management.", Journal of Intelligent Transportation Systems, Vol. 9, Issue 3, pp. 145-158, 2005.

Qiu, L., Nixon, A., "Effects of adverse weather on traffic crashes systematic review and meta-analysis," Transportation Research Record 2055, Transportation Research Board, Washington D.C., pp. 139-146, 2008.

Qu, X., Wang, W., Liu, P., and Noyce, D., "Real-time prediction of freeway rear-end crash potential by support vector machine," presented at the 91st annual meeting of the Transportation Research Board, Washington D.C., 2012.

Rama, P., "Effects of weather-controlled variable speed limits and warning signs on driver behavior." In Transportation Research Record 1689, Transportation Research Board, Washington D.C., 1999.

Riggins, G., Bertini, R.L., Ackaah, W., Margreiter, M., "Evaluation of driver compliance to displayed variable advisory speed limit systems: comparison between Germany and the U.S." Transportation Research Procedia, Vol. 15, pp. 640-651, 2016.

Riggins, G., Bertini, R.L., Ackaah, W., Bogenberger, K., "Measurement and assessment of driver compliance with variable speed limit systems: comparison of the United States and Germany." Transportation Research Record 2554, Transportation Research Board, Washington D.C., pp. 77-88, 2016.

National Research Council, Washington, D.C., pp. 53-59, 1999.

Sun, Jie., Sun Jian., "A dynamic Bayesian network model for real-time crash prediction using traffic speed conditions data," Transportation Research Part C, Vol. 54, pp. 176-186, 2015.

Shi, Q., Abdel-Aty, M., "Big data applications in real-time traffic operation and safety monitoring and improvement on urban expressways," Transportation Research Part C, Vol. 58, pp. 380-394, 2014.

Sturtz, S., Ligges, U., and Gelman, A.E., "R2Winbugs: A package for running Winbugs from R," Journal of Statistical Software, Vol. 12(3), pp. 1-16, 2005.

Shankar, V., Mannering, F., and Barfield, W., “Effect of roadway geometrics and environmental factors on rural freeway accident frequencies,” Accident Analysis and Prevention, Vol. 27, pp. 371-389, 1995.

Sawalha, Z., Sayed, T., “Transferability of accident prediction models.” Safety Science, Vol. 44, pp. 209–219, 2006.

Saccomanno, F., Cunto, F., Guido, G., and Vitale, A., “Comparing safety at signalized intersections and roundabouts using simulated rear-end conflicts.” Transportation Research Record 2078, Transportation Research Board, Washington D.C., pp. 90-95, 2008.

Shew, C., Pande, A., and Nuworsoo, C., “Transferability and robustness of real-time freeway crash risk assessment,” Journal of Safety Research, Vol. 46, pp. 83–90, 2013.

Smulders, S., “Control of freeway traffic flow by variable speed signs.” Transportation Research Record, Transportation Research Board, Washington D.C., 1990.

Soriguera, F., Torne, J.M., Rosas, D., “Assessment of dynamic speed limit management on metropolitan freeways.” Journal of Intelligent Transportation Systems, Vol. 17(1), pp. 78-90, 2013.

Soriguera, F., Martinez, I., Sala, M., Menendez, M., “Effects of low speed limits on freeway traffic flow.” Transportation Research Part C, Vol. 77, pp. 257-274, 2017.

Soriguera, F., Sala, M., “Freeway lab: testing dynamic speed limits.” Social and Behavioral Sciences, Vol. 160, pp. 35-44, 2014.

Sui, Y., Young, R.K., “Analysis of speed compliance in rural variable speed limit system.” ITE Western District Annual Meeting, July 2013.

Wang, L., Abdel-Aty, M., Shi, Q., and Park, J., “Real-time crash prediction for expressway weaving segments,” Transportation Research Part C, Vol. 61, pp. 1-10, 2015.

Wang, L., Shi, Q., and Abdel-Aty, M., "Predicting crashes on expressway ramps with real-time traffic and weather data," Transportation Research Record 2514, Transportation Research Board, Washington D.C., pp. 32-38, 2015.

Xu, C., Liu, Pan., Wang, W., and Li, Z., "Evaluation of the impacts of traffic states on crash risks on freeways," Accident Analysis and Prevention, Vol. 47, pp. 162-171, 2012.

Xu, C., Wang, W., Liu, P., Guo, R., and Li, Z., "Using the Bayesian updating approach to improve the spatial and temporal transferability of real-time crash risk prediction models," Transportation Research Part C, Vol. 38, pp. 167-176, 2014.

Xu, C., Tarko, A.P., Wang, W., and Liu, P., "Predicting crash likelihood and severity on freeways with real-time loop detector data," Accident Analysis and Prevention, Vol. 57, pp. 30-39, 2013.

Xu, C., Wang, Q., and Liu, P., "Identifying crash-prone traffic conditions under different weather on freeways," Journal of Safety Research, Vol. 46, pp. 135-144, 2013.

Xu, C., Liu, P, Wang, W., and Jiang, X., "Development of a crash risk index to identify real time crash risks on freeways," Journal of Civil Engineering, Korean Society of Civil Engineering, Vol. 17, pp. 1788-1797, 2013.

Yeo, H., Jang, K., Skabardonis, A., and Kang S., "Impact of traffic states on freeway crash involvement rates," Accident Analysis and Prevention, Vol. 50, pp. 713-723, 2013.

Yu, R., Abdel-Aty, M., "Utilizing support vector machine in real-time crash risk evaluation," Accident Analysis and Prevention, Vol. 51, pp. 252-259, 2013.

Yu, R., Adel-Aty, M., "An optimal variable speed limits system to ameliorate traffic." Transportation Research Part C, Vol. 46, pp. 235-246, 2014.

Yang, X., Lin, Y., Lu, Y., Zou, N., "Optimal variable speed limit control for real-time freeway congestions." Social and Behavioral Sciences, Vol. 96, pp. 2362-2372, 2013.

Zheng, Z., Ahn, S., and Monsere, C.M., “Impact of traffic oscillations on freeway crash occurrences,” Accident Analysis and Prevention, Vol. 42, pp. 626-636, 2010.